2015

MIRNAS AS BIOMARKERS FOR PROSTATE CANCER PROGRESSION

Gene C. Clark
Virginia Commonwealth University

MIRNAS AS BIOMARKERS FOR PROSTATE CANCER PROGRESSION

A thesis submitted in partial fulfillment of the requirements for the degree of Master of Science in Biochemistry at Virginia Commonwealth University

By

Gene Chatman Clark
B. S. 2012, Virginia Polytechnic Institute

Director: Zendra E. Zehner
Professor, Department of Biochemistry

Virginia Commonwealth University
Richmond, Virginia
July 22, 2015

Acknowledgement

Firstly, I would like to thank the many people here at VCU have inexplicably taken a chance on me. This includes, but could not possibly be limited to, Dr. Kimberly Jefferson who let me work in her lab when I was just a non-degree seeking student, Dr. Shirley Taylor who successfully encouraged me to pursue my love of research, and Dr. Louis DeFelice who suggested that I apply to the Pre-Medical Certificate Program here at VCU. I would also like to thank my amazing lab mates, Qianni Wu and Rhonda Daniel, whose insight and support were invaluable to this project. I have been lucky to have had them as partners and as friends. I would also like to thank Dr. Mike Holmes for his advice and for all of the time that he spent goofing off with me in the break room. Finally, I would like to thank Dr. Zendra Zehner for her much needed guidance. I could not have gotten anywhere without her. Because she is modest, she will tell you a different story. Do not believe her.

Table of Contents

List of Figures

List of Tables

Abbreviations and Symbols

ADAR: RNA specific Adenosine Deaminases

AGO: Argonaut

AKT1: Rac protein kinase alpha

ALL: Acute Lymphoblastic Leukemia

AML: Acute Myeloid Leukemia

AMPK: Adenosine Monophosphate Kinase

AR: Androgen Receptor

AUC: Area Under a receiver operating Curve

BCL2: B-Cell CLL/Lymphoma 2

BCL6: B-Cell CLL/Lymphoma 6

BPH: Benign Prostate Hyperplasia

BRG1: Brahma/SWI2-related gene 1

BRM: Brahma

C19MC: Chromosome 19 Megacluster

cDNA: complementary DNA

circRNAs: circular RNAs

CLL: Chronic Lymphocytic Leukemia

COSMIC: Catalogue of Somatic Mutations in Cancer

CPM: Count Per Million

CRPC: Castrate Resistant Prostate Cancer:

Ct: Cycle threshold

CV: Coefficient of Variance

DGCR8: DiGeorge Syndrome Critical Region Gene 8

DNA: Deoxyribonucleic Acid

EGF: Epidermal Growth Factor

EGFR: Epidermal Growth Factor Receptor

emPCR: emulsion PCR

EMT: Epithelial-Mesenchymal Transition

ErbB2 & 3: V-Erb-B2 Erythroblastic Leukemia Viral Oncogene Homolog

ERG: v-ets erythroblastosis virus E26 oncogene homolog

ETV4: Ets Variant 4

EV: Extracellular Vesicle

F6: Poorly Tumorigenic Prostate Cell Line 6

FFPE: Formalin Fixed Paraffin Embedded

G: Gleason

GLM: Generalized Linear statistical Model

HMGA: High Mobility Group AT-hook

HOX: Homeobox

Hsa: homo sapiens

HuR: Hu Antigen R

HVEC: Human Vaginal Epithelial Cells

IG-DMR: Intergenic Differentially Methylated Region

Igf2: Insulin-like growth factor 2

IPC: Induced Pluripotent Cells

KSRP: KH-Type Splicing Regulatory Protein

L: liter

lncRNA: long non-coding RNA

LR: Likelihood Ratio

lrECM: lamimin rich Extracellular Matrix

M12: Metastatic Prostate Cancer Cell Line 12

M2182: Moderately Metastatic Prostate Cancer Cell Line

MAPK: Mitogen Activated Protein Kinase

MDM2: Mouse Double Minute 2 Homolog

MEST: Mesoderm-Specific Transcript homolog protein

MET: Mesenchymal-Epithelial Transition

mg: milligram

miR: mature miRNA transcript

miRNA: microRNA

mL: milliliter

MMCT: Microcell Mediated Chromosome Transfer

mRNA: messenger RNA

Myc: myelocytomatosis viral oncogene homolog

ncRNA: non-coding RNA

NE: Neuroendocrine

NGS: Next Generation Sequencing

nt: nucleotide

p53: Transformation-Related Protein 53

p68: RNA Helicase Protein 68

p72: RNA-Dependent Helicase Protein 72

pCa: prostate Cancer

PCR: Polymerase Chain Reaction

pg: picogram

PI3K: Phosphoinositide 3 Kinase

PIN: Prostatic Intraepithelial Neoplasia

pri-miRNA: primary miRNA

PSA: Prostate Specific Antigen

PTEN: Phosphatase and Tensin Homolog

Ras: Kirsten Rat Sarcoma Viral Oncogene Homolog

RBD: RNA Binding Domain

RBP: RNA Binding Protein

RISC: RNA Induced Silencing Complex

RLC: RISC Loading Complex

RNP: Ribonucleoprotein

RPKM: Reads Per Kilobase Per Million mapped reads method

RPMA: Reverse Phase Protein Microarray

RT-qPCR: Real Time quantitative Polymerase Chain Reaction

SNP: Single Nucleotide Polymorphism

SV40T: Simian Virus 40 Large T Antigen

TC: Total Counts method

TE: transposable element

TF: Transcription Factor

TGCA: The Cancer Genome Atlas

TGT-Beta: Transforming Growth Factor

TMM: Trimmed Mean of M values method

TMPRSS2: Transmembrane protease, serine 2

TNF: Tumor Necrosis Factor

ug: microgram

uL: microliter

UTR: Untranslated Region

ZEB: Zinc Finger E-box binding homeobox 2

Abstract

MIRNAS AS BIOMARKERS FOR PROSTATE CANCER PROGRESSION

Gene Chatman Clark
B.S. 2012, Virginia Polytechnic Institute

A thesis submitted in partial fulfillment of the requirements for the degree of Master of Science in Biochemistry at Virginia Commonwealth University

Virginia Commonwealth University, 2015

Director: Zendra E. Zehner
Professor, Department of Biochemistry

Prostate cancer is one of the most challenging global medical issues today. In 2011, prostate cancer was the most diagnosed malignancy in the United States, making up 29% of new cancer cases. In that year it was the second leading cause of cancer related deaths among men in the USA and the second most common cause of cancer related death overall from the EU. The prostate remains, however, an under studied organ, making insights into the anatomy and biology of prostate cancer difficult to achieve. After 30 years, PSA screening of men of the appropriate age is still the first step in prostate cancer diagnosis, usually followed by a manual prostate exam which may lead to a transrectal biopsy. This study makes use of Next Generation Sequencing to successfully identify a superior miRNA based urinary assay for the detection of prostate cancer.

A receiver operating curve AUC of 0.90 was achieved for patients vs. non-patients using an additive risk model defined by empirically derived critical threshold values of eight urinary miRNAs identified with this method. This is superior to the PSA blood test's AUC of 0.66 which illustrates that a miRNA profile such as this has the potential to surpass protein biomarkers such as PSA in terms of specificity and sensitivity. It was also demonstrated that a geometric mean of three urinary miRNAs were useful for endogenous normalization.

One significant risk factor for prostate cancer is being African American. Again using Next Generation Sequencing technology, we have established a miRNA expression profile for the stages of a prostate cancer cell line progression model derived from the normal prostate epithelium of an African American man. Normal prostate epithelium was immortalized only with SV40 large T antigen (P69) and passaged three times in nude mice, producing the highly aggressive and metastatic M12 cell line. The M2182 cell line is an intermediate between the P69s and M12s having only been passaged twice and not yet having acquired metastatic potential. The F6 cell line was derived by reintroducing a copy of chromosome 19 missing from the M12 cell line via microcell mediated chromosome transfer. These profiles show a large downregulation of miRNAs early in tumorigenesis (from P69 toM2182) affecting the DLK1-DIO3 megacluster and the miR-200 family. The later acquisition of metastatic potential (from M2182 to M12) is concomitant with the upregulation of specific miRNAs including the HOX gene miRNAs miR-10a and miR-196 and miR-9. Thus, the analysis of this progression model has uncovered relevant miRs and genes the dysregulation of which contribute to prostate tumorigenesis.

INTRODUCTION

The Prostate

The prostate is a ductal exocrine organ located at the junction between the bladder and the urethra that makes an alkaline contribution to the seminal fluid designed to facilitate the survival of spermatozoa in the hostile environment of the vagina. As an exocrine organ, the bulk of the prostate is made up of tubuloalveolar glandular tissue from which 95% of prostate cancers (adenocarcinomas) originate.[5] This glandular tissue is divided up into the four distinct zones based on the location and appearance of their ductal openings in the urethra with reference to the verumontanum (seminal colliculus), the microscopic appearance of their glands, and the branching pattern of the tubular network.[5] Approximately 50-75% of glandular tissue makes up the peripheral zone constituting most of the base and lateral areas of the prostate's conical shape. Approximately 10-25% of the prostate's glandular tissue, the majority of the tissue that does not reside in the peripheral zone, resides in the central zone. Between 5% and 10% of glandular tissue resides in the transition zone which is separated from the rest of the prostate by a fibromuscular band. Finally the periurethral glands make up less than 1% of glandular tissue.[5]

Prostate Cancer

One inherent problem to the characterization of miRNA involvement in prostate carcinogenesis is that, compared to other more well studied malignancies, little is known about crucial molecular mechanisms driving pCa, leaving us with no place to start looking. It is hoped at this stage that as miRNA studies move forward in tandem to studies involving more classical oncogenes, that the two will complement each other, with an integrative model being the final goal. However, some key molecular aberrations in prostate cancer that have been observed

include the TMPRSS2:ETS genetic rearrangement, GSTP1, NKX3.1, PTEN, p27, and the androgen receptor (AR)[8] and many reports show aberrant miRNA contribution to prostate carcinogenesis.[2]

The Relevance of miRNAs

Non-coding RNA (ncRNA) has been reported to account for up to 90% of transcription in eukaryotes, and yet for a long time was considered to make no significant contribution to the biology of the cell.[1] The discovery of the importance of miRNAs and the many other functional ncRNAs has helped to overturn this thinking. miRNAs are phylogenetically conserved[3], 19-24 nucleotide (nt) long non-coding RNAs that make up an endogenous and extremely diverse part of translational regulation. Based on Watson-Crick base paring alone, it is estimated that 60% of protein encoding genes could be regulated directly by miRNAs.[1] However, a more modern view of miRNA targeting allowing for G:U wobbles and the possibility for strong binding despite central mismatches has led contemporary researchers to expand that estimation to as high as 90%.[38] In addition to this, most genes contain multiple binding sites for different miRNAs allowing for the formation of complex regulatory networks. What is known is that miRNAs have been shown to regulate almost all physiological processes and to be involved to some degree in the pathology of all tissues.[1] In the last decade, more than 10,000 papers reporting on the involvement of miRNAs in cancer were deposited to PubMed.[58]

Extracellular miRNAs and the Tumor Microenvironment

The ability of miRNAs to act on local or even distant tissues has captured the imagination of many researchers. Evidence has accumulated for many possible secretory mechanisms including passive diffusion from platelets and cells undergoing apoptosis, and active secretion

via exosomes, microvesicles, apoptotic bodies, and exocytosis in complex with proteins and lipoproteins.[3,19] However, none of these has received more attention in the past decade than exosomes. Exosomes range from 30-100 nm and are formed through inward budding of endocytic membranes, resulting in multivesicular bodies that eventually fuse with the cell membrane to release the exosomes into the extracellular milieu. Studies have suggested that a common 3' UTR motif may allow for selective packaging of certain mRNAs into exosomes, perhaps via interactions with as of yet unidentified ribonucleoproteins (RNPs).[11] Upon reaching their destination, miRNAs can enter target cells by endocytosis, membrane fusion, binding to specific receptors, or passive diffusion.[9]

Exosome production occurs in most healthy cells but it has been demonstrated that exosomes are shed in greater numbers from cancer cells. In fact circulating exosome levels have been demonstrated to be upregulated in breast cancer patients when compared to healthy controls[34] and cancer patients in general have been shown to have more RNA from extracellular vesicles (EVs) in their blood. This is thought to serve cancer cells both in the cultivation of the tumorigenic microenvironment and in the shedding of proteins and RNAs that hinder their proliferation.[11] The tumor microenvironment is integral to the development of every in vivo tumor. It is mostly populated by cells other than tumor cells such as cancer associated fibroblasts, endothelial cells, stromal progenitor cells, pericytes, and inflammation mediating immune cells such as macrophages.[3,4] Studies have shown that communication between tumor cells and these cells that make up the surrounding environment is strongly mediated by non-coding RNA (ncRNA) and a majority of these are miRNAs.[3] To illustrate the importance of exosomes in tumor associated miRNA signaling, it has been established that in normal tissues, of the miRNAs that reside in the ECM, 90% are bound to proteins of the AGO family and 10%

reside in exosomes and other vesicles of various origins. However, in a tumor's "sphere of influence", the concentration of miRNAs residing specifically in exosomes dominates.[9,19]

Canonical and Non-Canonical Pathways

About 40% of miRNAs in *Homo sapiens* are encoded in clusters and co-transcribed together as one long primary miRNA (pri-miRNA) transcript. These pri-miRNAs sport multiple local hairpin structures each of which contains a future mature miRNA.[1] Pri-miRNA transcripts are on the average 1kb long, have 5' caps, polyA tails and are transcribed mostly in a Pol II dependent manner. Evidence does exists for a Pol III dependent mechanism for the transcription of viral miRNAs and miRNAs encoded within Alu sequences.[1] In the "canonical" pathway, pri-miRNAs are processed in the nucleus by an RNaseIII type enzyme called Drosha in complex with the essential cofactor DGCR8 (together referred to as the Microprocessor), and other non-essential cofactors such as p68 and p72.[61] Together, these proteins produce a 60-110 nt hairpin structure with a single 3'-OH 2 nt overhang referred to as a pre-miRNA.[7] Pre-miRNAs are transported from the nucleus into the cytoplasm by Exportin-5 in a Ran-GTP dependent manner where they are further processed by Dicer1, another RNaseIII type enzyme, in complex with multiple cofactors such as TRBP and KSRP.[7,61] Dicer processing produces a dsRNA 19-24 nucleotides long with two 2 nt 3' overhangs. The duplex is then loaded into one of four Argonaut (AGO) proteins with the help of RISC Loading Complex (RLC). A principal component of the RLC is the Heat Shock Cognate 70- Heat Shock Protein 90 complex which upon hydrolysis of an ATP, manipulates the conformation of the apo-AGO protein to allow for loading. Once inside the AGO protein, the passenger strand is most likely degraded by an unconfirmed nuclease or unwound by AGO. The mature single stranded miR and the Ago protein constitute the minimal RNA Induced Silencing Complex (RISC) and once properly loaded, the miRNA sets to guiding

the RISC to its targets. The target sequence is usually located in the 3'-UTR of a cytoplasmic mRNA transcript but a few complementary sequences are also found in coding regions and in the 5'UTRs.[1,10] The favoring of 3'-UTR target sites could possibly reflect the mechanism of acquisition of target transcripts by the RISC complex.

The processing of some miRNAs are Drosha or Dicer independent, and are thus referred to collectively as "non-canonical" pathways. For Instance, the processing of pre-miRNA-451, the single most abundant circulating miRNA, is Dicer independent and instead relies on AGO2's RNaseH –like endonuclease activity to produce its mature miRNA transcript (miR).[27] However, despite some high profile exceptions like this one, a vast majority of miRNAs are processed via the canonical pathway with only about 1% of conserved miRNAs being either Dicer or Drosha independent.[61]

miRNA Action

Animal miRNAs tend to recognize targets via a 6-8 nt seed sequence located at position 2-7 from the 5' end of the miRNA. Bases at positions 8 and 13-16 also play a smaller role in target recognition.[61] Near perfect matching allows Ago2 mediated mRNA cleavage of mRNA transcripts.[1] However, as opposed to in plants, the vast majority of animal miRNAs only have partial complementarity to their target sequences which leads to translational inhibition or mRNA destabilization. One promising model for translational repression suggests that mRNA-miRNA complexes are sequestered in P bodies where they are de-capped. Another suggests that the RISC complex can repress the activity of eIFs, stalling translation at the initiation stage.[1] Interestingly, the most recent evidence suggests that translational inhibition might take a back seat to mRNA destabilization, although this has yet to be fully accepted by the scientific community. Some evidence has suggested that recruitment of CCR4 and CAF1 deadenylases by

GW182 is the most common pathway for regulation in mammals.[27] On the whole, it is likely that miRNAs are capable of inhibiting protein expression through many mechanisms although the context and relative contribution of each remains to be explored.

These mechanisms function to two important effects. miRNAs create overlapping networks of regulation[2] in order to achieve sharp spatial and temporal control of fluctuating mRNA levels. This is especially important during embryonic development and during modular cellular mechanisms, which are controlled by homeostatic regulation of various determinates of the cell state. miRNAs are known to play a part in almost all cellular processes including but not limited to proliferation, development, apoptosis, EMT, and differentiation. miRNA are also known to at least participate in, if not truly define, the signaling architecture that establishes and protects the state of the cell through the propagation of an elegantly complex web of positive and negative loops. See below for a more detailed explanation.

miRNA Expression and Regulation

Some miRNAs are autonomously expressed and their promoters are very similar to those of protein encoding genes. Many feature CpG islands, TATA boxes, response elements, initiation elements, and other classic promoter components.[1] Interestingly, miRNAs are often found to regulate the transcription factors (TFs) that activate or repress them either positively or negatively creating various control loops.[1] For instance, the transcription factor PIT3 upregulates the transcription of miR-133b which targets the mRNA that codes for PIT3, forming a negative loop that controls dopaminergic neuron differentiation. Another, more elaborate example of this is how the miRNAs lys6 and miR-273-5p interact with the transcription factors DIE-1 and COG-

1 to form a double negative loop that controls the two alternative fates for chemosensory neurons in *C. elegans*.[27] During development and during the determination and maintenance of the cell state, auto-regulatory feedback loops are the most common form of miRNA regulation. miRNAs are uniquely suited to participate in regulatory loops due to the fact that they do not need to be translated in order to act. It is easy to imagine how this might be attractive in terms of a conservation of energy and precision of timing and targeting due to their immediate and direct effect. In keeping with this concept, it has been discovered that some miRNAs can actually directly self-regulate, binding to their own primary transcripts in a feed forward manner.[1]

Another facet of miRNA regulation is the global control of miRNA production by various mechanisms. For instance, miRNA activity is related to the concentration of the Drosha and DGCR8 complex in the nucleus. The concentration of this complex is controlled by an interesting auto-regulatory relationship between these two proteins. Drosha is stabilized by DGCR8 and without it, it has almost no RNase activity. However, the functional Drosha/DGCR8 complex destabilizes DGCR8 mRNA by excising a miRNA-like hairpin from one of its exons.[61,1] This relationship is deeply conserved across the animal kingdom and, although the overall levels of this complex can be manipulated by other factors, its expression is homeostatic. A similar relationship exists between the Dicer1 mRNA and miRNA-let-7, which is also hypothesized to contribute to homeostatic control of miRNA production. Overall miRNA activity can also be perturbed by different post-translational modifications on miRNA processing machinery and by some transcription factors such as p53, MYC, ZEB1/2, and MYOD1.[61]

Activation of different RNA binding (RBD) proteins that function along with the microprocessor to either upregulate or down regulate a group of miRNAs also plays a large part in control of miRNA expression. For example KSRP binds to the terminal loops of the primary

transcript of miRNA-let-7 to facilitate Drosha/DGCR8 processing while LIN28A/B, which is exclusively expressed in undifferentiated cells, functions in a similar way to suppress it.[61] Seventy-five % of 3'-UTRs that contain miRNA binding sites also contain a binding site for HuR, an RBD that functions by directly binding mRNAs in a way that protects them from the RISC, but allows for translation.[1] Controlling the expression of the many different types of RBDs is an important aspect of global miRNA control.

3p vs 5p

Until recently, it was widely believed that only the duplex strand that comes from the 5' end of the pre-miR became the active strand in the RISC complex, but now we know that both the 5' and 3' ends can be active strands.[1] This is reflected in the recent change in "official" nomenclature from the miRNA/miRNA* designation to the miRNA-5p/miRNA-3p. Much evidence suggests that, for the most part, it is the strand with the lowest free energy of its 5' end within the miRNA duplex that becomes the active strand.[27] It also seems to be the case that AGO proteins preferentially select for guide strands with a U at their 5'-end. However, it has been demonstrated that for some miRNAs, both strands can function as the active strand, with their relative use varying depending on tissue and context.[1] For instance, miR-142-5p is the dominant strand in adult brain, testes, and ovary tissue while miR-142-3p is the dominant strand in embryonic and neonatal tissues.[61] Interestingly, despite having completely different seed sequences, the targets of the 3' and 5'strand sometimes overlap to some degree, suggesting that alternate strands could be intentionally selected to regulate alternate portions of the same pathways. How this selection is made is beyond what we currently understand, but it could be related to alternate Drosha/DGCR8 processing.[65]

Many examples illustrate the importance of strand selection phenomenon in cancer. Specifically, one study found arm switching in colorectal cancer of miR-28 could be explained by the fact that expression of miR-28-5p reduced cell proliferation by targeting the CCND1 and HOXB3 proteins while miR-28-3p expression increased in vivo migration and invasion by targeting the metastasis suppressor protein NM23-H1.[58]

The General Silencing of miRNAs in Cancer

The general dysregulation of homeostatic control of miRNA signaling is the most common miRNA related phenomenon seen in cancers.[66] For a vast majority of miRNAs, this general dysregulation amounts to suppression, with only a small subset of miRNA families governing oncogenic events experiencing upregulation. Considering the vastly complicated regulation of miRNA machinery, there are many ways in which global miRNA signaling can be perturbed, but two of the most common aberrations seen in cancers are hypermethylation of CpG islands and a loss of core miRNA machinery genes.

Under normal physiological conditions, most CpG island promoters are unmethylated (although not necessarily active) while in most tumors, a majority of genes are hypermethylated.[4] This leads to a general silencing of tumor suppressor genes.[1] The tumorigenic effect of this illustrates that tumor suppressors are more important to lose than oncogenes are to gain. About half of all miRNA genes are associated with CpG islands and so, the general hypermethylation associated with tumors leads to a global dampening of miRNA networks. In fact, this is currently thought to be the most common cause of miRNA silencing in miRNAs.[58] As a further complication, miRNAs can themselves regulate important components of the epigenetic machinery.[1]

Knockdown of Dicer and Drosha leads to tumorigenesis.[7] There is evidence that Dicer1 acts as a haplo-insufficient tumor suppressor in mice[61] and in breast cancer cell lines, Dicer1 expression was found to be lower in cells that displayed a mesenchymal phenotype than an epithelial one.[61] The same observation was made by a different group for breast cancer metastases derived from a cell line.[7] It could be that inactivation of Dicer1 is a simple way of breaking down the protection that miRNA signaling gives to the cell state. However, Dicer1 is not downregulated in all cancer types and in fact, in prostate cancer it is much more commonly upregulated.[7] Knockdown of EXP5 results in a reduction of miRNA levels without an accumulation of pre-miRNAs in the nucleus, which suggests that there is a certain level of nuclease activity in the nucleus and EXP5 functions to protect the pre-miRNAs before they are delivered to the cytoplasm. In some tumors, XPO5, the gene that encodes EXP5, is mutated.[61] Prostate cancer is a malignancy in which mutations in the XPO5 gene are seen in appreciable levels.[66] Interestingly, AGO2 specifically is commonly seen to be upregulated in cancers, including 14.8% of metastatic prostate adenocarcinoma. This phenomenon correlates well with EGFR amplification or upregulation.[66]

Another mechanism for global miRNA dysregulation that is less commonly discussed is the hyper expression of viral miRNAs. Several viruses encode both stolen human microRNAs and novel unique viral microRNAs that participate in the establishment of viral latency, entry into the lytic life cycle, cellular proliferation, immune evasion, and tumor progression.[57] It has been demonstrated that in lymphoma cells infected by Kaposi sarcoma associated herpesvirus, viral encoded microRNAs represent the majority (more than 80%) of expression.[57] This suggests that the concentration of miRNA machinery in the cell is rate limiting and that a miRNA that is

pathogenically over expressed may dominate the miRNA profile of a cell in a way that effectively silences other tumor suppressor miRs.

The Epithelial-Mesenchymal Transition

Complications due to metastasis is the main cause of cancer related death, responsible for up to 90% of deaths in patients with solid tumors.[7] Considerable research has been done in the field of miRNA involvement in the EMT, due to their known role in this modular process and the crucial part that the EMT plays in the escape of clonal cells from the local tumor environment. Most impressively, a double negative loop involving the miRNA-200 family and the ZEB1/2 transcription factors has been demonstrated to stabilize either the epithelial or mesenchymal phenotype in a mutually exclusive manner.[28] This research can be retroactively applied to the stratification of prostate cancer patients on the basis of tumor aggressiveness and likelihood for post-surgery recurrence. This is very relevant clinical information as knowing whether or not recurrence is likely could spare an elderly patient the consequences of chemotherapy.

Why Next Generation Sequencing (NGS)

Several factors such as their size, high homology, and low abundance, make the profiling of microRNAs technically challenging. The most crucial factor affecting the outcome of any profiling study is the choice of platform as inter-platform differences have been demonstrated to be high.[45] Our choice to pursue NGS as opposed to microarray or qRT-PCR technology was a direct result of the advantages that it posed to our specific study.

Firstly, it is more sensitive, providing a picture of miRNAs present at very low copy numbers that would have been impossible to see on any microRNA array. In addition to this, a recent review of miRNA platforms demonstrated that of all available technologies, Illumina

sequencing specifically demonstrated one of the highest abilities to differentiate between small differences in gene expression.[45] These advantages opened us to the possibility of more deeply evaluating changes in low copy number miRNAs as opposed to high copy miRNAs. The importance of low copy miRNAs is discussed in the discussion section of Chapter 1. However, one caveat of NGS is that the number of adaptor sequences within a sample lane is rate limiting and so high copy miRNAs can be disproportionately represented in the resulting sequencing profile compared to low copy miRNAs. This should be kept in mind so as not to unnecessarily disregard potentially impactful miRNAs when choosing candidates for further validation.

Secondly, NGS has the ability to distinguish miRNAs that differ by as little as a single nucleotide. As with the multiple members of the Let-7 family, singular differences that fall in a miRNA's seed region can drastically effect the genes that it targets, which means that differentiating between them is of significant clinical importance.[78] This also means that NGS can discriminate between isomiRs, which are a result of post transcriptional additions to the 3' end, and less frequently the 5' end, of mature miRs. Although this was not utilized in this current study, the sequencing data can be reanalyzed in future experiments to highlight these differences. Last but not least, it was reasoned that the greatest potential advantage in using miRNAs as biomarkers stems from their diversity and investigating only a selective panel for which primers are available was considered an unacceptable limitation. The profiling by sequencing approach does not have this limitation. For the same reason, NGS also allows for the discovery of novel miRNA transcripts whose validation in future experiments will be valuable irrespective of their relationship with prostate cancer or their utility as a biomarker.[35]

Chapter 1: A Urinary Assay for the Detection of Prostate Cancer

Specific Aims

In the 1970's, only the healthiest and most promising of patients could hope to survive a surgical cure for prostate cancer. However, Dr. Patrick Walsh's accurate anatomical descriptions of the 1980's led to the improved management of the dorsal penile veins allowing for a careful operation to occur in a field cleared of blood. This, in turn, led to the improved management of both the striated sphincter and the newly described autonomic neurovascular bundle of the prostate. These advancements made low risk prostatectomy with the retention of potency and urinary continence a potentially curative option for prostate cancer patients.[5] However, the curative potential of surgical treatment depends on the stage of the disease at the time of diagnosis with truly localized cancer having the greatest success rate.[5]

The next advancement in prostate cancer medicine was the advent of PSA testing in the 1980's. It is estimated that PSA screening affords patients and their physicians a lead time of 5.4 to 6.9 years, resulting in patients who present with lower grade disease at the time of diagnosis.[67] Despite a 70% increase in prostate cancer incidence since 1980, by 2008 prostate cancer mortality rates had dropped by 40% in the United States. This is in contrast to 12% reduction in mortality in the United Kingdom where routine PSA screening was never adopted.[67] However, PSA testing is plagued by a low sensitivity that makes it less than optimal. Today, more than 15% of pCa patients present with a serum PSA level below the empirically defined cut off point for biopsy referral of 4 ng/ml, suggesting that many prostate cancers go undetected for a long time.[37] Currently, 4% of patients have progressed all the way to metastasis at the time of diagnosis giving them limited treatment options.[28] The low specificity of PSA testing is also a cause for major concern in terms of patient outcomes. Circulating PSA levels can also be the result of other, non-malignant pathologies of the prostate such as benign prostate hyperplasia

(BPH) and prostatic intraepithelial neoplasia (PIN). Because PSA screening and digital rectal examination are the only diagnostic criteria in use for the recommendation for biopsy, an astounding 75% of biopsies come back negative for pCa.[20]

microRNAs (miRNAs) are short non-coding RNAs (18-24 nt) involved in an expansive list of biological processes. Generally speaking, miRNAs effect gene regulation at the level of translation by either inhibiting translation or by destabilizing mRNA transcripts. However, in addition to their intracellular functions, miRNAs are increasingly being recognized for the role they play outside of the cell. In fact, it has been proposed that non-coding RNAs may dominate the bulk of signaling between tumor and tumor associated cells that propagate the tumor microenvironment. The modern development of detection technologies such as RT-PCR, microarrays, and deep sequencing, has produced evidence that almost all of the body fluids, including blood, urine, saliva, and semen of cancer patients possess distinct miRNA profiles from those of healthy individuals.[3,9] Surprisingly, these miRNA body fluid profiles have been found to be less variable and more powerfully correlated to individual pathologies than any combination of mRNA or proteins, making them a promising potential source of accurate biomarkers.[21] *In this study, we took advantage of next generation, high throughput sequencing technology to identify potential biomarkers for prostate cancer in the urine of patients and controls.*

Urine Over Blood and Semen.

In general, urine was thought to be a good biofluid candidate for diagnosis because it was thought that due to the necessity of urine to pass through the prostatic urethra and the prostate's direct connection to the urethra via its multiple large ducts, the urine may be particularly enriched for miRNAs derived from the prostate. Urine was chosen over blood because

circulating miRNAs thought to be derived from all of the tissues in the body constitute a large signal whereas the miRNA population of the urine is much smaller and derived from a smaller subset of tissues. This means that miRNA signals in the urine associated with changes in the prostate will have less background noise with which to compete. Also, biomarkers that are secreted by prostate cancer into the urine are diluted into a smaller volume than biomarkers that are secreted into the blood (a few ounces of urine vs. 5 liter of blood), making biological differences in gene express easier to detect.

Also, it was thought that in the case of urine, sufficient amounts of sample could be obtained from each subject in order to perform sequencing with high confidence. Urine was chosen over semen because it was thought that older patients with prostate problems would be less likely to produce a semen sample, making sample acquisition difficult, and that even the most robust of the samples obtained may not provide enough material to perform sequencing with an acceptable level of confidence. However, because the prostate normally contributes about 50-70% of the seminal fluid, semen deserves further investigation for the purposes of prostate cancer diagnosis as it is likely to be greatly enriched in material from the prostate as compared to other candidate biological fluids.

Materials and Methods

RNA Extraction from Urine

Many past studies have used the pellet obtained from urine after a low speed spin for further analysis of miRNA content. However, it has been discovered that a large amount of low

quality and degraded RNA exists in this compartment, possibly due to the high level of RNase activity characteristic of the urinary tract.[31] These low quality RNA fragments create noise and introduce a high rate of false positives in miRNA sequencing studies due to their small size and alignment to the genome. Considering this, we opted to analyze the cell free component of urine, as the centrifugation steps used to remove whole cells and cell fragments are not likely to remove either free miRNAs or those contained in exosomes or in complex with AGO2 proteins, which would require ultracentrifugation speeds to pellet.

The cell content of the urine is vastly smaller than that of the blood and only 10% of the cells that are found in the urine are from the prostate. On top of that, the portion of these prostate cells that are derived from the tumor is negligible, except in rare and extraordinary circumstances. Also, since it has been established that the tumor derived signal in blood is independent of the presence of circulating whole cells,[23] we reasoned that excluding the cellular compartment from the urine would not significantly reduce our chances of finding a diagnostic marker. Urine samples were subjected to a 2,000 x g spin for 30 min in order to pellet any intact cells in the fluid. After transfer to new tubes, each sample was then subjected to a 12,000 g spin to pellet any remaining large cell fragments. It cannot be ruled out, that some miRNAs derived from whole cells or cell fragments lysed during the extraction process are still present in the samples.

Because it is difficult to obtain sufficient RNA from urine to construct cDNA libraries for high throughput deep sequencing, many past researchers have pooled patient samples together.[31] However, in an attempt to preserve individual variability, we used a slurry based total RNA extraction method capable of concentrating RNAs from large urine volumes into a small (<200 ul) eluent. It was also thought that this would be an interesting approach because the intact

population of miRNAs extracted from this compartment, without enrichment for exosomes, has yet to be analyzed, especially not for individual, un-pooled samples. For sequencing, extracted RNA from a select number of samples was concentrated further under lyophilization conditions using a rotovap at low temperature and pressure in order to meet the minimum concentration (100ng RNA/6ul) required for sequencing. However, RT-PCR validation was performed separately on un-concentrated samples due the sensitivity of RT-PCR.

Illumina

For the urine profiling experiment, 9 patient and 5 control samples were prepared as described above and sent to the Nucleic Acids Research Facility at Virginia Commonwealth University for paired end sequencing on the Illumina platform using the manufacturer's recommended protocols. It should be noted that this standard protocol included a gel electrophoresis size fractionation step that restricts sequencing to the appropriate size range of cDNA products. Samples identifiers, their cancer stage, and "miRNA" concentration as reported by the Agilent Bioanalyzer's small RNA chip are recorded below. When Gleason score was not available, pCa was used to designate patients. Downstream analysis was performed using multiple programs including Partek Flow, RStudio, and edgeR.

Trimming of the bases and adaptors attached to the 3' and 5' ends of the read sequences by the Illumina sequencing TruSeq Small RNA sample preparation kits (AGATCGGAAGAGCACACGTCT) was performed in Partek Flow. Two deviations from the default settings were used to appropriately accomplish this for our unique project. Firstly, match times were increased from the default of 1 to 3 to allow sequences to be cleaved multiple times. Trimming multiple times is important because it is possible for adaptors to anneal more than once to a single read. Trimming of bases further increases quality scores by removing partial

junk sequences that could affect alignment. Secondly, the minimum read length was changed from the default of 25 nt to 16 nt to accommodate the size of miRNAs. A pre-alignment QA/QC report was generated to assess RNA quality (Phred) and the results are reported in Figure X. A Phred score of higher than 30 is considered exceptional and is defined as $(10)(-\log_{10}X)$ where X is the chance that an incorrect base has been incorporated into a sequence. For instance a Phred score of 30 indicates that 1/1000 (10^{-3}) bases is incorporated incorrectly, indicating a base call accuracy of 99.9%. After trimming, the reads were aligned to the human genome (GRCh38) using the Bowtie Aligner. The Bowtie Aligner was chosen because it is the most suitable for short reads with high similarity but unique alignments. Seed mismatch was decreased from 2 to 1 to increase stringency and the alignments reported per read was increased from 1 to 3. Again, the minimum read length was altered from 28 to 16 to accommodate the size of miRNAs. Trimmed reads and alignments (3x) are reported in Figure X.

RT- PCR

In a recent study comparing commercially available miRNA profiling technologies based on NGS, microarray, or qRT-PCR, the greatest overlap between any two platforms in terms of the validation of differential gene expression in a set of mixed standards was only 54.6%.[45] Because of this low level of confidence, it is considered good practice to validate profiling results using another platform. For this purpose, we have chosen qRT-PCR because of all of the microRNA platforms, qRT-PCR possesses the greatest consistency and sensitivity.[45]

The quanta kit, which employs a universal tailing method to prime miRNAs for cDNA synthesis, was chosen based on the results of a study that reported that this platform possessed a higher sensitivity than a similar competitor and it was thought that this would be useful given the

possible importance of low miRNA abundance in urine.[42] cDNA synthesis and qPCR were performed according to the manufacturer's protocol with the exception that each qPCR reaction was scaled down to save reagents as follows: 6.25 ul SYBR Green Master Mix, 0.25 ul primer, 4.0 ul RNase Free H_2O, 2.0 ul cDNA for a final volume of 12.5 uL.

Although it is true that it becomes more difficult to specifically target RNAs as they get smaller, modern primer specificity is such that size selection is not necessary for qPCR experiments and they can be performed on total RNA samples.[57] However, the universal tailing system employed by the Qiagen RT-PCR assay has been demonstrated to confer a likelihood for false positives related to non-specific amplification.[57] Because of this, low expressed qPCR results were held to the highest possible scrutiny.

Results

NGS Normalization

RNA ligase preferences, factors pertaining to reverse transcription, library PCR amplification efficiencies, the length of each individual gene transcript, the overall sequencing depth, and RNA composition of individual samples are all factors likely to contribute technical biases to the final data output of next generation sequencing results.[56] For these reasons it is important to carefully normalize across different samples in order to detect true biological differences in expression.[76] However, currently no consensus exists as to how to do this and many RNA sequencing studies do not report on their normalization methods at all. Thus,

normalization methods must first be discussed and stablished before proceeding with subsequent data analysis.

It is common practice to normalize RNA sequencing results using either the "Reads Per Kilobase Per Million mapped reads" (RPKM) method, the "total counts" (TC) method, or the "Trimmed Mean of M values" (TMM) method. This first method, RPKM, is designed around the concept that the number of reads of a particular gene in a sequencing data set is proportional to the length of that gene and corrects for this mathematically.[70] This particular issue however seemed to be of little impact to our size fractionated library, since microRNAs are of the same approximate size. The second method, TC, takes the number of transcript raw reads from a sample and simply divides it by the total number of raw reads in that sample. In this way, each gene product is adjusted for library size in each sample.[71] These two methods attempt to minimize the effect that different library sizes (or disproportionate library fractions) may have on sequencing depth by taking into account gene length and relative expression level. However, both these methods are susceptible to RNA composition bias, limiting their utility in situations where comparisons are made between samples of very different composition such as between tissue types.[56] It results when technical bias is introduced by highly expressed genes in a data set overriding the representation of rare genes within a sample. (Please look to Chapter 2 for a discussion on high copy number vs low copy number miRNAs.) This can have a powerful impact on downstream analysis by producing an unacceptably inflated false positive rate.[69]

Composition bias was likely to be an obstacle in our study for two reasons. Firstly, we intended to compare data from samples composed of whole tumor tissue, obtained from The Cancer Genome Atlas (Chapter 2), to data from our own cell line samples (Chapter 2), from both of these tissue samples to our body fluids (Chapter 1), urine and blood, and between these body

fluids. The rationale behind this last comparison was that blood and urine samples taken from the same patients might yield clues as to where in the body a particular miRNA signal originated. For instance, if a miRNA seemed to be simultaneously upregulated in the blood and urine of the same patient, it might be reasoned that this miRNA is seeping into the circulation from the prostate and filtering into the urine through the kidneys. If a miRNA is upregulated in the urine but not the blood, it might be possible that it is making its way into the urine through the prostate's ductal connections to the urethra. If a miRNA is elevated in the blood but not the urine, it could be that this miRNA is not coming from the prostate tumor at all. The second reason why composition bias became an important factor in our experiment was because, when comparing the results of the Bioanalyzer data used to determine small RNA concentration, it became clear that RNA composition was likely to be drastically different between individual urine samples.

Figure 1: A comparison between samples of RNA in small size range. A) An electropherogram in the small RNA range of a typical control sample (1ul) . B) An electropherogram in the small RNA range of a typical patient sample (1ul). A comparison of the electropherograms of controls and patients demonstrates that patients are more likely to have more material of this size range in their urine.

A)

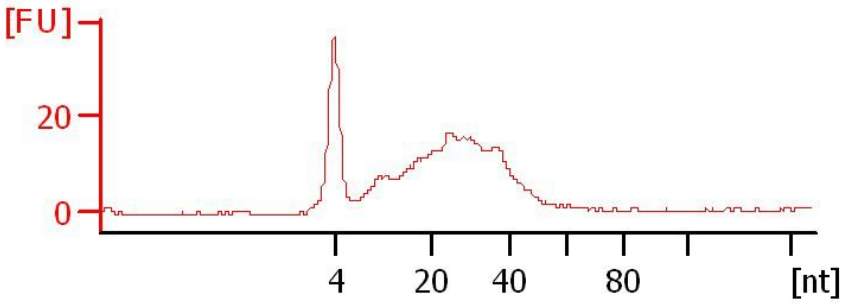

B)

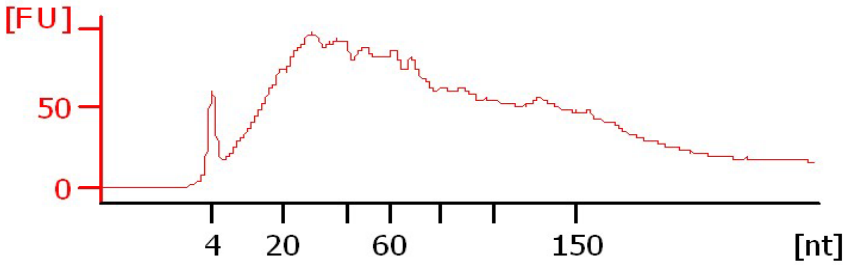

For example, as illustrated in Figure 1, controls typically contained much less material in the small RNA size range than patients.

The TMM method normalizes for the RNA composition with a scaling constant called a TMM factor calculated individually for each sample library with one middle sized sample library acting as a reference.[69] The TMM factor is calculated as a weighed mean of the log ratio between the expression of the most abundant genes in the reference library to those same genes in each test sample.[73] Firstly, for pairwise comparison, the log fold change for each gene is defined as

(1) $Mg = \log_2(Ygk/Nk)/(Ygk'/Nk')$

where "Mg" is the value of the fold change of gene g, commonly referred to as the "M value," "Ygk" is the raw read count for gene g in library k, and "Nk" is the total number of raw reads in library k. Then the absolute expression is calculated for each gene by

(2) $Ag = (½)\log_2[(Ygk/Nk)(Ygk'/Nk')]$

where, "Ag" is the "A value," a relative measure of absolute expression for gene g. After the M value and A value were calculated for all genes, genes with exceptional values were trimmed by excluding the top and bottom, 30% of M values and 5% of A values, and a "weighted" mean is calculated from the remaining genes by the edgeR program. These correction factors were used to populate a Generalized Linear statistical Model (GLM) and analysis of the normalized reads was performed with the appropriate tests (Fisher's exact test and GLM likelihood ratio test).[72] Although the TMM method does rely on the assumption that the majority of genes common to

both patient and control samples are *not* differentially expressed[72], something that we cannot assume about our body fluid samples, it has been demonstrated to be relatively resistant to deviations from this assumption.[56] Adjusted P values, referred to as the False Detection Rate or FDR, were obtained with the Benjamin-Hochberg method, which mitigates familywise error for multiple comparisons.[76] A false positive rate lower than 0.2 was considered to be significant. The Likelihood Ratio (LR) is a number generated by the edgeR statistical analysis program which is reported below. %GC is usually reported in sequencing studies in an effort to assess technical differences.

RNA-sequencing

9 patients and 5 controls were chosen for sequencing. When a Gleason score was not available, pCa was used to designate patients.

Table 1: Candidates for RNA Sequencing

Sample name	Stage	miRNA concentration (pg/ul)
12042014-EMR	G6	935.1
03082013	G6	323.1
10242013	G6	6233.7
11202014-KAB	G7	269.6
11262014-CTL	G7	1096
04192013-2	G8	1782.6
010812	G9	474
04042013-Pre	G9 + mets	796.1
111612	pCa	11826.6
07152014	Control	1076.7
08062013-Post	Control	2127.5
10212014	Control	356.9
WMH	Control	3028.0
GCC	Control	1601.8

Table 2: Sequencing Statistics

Sample name	Stage	Total reads	Total alignments	Avg. length	Avg. quality (Phret)	%GC
10242013	G6	2,525,470	6,049,884	29.09	38.59	50.41%
03082013-	G6	344,505	480,916	26.08	38.38	50.96%
12042014-EMR	G6	415,779	974,864	29.7	36.48	53.81%
11202014-KAB	G7	398,747	1,009,080	24.97	36.51	43.33%
11262014-CTL	G7	1,964,389	3,726,877	25.91	36.21	55.08%
04192013-2	G8	1,908,994	2,803,715	28.29	38.51	51.33%
010812-	G9	2,111,229	4,717,551	29.49	38.64	52.66%
04042013-Pre	G9	1,170,650	2,363,672	20.12	37.85	58.45%
111612	pCa	2,342,875	5,436,338	30.98	38.71	53.42%
07152014-	Control	3,225,726	8,762,098	31.66	36.59	56.53%
08062013-Post	Control	2,165,549	5,545,114	32.78	36.67	55.98%
10212014-	Control	2,246,868	5,786,297	31.19	36.68	52.17%
GCC	Control	383,885	641,523	25.68	38.25	52.88%
WMH	Control	1,981,890	3,715,430	26.59	38.4	53.52%

These results show that a high number of total reads in the appropriate size range align to the genome and are indeed validated human miRNAs. The disparities between the average lengths and total amount of reads between samples suggests that there are indeed considerable compositional differences, reaffirming our choice of TMM as our normalization method. %GC is consistently around 50% and Phret scores are consistently well above 30.00 confirming that our sequencing data is of high quality.

Table 3: microRNA Sequencing Results of Urine Samples

Gene Name	logFC	logCPM	LR	PValue	FDR
hsa-miR-223-3p	**5.940734**	**10.614319**	**16.24019**	**5.58E-05**	**0.013336**
hsa-miR-223-5p	**5.95683**	**7.6441786**	**13.45336**	**0.000245**	**0.029226**
hsa-miR-142-3p	**6.801603**	**9.4414229**	**12.68913**	**0.000368**	**0.0293**
hsa-miR-199a-3p	**4.884872**	**8.3158747**	**11.69224**	**0.000628**	**0.0375**
hsa-miR-363-3p	**-2.4222**	**11.602927**	**11.15461**	**0.000838**	**0.040067**
hsa-miR-199b-5p	4.974522	7.5241254	10.1309	0.001458	0.058079
hsa-miR-199b-3p	4.59329	7.3669649	9.558437	0.00199	0.067955
hsa-miR-143-3p	**3.957342**	**10.998673**	**8.453135**	**0.003644**	**0.108869**
hsa-miR-184	**5.863426**	**12.214555**	**7.873185**	**0.005017**	**0.133238**
hsa-miR-629-5p	2.227044	9.2003383	7.185232	0.007351	0.175679
hsa-miR-941	2.812312	10.376636	6.913948	0.008553	0.185825
hsa-miR-205-5p	**2.799235**	**11.093862**	**6.44201**	**0.011145**	**0.221976**
hsa-miR-146a-5p	**2.617289**	**11.905298**	**6.268341**	**0.012291**	**0.224996**
hsa-miR-185-5p	1.792165	10.981644	6.009805	0.014227	0.224996
hsa-miR-34c-5p	4.915895	9.5787856	5.939451	0.014806	0.224996
hsa-miR-375	**-2.25697**	**15.598242**	**5.837234**	**0.01569**	**0.224996**
hsa-miR-618	4.634886	8.8283879	5.737391	0.016607	0.224996
hsa-miR-204-5p	**-2.28501**	**11.863405**	**5.651272**	**0.017443**	**0.224996**
hsa-miR-221-3p	2.323762	11.741003	5.607212	0.017887	0.224996
hsa-miR-145-5p	4.683413	7.6031015	5.48455	0.019185	0.229264
hsa-miR-135a-5p	**-2.25086**	**9.7143463**	**5.31853**	**0.0211**	**0.240002**
hsa-miR-3613-5p	2.656422	8.6492001	5.238507	0.022092	0.240002

12 Candidates were selected for further investigation (bold above) with qRT-PCR based on their adjusted p value and considering a maximum FDR of 0.2. miRNA candidates were excluded from further investigation based on the range of read counts between samples. 135a-5p was considered for further validation despite its poor FDR because when the data was reconsidered deleting one particular outlier sample (10242013 G6), 135a-5p became the second most dysregulated miRNA (see Appendix). An interesting thirteenth candidate, 126-3p, was selected, not based on the sequencing data, as described below. Before validation with qRT-PCR could be performed, an appropriate normalization method had to be selected.

Possible prostate specific miRNAs: 126-3p

Some miRNAs, and their subsequent role in tumor progression, seem to be organ specific. For instance, down regulation of miR-122-5p, which is normally highly expressed in the liver and nowhere else, allows for the formation of intrahepatic metastases.[17] Likewise, the expression of miR-208 is restricted to cardiomyocytes and the 46 miRNAs of the chromosome 19 mega cluster are restricted to the embryonic placenta.[80] An analogous prostate specific miRNA could drastically increase the specificity of a new biomarker assay even if that miRNA plays no role in prostate cancer progression. The logic behind this idea is that if the prostate is the only tissue that makes a particular miRNA, then the amount of that miRNA in the urine or in circulation could specifically indicate pathology in the prostate. The PSA assay functions under the same logic. However, so far, no such miRNA marker has been found. A similar alternative would be a miRNA that acts differently in the prostate or prostate cancer than in any other cancer or tissue. For instance, miR-221-5p has been demonstrated to be upregulated a variety of cancers, but is downregulated in the tissue of TMPRSS2:ERG fusion positive pCa.[15] However, our sequencing data did not support further investigation of this miRNA as a urinary biomarker.

miR-126-3p was included in the qRT-PCR validation step despite dysregulation not being supported by our sequencing data as an intellectual experiment. miR-126-5p has been shown to play a positive role in the acquisition of angiogenesis and metastasis of multiple cancers, including prostate.[80] Among its many validated targets is a prostate specific protein called prostein, also called prostate cancer-associated protein 6, encoded by the Solute carrier family 45 member 3 *SLC45A3* gene. The expression of this protein has been demonstrated to decrease with the progression of prostate cancer, possibly because of putative tumor suppressor properties or because this protein is prostate specific and looses expression as prostate cancer

cells become more dedifferentiated. Surprisingly, this validated target is shared by its 3' counterpart, despite having different seed sequences. Since 126-3p has few other predicted targets, it was hypothesized that its expression would be more powerfully effected by changes in the presence of this lonely target.

Normalization of qRT PCR Analysis of Urine

Currently, there is a lack of consensus on how to normalize for qRT-PCR experiments that require high resolution such as those dealing with miRNAs.[19] It is for this reason that special attention will be paid to the method used here. The normalization strategy that we used has three parts. Firstly, total RNA was extracted from an equal volume of each urine sample (40 mL). This method is easy to criticize due to the inherent difficulty there is in being precise with heterogeneous biological samples. Secondly, an equal amount of small RNA in the 10 – 40 nucleotide size range, as measured by an Agilent Bioanalyzer, was used to make cDNA for each experiment (1.5 ng). It is important to control for the different overall concentrations of microRNA within each sample as there are many reasons other than the presence or absence of cancer for why they might be variable. For instance, it has been established that blood samples from HIV patients that suffer from an advanced stage of immune suppression will produce less RNA than healthy individuals due to their low CD4 cell count.[33] However, this approach is easily confounded by the presence of varying amounts of degradation products in this size range. Also, the reproducibility of quantitative values produced by the bioanalyzer small RNA chip has been reported to represent a Coefficient of Variance (CV) of as large as 25%.[49] In fact, it was found that every sample normalized by the previous two methods consistently produced either higher or lower Ct values within each sample for all miRNAs tested. This suggested that the actual amount of miRNA present in each sample was still variable and an endogenous

normalization was needed. Also, this approach was partially abandoned in a later round of validation by PCR that was intended to fill in missing data for low expression miRNAs by utilizing the highest RNA content possible.

A normalization factor was obtained from the combined expression of three endogenous miRNAs for use in the comparative ΔΔCt method of Livak using the Normfinder program. Multiple miRNAs were incorporated in an effort to increase the resolution of the experiment and because it is the opinion of most miRNA researchers that due to the natural level of individual miRNA expression between individuals, normalizing to a single miRNA is not appropriate.[56] The use of this strategy to find a non-classical endogenous normalization standard, as opposed to one commonly used for miRNA experiments such as RNU48, was necessitated by the unusual and cell free content of the sample under examination. For these reasons, it is the growing opinion that the classical reference genes, such as RNU48, are inappropriate for quantitative experiments of this level of resolution.[33] It has been argued that normalization is best performed between genes of the same class so as to ensure that the factor used for normalization accurately mirrors the physiochemical properties of the target molecule.[56] All things considered, it is the opinion of many in the field that the best way to normalize miRNA expression data is via a global mean normalization of three or more stable reference miRNA genes. This is achieved by taking the geometric mean of the reference genes and controls best for outliers and differences in sample size, which are the most common sources of error in miRNA analyses.[57]

To identify potential endogenous miRNAs for normalization, 6 candidate genes were selected based on abundance and minimal overall variance of normalized reads as reported by the NGS data, presence in the literature as a potential normalization factor, and by long hand

pairwise comparison of exploratory RT-PCR data. They were miR-197-3p, miR-16-5p, miR141-3p, miR-let7g-5p, miR-let7d-5p, and miR20a-5p.

Table 4: NGS Sequencing Results for Normalization Candidates

Gene Name	logFC	logCPM	LR	PValue	FDR
hsa-miR-20a-5p	-0.46117	9.7100253	0.238656	0.625178	0.820976
hsa-let-7g-5p	0.946926	14.97011	1.145196	0.284557	0.647706
hsa-let-7d-5p	-0.1593	10.553354	0.026416	0.870888	0.954781
hsa-miR-197-3p	1.519523	9.8423829	1.736972	0.187523	0.558102
hsa-miR-141-3p	-1.29889	10.741446	1.405796	0.235755	0.604689
hsa-miR-16-5p	1.028633	9.5983274	2.064657	0.150749	0.551875

A RT-PCR experiment was designed to test the expression of these six miRNAs in eight control urine samples and eight patient urine samples for subsequent Normfinder program analysis. The program dictates the use of a constant number of control and experimental samples and a minimum of 5 gene candidates to be analyzed. Everything was performed in duplicate instead of in triplicate due to budgetary constraints. It was felt more weight should be given to biological replicates over technical ones in search of possible normalizing microRNAs.[46] Since few PCR reactions were unsuccessful and the quality and number of replicates was satisfactory, missing values were dealt with not by unit imputation but by simple exclusion from downstream analysis. This approach was chosen over the various methods of unit imputation so as not to inflate or unjustifiably skew the stability value for our normalization factor.[46] The least variable three genes were found to be miR-20a-5p, miR-let7g-5p, and miR-let7d-5p, in that order. Thus, for all subsequent validation RT-PCRs, a geometric mean of these three genes was used to generate a ΔCt.

Table 5: Normfinder Stability Values

Gene name	Stability value
20a-5p	0.008
let7g-5p	0.013
let7d-5p	0.016
16-5p	0.017
141-3p	0.020
197-3p	0.021

Normalizing to small RNA concentration therefor further reduces the error due to variable sample size. It must be noted however that normalizing to sRNA concentration instead of total RNA concentration produced data that reflects the concentration of single miRNAs compared to the whole miRNA population, essentially a ratio, and will hide the fact that each sample might have different overall miRNA expression levels. However, since the Bioanalyzer data provides a measure of overall RNA expression for a wide range of sizes, this did not seem to be a great loss of information. Also, normalization to total RNA was not a more attractive option due to the fact that cell free urine has very little ribosomal RNA and other species present in the urine are expressed at comparatively low levels and are otherwise uncharacterized in terms of expression.[33]

Why Normfinder

The apparent difference in gene expression between two samples for a given gene as assessed by RT-PCR is a combination of two values. These are the actual biological difference in expression and a sum of confounding factors that result in non-specific variation such as

extraction yields, differences in enzymatic activity, and input variation between technicians. Normalization is meant to eliminate as much of these non-specific effects as possible, but which normalization method is best is often in dispute. The use of endogenous reference genes is currently the favorite when considering microRNA assays. However, this method presents a special challenge when working on miRNAs present in the urine. A good reference gene is both stably expressed between patients and controls and is also of a character so as to best represent the biological context of the target genes, in this case microRNAs.[41] In the past, a favorite control has been RNU48, a snoRNA that has been demonstrated to be present in significant amounts the urine. However, this candidate falls short on the above two points as it has been demonstrated to vary to an unacceptable degree under different experimental conditions and it is not a miRNA. Therefore, we determined that new endogenous controls were needed. However, how can a candidate for normalization be evaluated if there does not exist a reliable method to normalize the candidate? The Normfinder program represents a user friendly, excel based version of an algorithm developed to assess the stability of a set of candidate genes and produce the best possible combined normalization factor should no single gene be suitable. This is usually the case for fine measurement required of validation of microRNA expression via qRT-PCR where differences of 2 or 3 fold are considered to be significant.

Normfinder was chosen over other such programs because the authors demonstrated that their model based approach is not susceptible to bias related to the co-regulation of normalization candidates in the way that the pair-wise comparison approach is.[44] In order to evaluate the systemic error introduced by the use of a particular gene as a normalizer, the program uses a linear mixed effects model where overall variation of the candidates and the overall variation between sample groups is taken into account. The intergroup and intragroup variation are then

combined into a single value by which the candidate reference genes are ranked. This advantage is of particular interest to miRNA studies because the relationships between microRNAs are difficult to predict and have been shown to change confusingly in different contexts and in different tissues. Also, the rate limiting nature of the miRNA processing machinery could have confounding effects on miRNA expression ratios that could resemble co-regulation, particularly since many miRs are processed from a single precursor transcript, but differ in amounts of final mature miR product due to differential processing. This may be especially true of prostate cancer where the loss of Dicer1 is a common hallmark. This might threaten the integrity of a normalization factor derived by a pair-wise comparison approach. For these reasons, it is this author's opinion that co-regulation between individual miRNA's is difficult to predict. Therefore, it may be inappropriate to rely solely on the pairwise comparison approach as advocated by programs such as Bestkeeper to provide an endogenous normalization factor, where even a small degree of co-regulation introduces bias. This discussion is at the forefront of miRNA research as it is possible that standardizing normalization methods could do a lot to resolve some of the ambiguous results between seemingly similar microRNA experiments from the past.

qPCR samples

It has been demonstrated that the non-specific amplification methods used to prepare RNA samples for qPCR analysis have a negative effect on the linearity of the final assay.[57] Considering this, all samples that did not possess a sufficient concentration to meet the empirically derived minimum of 1.5 ng miRNA equivalent/PCR reaction were excluded from the first round of validation (6ul of cDNA are allowed per PCR reaction). This left us with the

following 17 patients and 12 controls in which we tested all thirteen candidate miRNAs identified by the data from RNA sequencing.

Table 6: Samples Used for the First Round of Validation

Sample Name	Stage	miRNA concentration (pg/ul)
11262014-QMA	G6	450.6
09172014	G6	895.6
12042014-EMR	G6	935.1
03082013	G6	323.1
11202014-KAB	G7	269.6
11202014-PYJ	G7	306
12042014-DT	G7	524.6
01222015-DLD	G7	674.2
11262014-CTL	G7	1096
02102015-EWJ	G8	257.3
11262014-WJC	G8	415.3
010812	G9	474
07112013-Pre	G9	225.9
04042013-Pre	G9	796.1
111512-PreB	pCa	287.8
03052013-Post	pCa	7158.4
111612	pCa	13494.5
111512-Pre	Control	222.2
10212014	Control	356.9
07092014-pnp	Control	516.2
07112014- nps	Control	519.4
07152014	Control	719.5
08062013-Post	Control	1292.5
07112014- wps	Control	1606.3
09172014	Control	1693.9
10172014a	Control	1926.4
12162014	Control	2450.3
10242013	Control	5312.6
10232013	Control	532.7

However, in an attempt to strengthen our conclusions about the final assay, the best eight miRNAs from the first round of validation were tested in an additional 10 patients and 6 controls that either did not meet the original concentration criteria or otherwise could not be included in the first round of validation.

Table 7: Additional Samples used for the Second Round of Validation

Patients	Stage	miRNA Concentration (pg/ul)
02102015-WHC	G6	164.2
02052015-RLJ	G6	110.9
12042014-HEW	G6	111.7
10242013	G6	7248.5
03022015-JRD	G7	102.3
12172014a-	G7	173.9
10172014c-	G7	162.2
04192013-2	G7	1166.6
04042013-2	G8	139.4
101112-Pre	pCa	699.1
12192014-51	Control	168.4
09082014-66	Control	102.1
Rhdad	Control	195.5
09032014-66	Control	233.8
09302014-	Control	777.2
08212014-	Control	704.6

In total, our final assessment included 27 patients and 18 controls. When a Gleason score was not available, pCa was used to designate prostate cancer patients.

Accuracy vs Area Under the Curve

Two metrics of evaluation are commonly used to describe the usefulness of a biomarker. The first is the accuracy metric which is obtained simply by dividing the number of accurate classifications by the total number of attempted classifications. The threshold value at which

each marker is evaluated can either be a single critical value consistently applied to all markers under consideration, or the value that produces the highest accuracy for each individual candidate. All of the accuracies reported in this study were produced by this second approach. One drawback to using this metric is that it is less useful for data sets with unevenly distributed values. If one range of values within the data set is more common than others, then a particular classifier may receive a higher accuracy if it correctly classifies the common range of values, but fails to classify the less common ones. This situation would be unacceptable in the clinic, which brings us to our second metric.

The Area Under a receiver operating Curve (AUC) is a metric that is not affected by data skewedness and can be interpreted as the probability that the classifier in question will assign a higher value to a randomly chosen positive instance than to a randomly chosen negative instance. It is a combined metric that is indirectly derived from both the sensitivity and specificity of a binary classification system. Sensitivity can be defined statistically as the chance that a sick individual will be assigned a positive classification by the assay and is represented by the following equation: Sensitivity = (# of true positives)/(# of true positives + # of false negatives). Specificity is defined as the chance that an individual who does not have the disease will be assigned a negative classification and is represented by the following equation: Specificity = (# of true negatives)/(# of true negatives + # of false positives). A ROC curve can be obtained by plotting sensitivity against 1 – specificity for all possible critical values of the classifier in question. The AUC is defined as the area under the resulting curve.[20]

qRT-PCR Results

MicroRNAs from Table C were subjected to qRT-PCR and AUC analysis. All qRT-PCR values are normalized to the global mean of the three normalizers (let 7d, let7g and miR 20a) and recorded as the ΔΔCt. For each miR, individual Ct values from patient and control samples are shown as Box plots (Figures 2-9). ROC curves and box plots are included for eight miRNAs* with the most diagnostic potential as judged by their AUC.

Table 8: Summary of qRT-PCR Results

Gene name	DDCt	P Value	Accuracy	AUC (fitted)
204-5p*	2.348913	0.0146	0.821429	0.756*
205-5p*	3.545608	0.0341	0.75	0.736*
223-3p*	2.565212	0.0800	0.714286	0.688*
199a-3p*	1.804074	0.0973	0.714286	0.637*
223-5p*	1.150305	0.1285	0.714286	0.618*
126-3p*	0.980553	0.231	0.642857	0.638*
143-3p*	1.315572	0.231	0.642857	0.648*
184-5p*	1.509285	0.2919	0.714286	0.599*
146a-5p	0.753938	0.3814	0.678571	0.597
375-5p	1.18963	0.519	0.642857	0.561
135a-5p	0.478416	0.6784	0.607143	0.559
363-3p	-0.16605	0.7125	0.571429	0.509
142-3p	0.430455	0.8538	0.535714	0.536

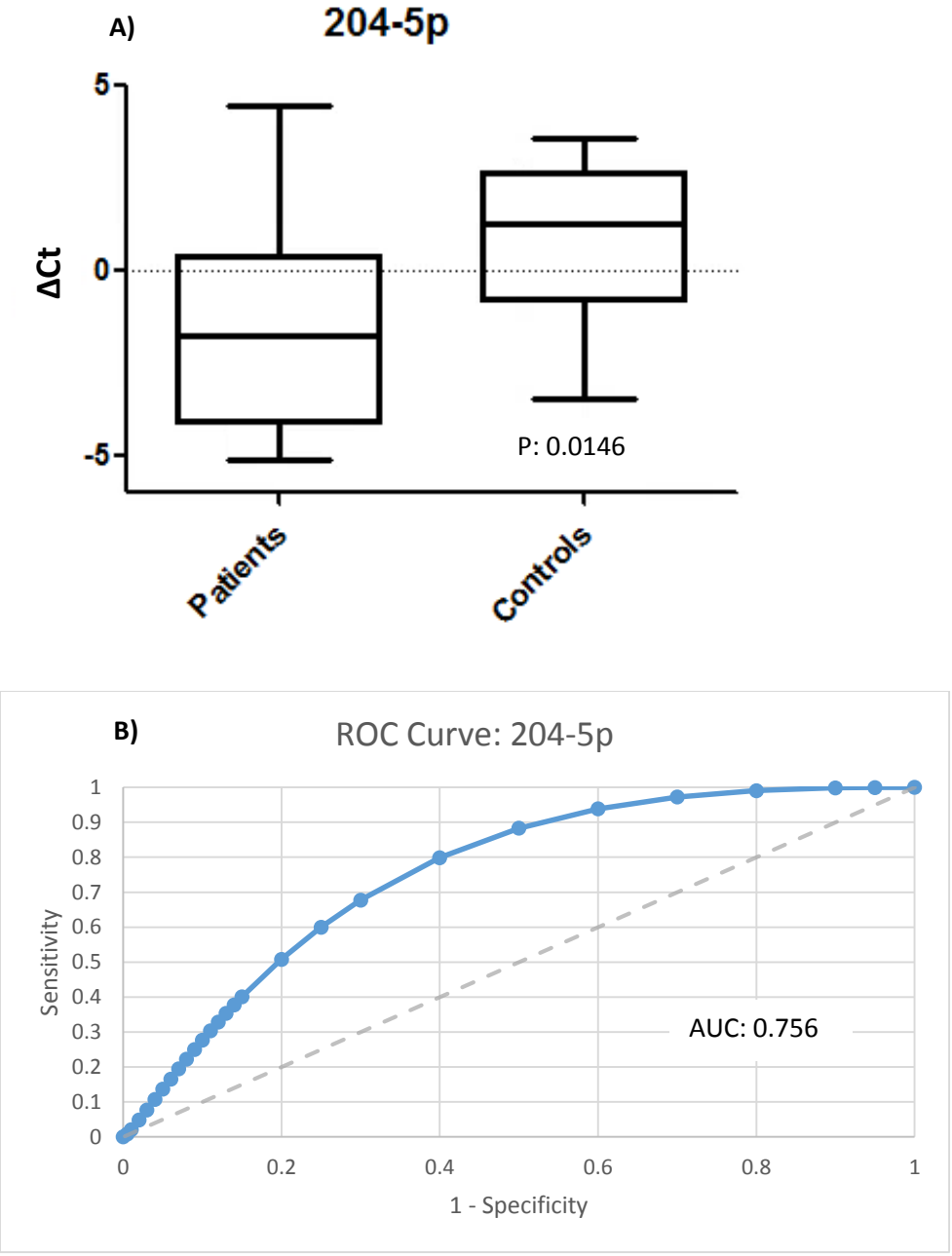

Figure 2: RT-PCR Analysis for miR-204-5p. A) Box plot for miR-204-5p. Center line demonstrates the mean ΔCt while the box's edges demonstrate the second (above) and third (below) quartiles. Whiskers demonstrate the minimum and the maximum. A p-value of 0.0146 demonstrates a statistically significant difference between patients and controls. B) ROC curve

for miR-204-5p. An AUC of 0.756 demonstrates a diagnostic potential superior to the PSA blood test (AUC = 0.678[103]).

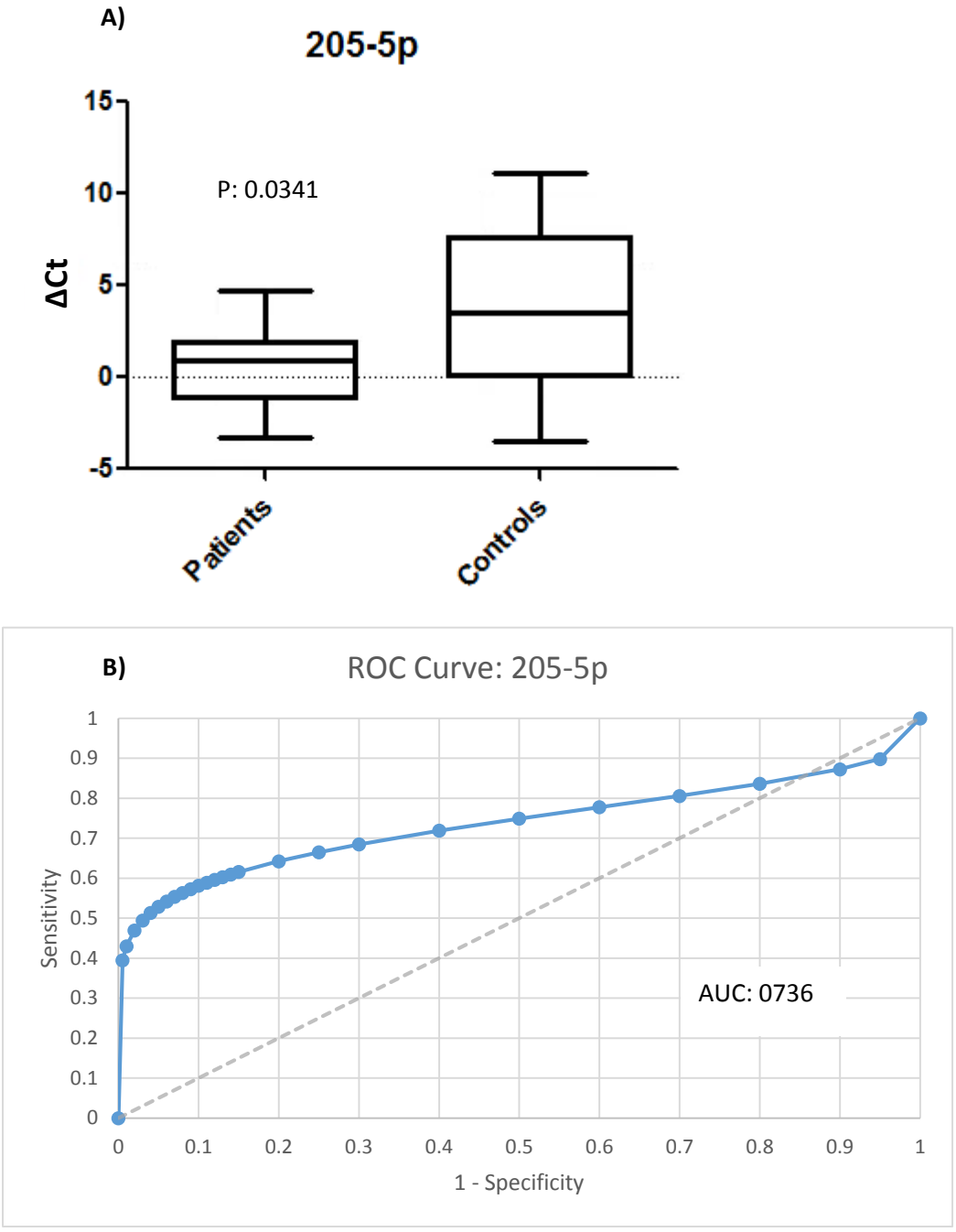

Figure 3: RT-PCR Analysis for miR-205-5p. A) Box plot for miR-205-5p. Center line demonstrates the mean ΔCt while the box's edges demonstrate the second (above) and third (below) quartiles. Whiskers demonstrate the minimum and the maximum. A p-value of 0.0341 demonstrates a statistically significant difference between patients and controls. B) ROC curve

for miR-205-5p. An AUC of 0.736 demonstrates a diagnostic potential superior to the PSA blood test (AUC = 0.678[103]).

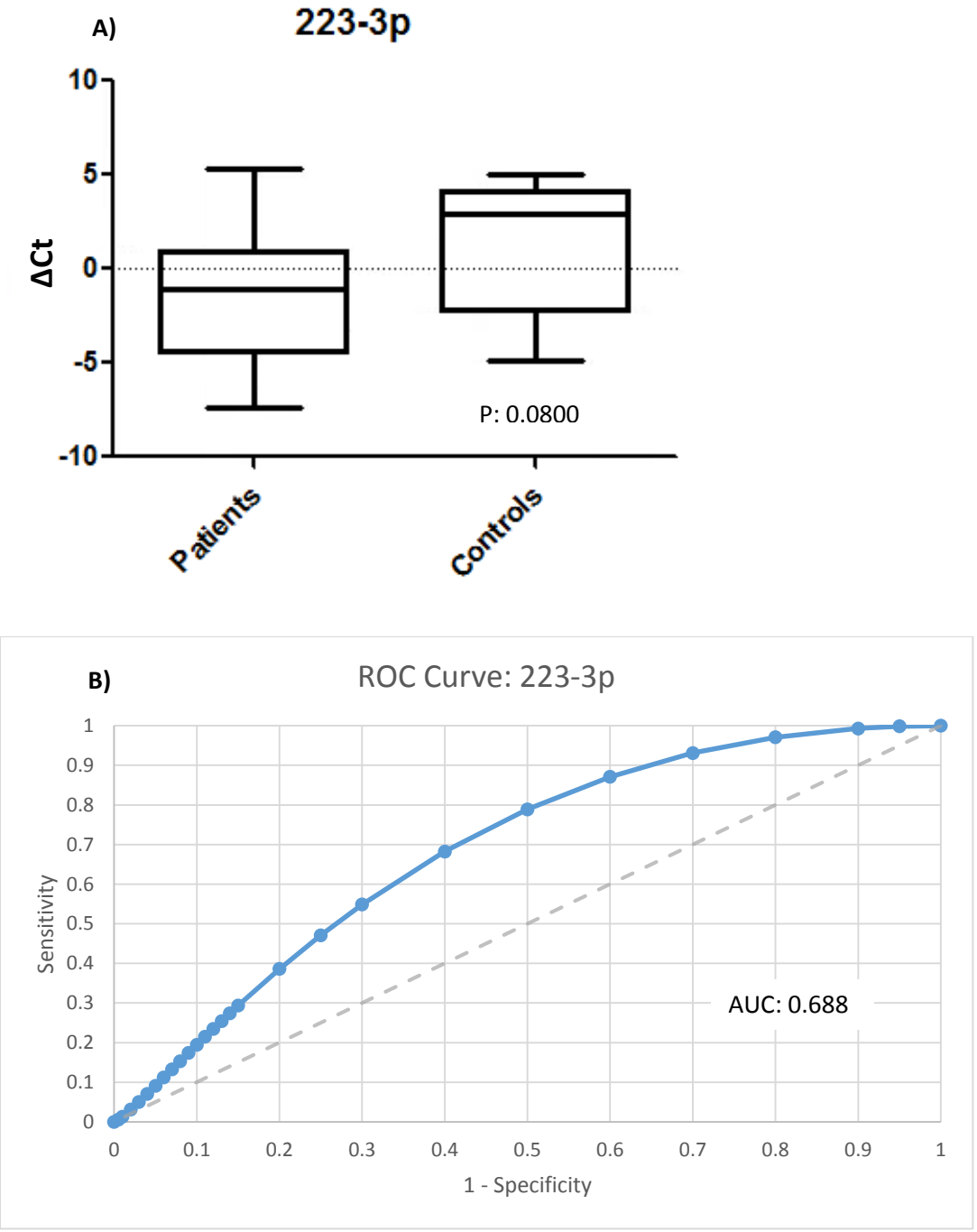

Figure 4: RT-PCR Analysis for miR-223-3p. A) Box plot for miR-223-3p. Center line demonstrates the mean ΔCt while the box's edges demonstrate the second (above) and third (below) quartiles. Whiskers demonstrate the minimum and the maximum. A p-value of 0.080 demonstrates an almost statistically significant difference between patients and controls with

only 28 samples. B) ROC curve for miR-223-3p. An AUC of 0.688 demonstrates a diagnostic potential slightly superior to the PSA blood test (AUC = 0.678[103]).

Three miRNAs miR-204-5p, miR-205-5p, and miR-223-3p (Box plots Figure C-H) display relevant dysregulation of expression comparing patients to controls. More importantly, these three miRs demonstrate a larger AUC value than the PSA blood test (0.756, 0.736, and 0.688 vs 0.678[103] respectively), suggesting that they perform better in terms of specificity and sensitivity as a diagnostic marker than the current PSA blood test.

However, 5 others (Figures 5-9) miR-199a-3p, miR-223-5p, miR-126-3p, miR-143-3p, and miR-184-5p all demonstrate some dysregulation by box plot analysis and AUC values greater or equal to 0.60, suggesting that they too have significant diagnostic value despite their lack of statistical significance within this small sampling group.

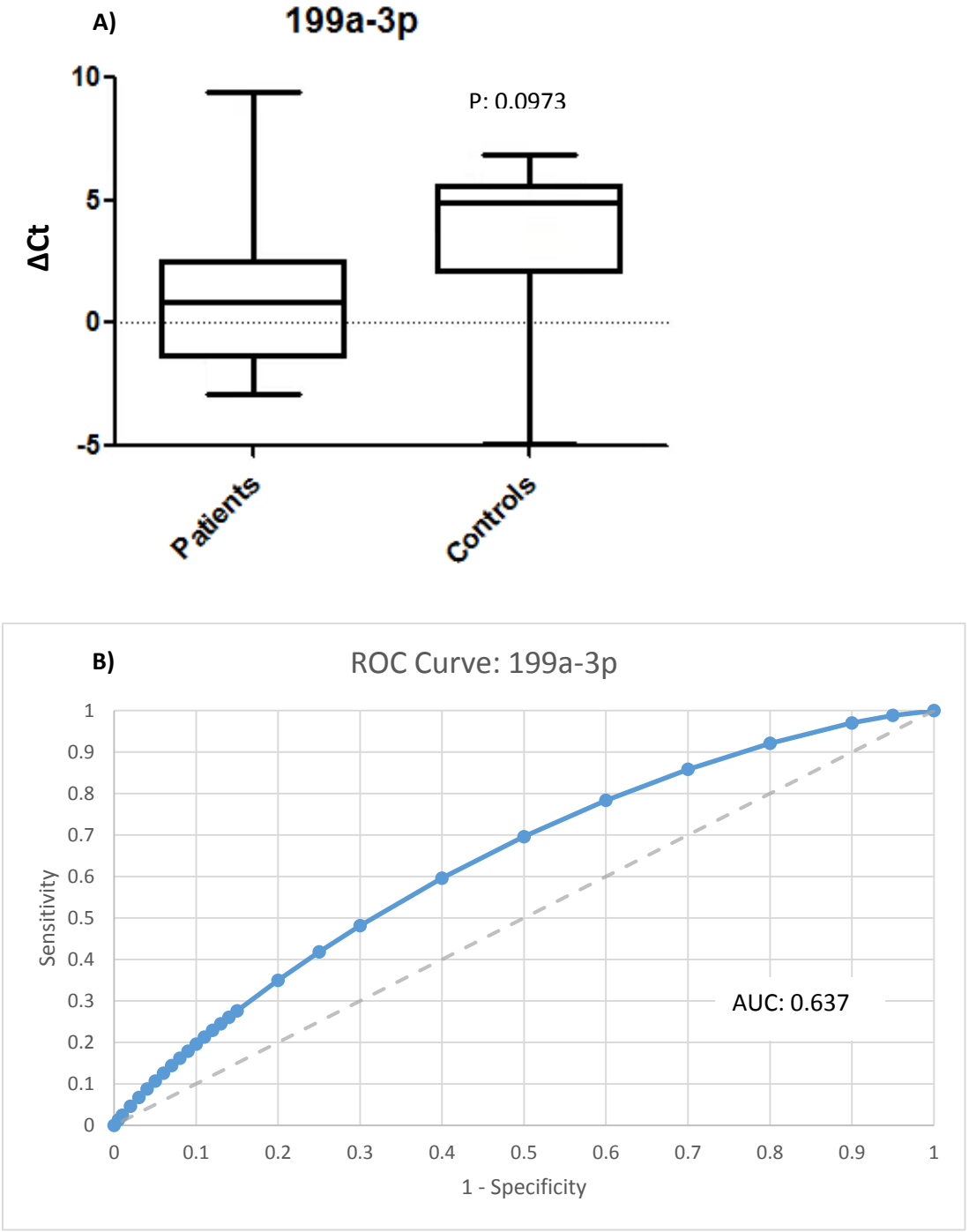

Figure 5: RT-PCR Analysis for miR-199a-3p. A) Box plot for miR-199a-3p. Center line demonstrates the mean DCt while the box's edges demonstrate the second (above) and third (below) quartiles. Whiskers demonstrate the minimum and the maximum. A p-value of 0.0973

demonstrates an almost statistically significant difference between patients and controls with only 28 samples. B) ROC curve for miR-199a-3p. An AUC of 0.637 demonstrates a diagnostic potential comparable to the PSA blood test (AUC = 0.678[103]).

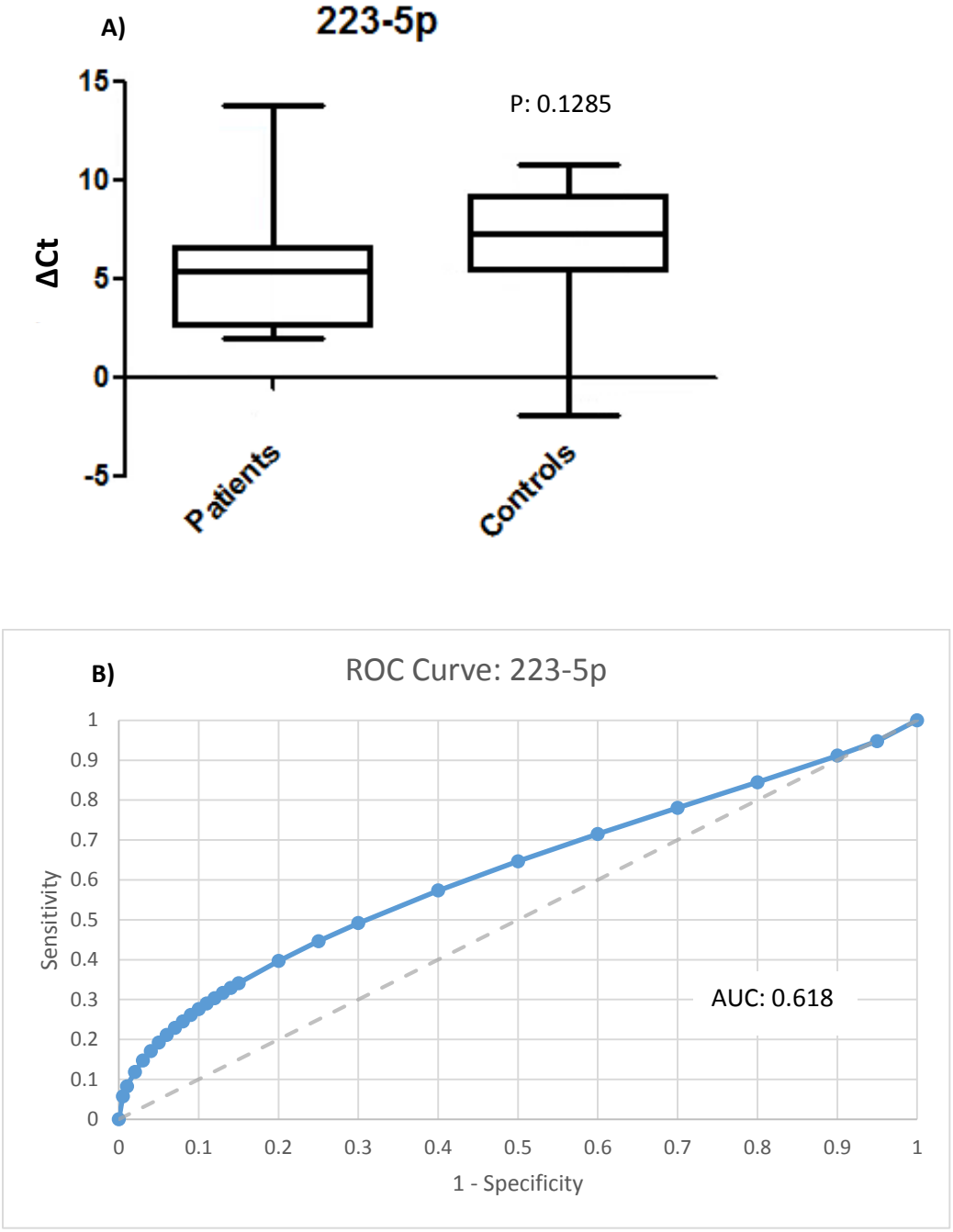

Figure 6: RT-PCR Analysis for miR-223-5p. A) Box plot for miR-223-5p. Center line demonstrates the mean ΔCt while the box's edges demonstrate the second (above) and third (below) quartiles. Whiskers demonstrate the minimum and the maximum. A p-value of 0.1285 demonstrates an almost statistically significant difference between patients and controls with

only 28 samples. B) ROC curve for miR-223-5p. An AUC of 0.618 demonstrates a diagnostic potential comparable to the PSA blood test (AUC = 0.678[103]).

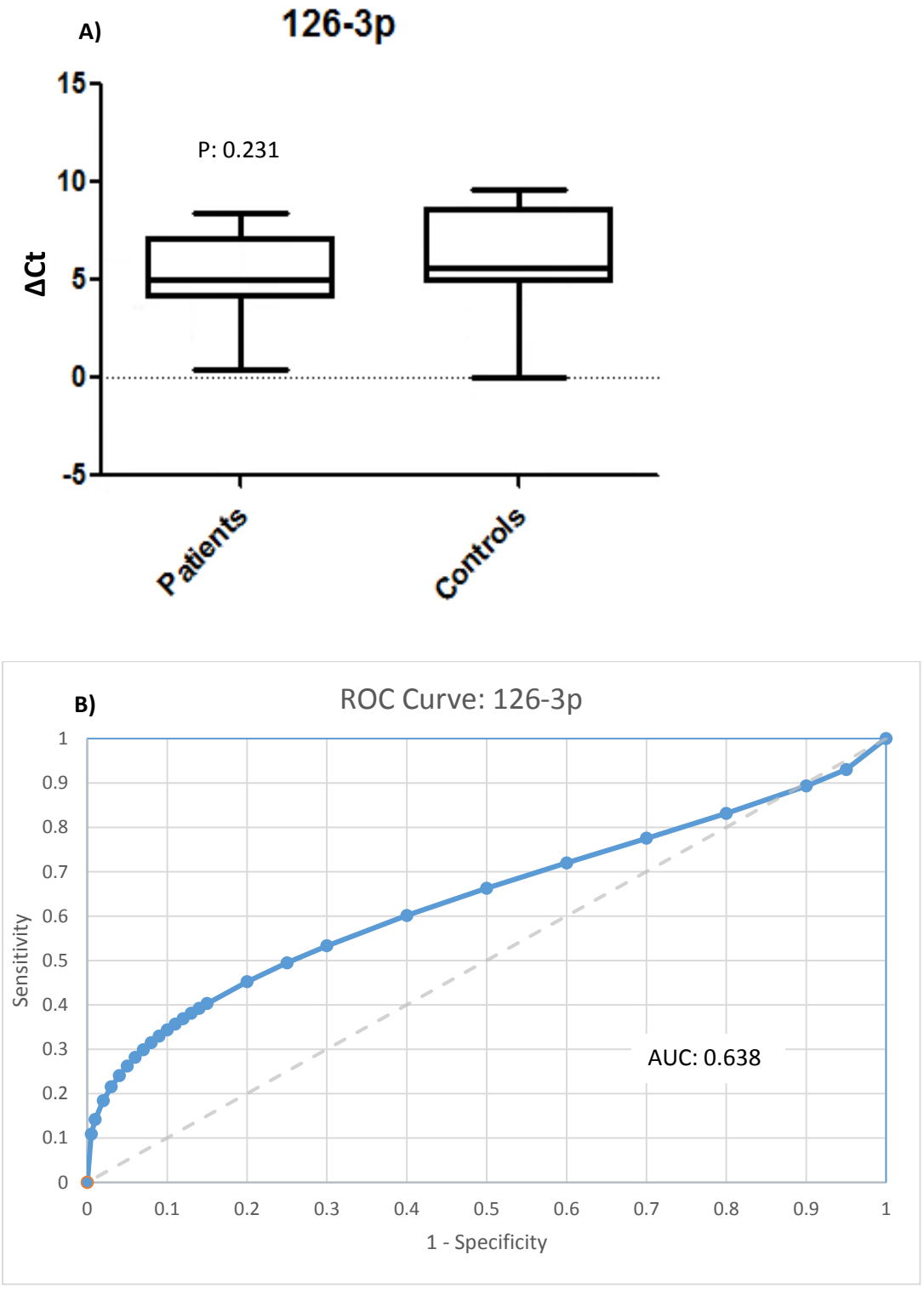

Figure 7: RT-PCR Analysis for miR-126-3p. A) Box plot for miR-126-3p. Center line demonstrates the mean ΔCt while the box's edges demonstrate the second (above) and third

(below) quartiles. Whiskers demonstrate the minimum and the maximum. A p-value of 0.231 does not demonstrate a statistically significant difference between patients and controls within the primary 28 sample group. However, an expansion of sample group size to 45, as described above, may reveal a more significant difference. B) ROC curve for miR-126-3p. An AUC of 0.638 demonstrates a diagnostic potential comparable to the PSA blood test (AUC = 0.678[103]).

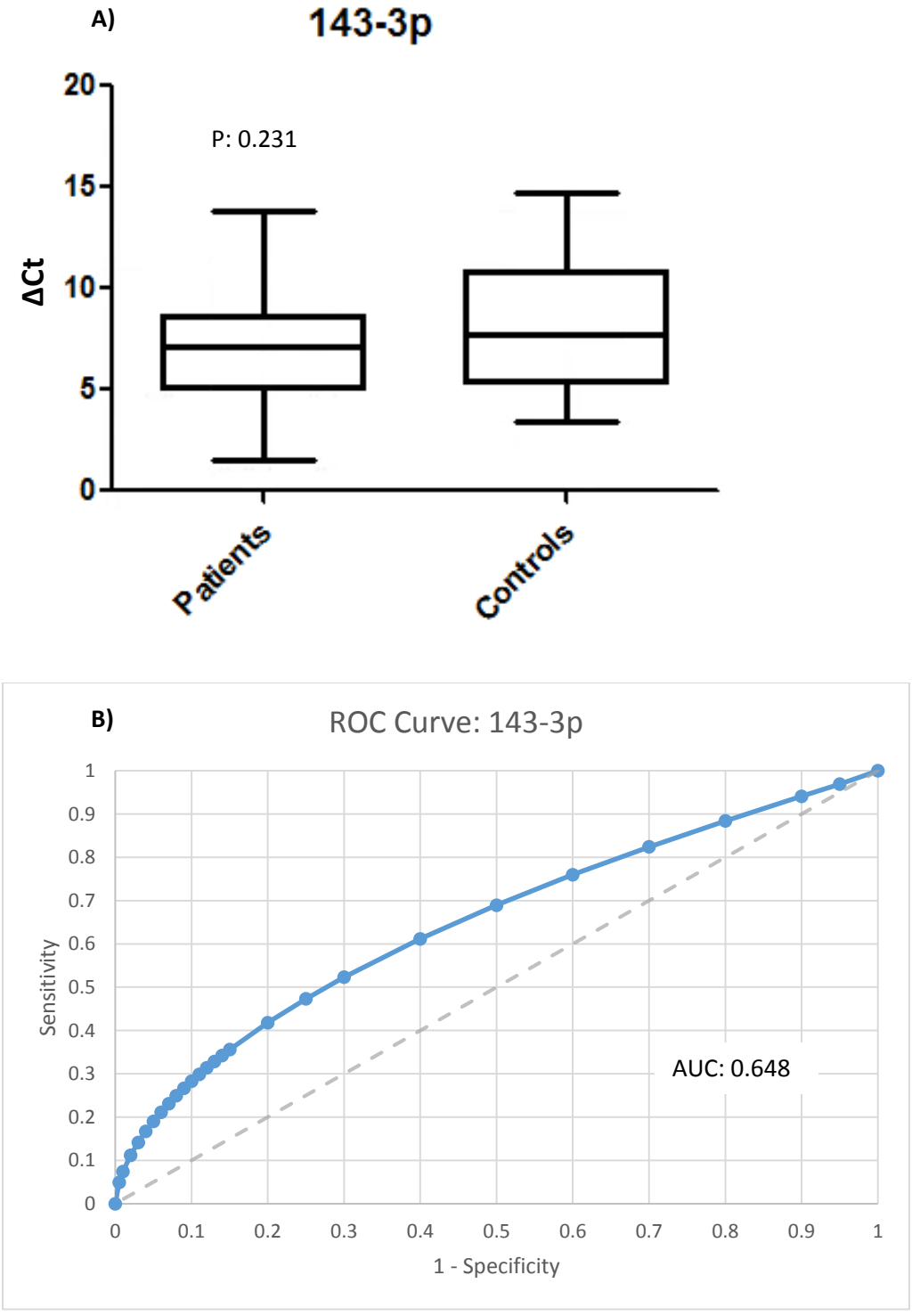

Figure 8: RT-PCR Analysis for miR-143-3p. A) Box plot for miR-143-3p. Center line demonstrates the mean ΔCt while the box's edges demonstrate the second (above) and third

(below) quartiles. Whiskers demonstrate the minimum and the maximum. A p-value of 0.231 does not demonstrate a statistically significant difference between patients and controls within the primary 28 sample group. However, an expansion of sample group size to 45, as described above, may reveal a more significant difference. B) ROC curve for miR-143-3p. An AUC of 0.648 demonstrates a diagnostic potential comparable to the PSA blood test (AUC = 0.678[103]).

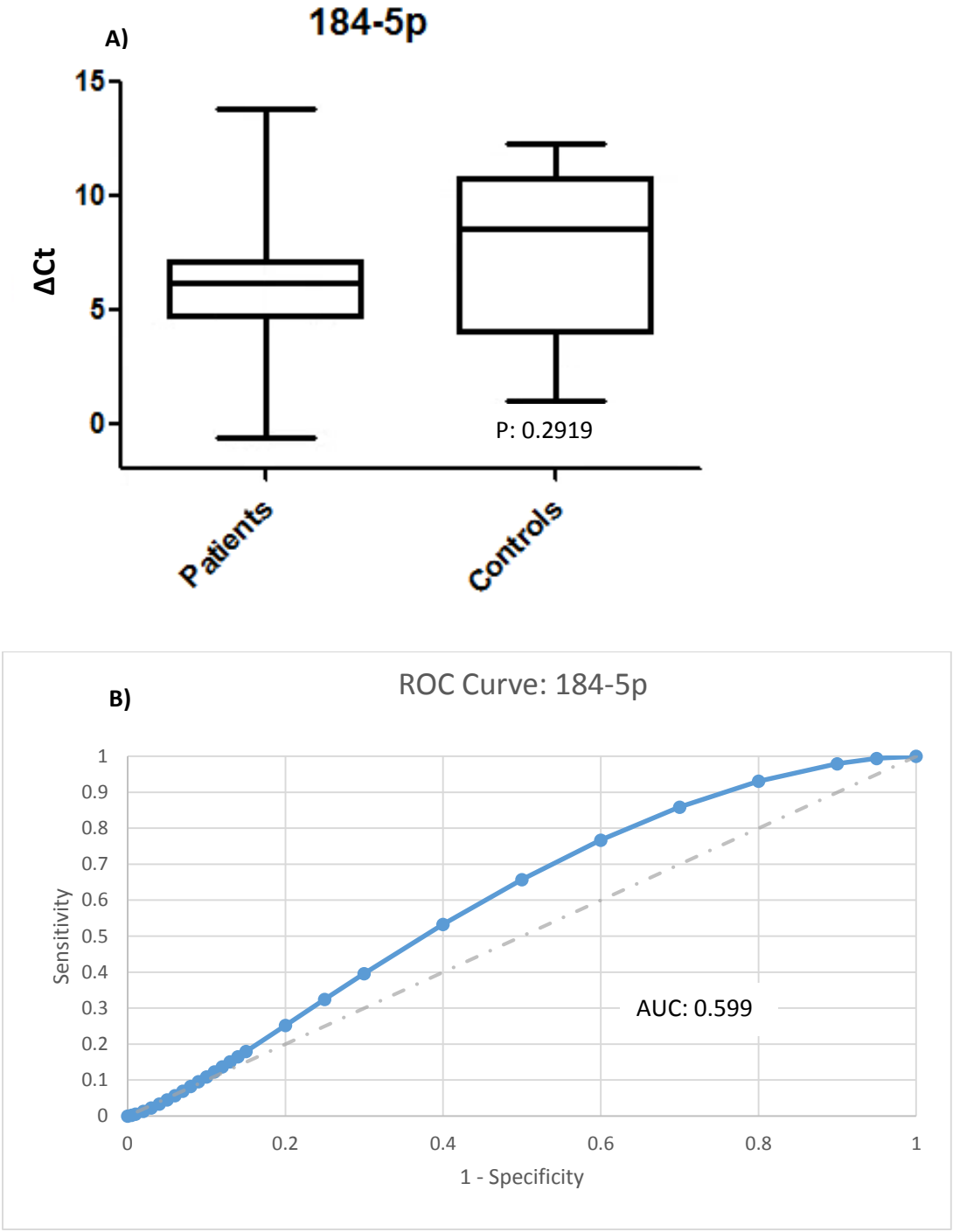

Figure 9: RT-PCR Analysis for miR-184-5p. A) Box plot for miR-184-5p. Center line demonstrates the mean ΔCt while the box's edges demonstrate the second (above) and third (below) quartiles. Whiskers demonstrate the minimum and the maximum values. A p-value of

0.2919 does not demonstrate a statistically significant difference between patients and controls within the primary 28 sample group. However, an expansion of sample group size to 45, as described above, may reveal a more significant difference. B) ROC curve for miR-184-5p. An AUC of 0.599 demonstrates a diagnostic potential comparable to the PSA blood test (AUC = 0.678[103]).

It was hypothesized that the diagnostic power of a combined assay could be more significant than any single miRNA on its own. A threshold value was determined by hand for the 8 most significant miRNAs that would most accurately segregate patients and controls. Then, each patient or control sample received a numerical classification 1-6 representative of the number of miRNAs out of the top eight for which it showed expression above that threshold. Having 4 points out of 6 (5 miRNAs out of 8) resulted in a positive classification while 3 points and below resulted in a negative classification. The compiled AUC for this combinatorial group of eight is shown in Figure S and final assay statistics in Table I (below).

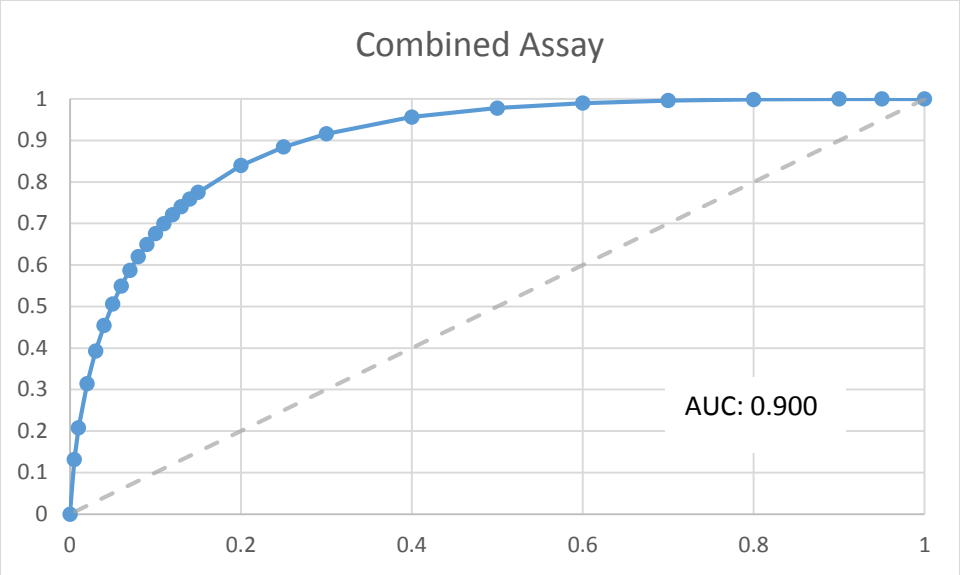

Figure 10: The combined assay**.** A combined assay, based on the number of miRNAs with in each individual sample to reach an empirically defined threshold value, produced an AUC of 0.900, demonstrating a diagnostic potential remarkably superior to the PSA blood test (AUC = 0.678[103]).

Table 9: Final Assay Statistics

Number of Cases	28
Number Correctly Classified	23
Accuracy	82.10%
Sensitivity	93.30%
Specificity	69.20%
Positive Cases Missed	1
Negative Cases Missed	4
Fitted ROC AUC	0.900
Empiric ROC AUC	0.885

It can be seen here in this final combined assay that the specificity and the sensitivity of miRNAs biomarkers is additive and superior to that of PSA. This demonstrates that miRNAs, which have been repeatedly demonstrated to be more powerfully correlated to the cell state than any other biological molecule, are the perfect candidates to make up for PSA's poor characteristic as a biomarker.

Discussion

The Assay

There is no question that overall, PSA screening has had a positive effect on public health. However, considering the effects of over-diagnosis, the high risk of false positives, the potential for over treatment of indolent disease, and the crucial age dependence of PSA screening's harm/benefit ratio, screening has the potential to do more harm than good for certain cadres of patients. This negative harm/benefit ratio is a direct result of the weak diagnostic power of the PSA test itself and the fact that almost all prostate cancers are aggressively treated once diagnosed, no matter the co-morbidities that might be present in its carrier.[67]

Here, we have presented a urinary diagnostic test that is superior in terms of specificity and sensitivity to the PSA blood test. The novel approach utilized in this study was the use of an additive threshold model based on the expression of multiple miRNAs. Since this test only incorporates a handful of miRNAs and there are 2588 miRNAs currently included in miRBase v21, this concept has an almost endless potential for sophistication. In the future, it is anticipated

that expanding the diagnostic panel with more appropriate miRNAs will allow us to differentiate between different strata of patients as well as other genitourinary pathologies.

The truly amazing thing about this additive risk model is that on their own, only two of these eight miRNAs would show a diagnostic potential comparable to PSA, but cumulatively, they are in fact superior. This final result demonstrates two things: that whole miRNA profiles are powerfully correlated with the cell state and that the urine is especially enriched for miRNAs from the prostate.

Contemporary Attempts at a Urinary Test for pCa

Although many urine biomarkers have been proposed and investigated, very few have ever made it to the clinic. The three most promising biomarkers currently in development are urinary PC3, urinary detection of LOH, urinary TMPRSS2:ERG fusion proteins, and combinations thereof. In the clinical study submitted for approval to the FDA for the use of PCA3 urinary mRNA based prediction of prostate cancer, urinary PCA3 had an AUC of 0.68 compared to serum PSA's AUC of only 0.52. Moreover, a different researcher reported that urinary PCA3 has no ability to differentiate aggressive from indolent disease.[37] A study assessing the sensitivity of LOH detection in the urine of prostate cancer produced a sensitivity of 87% between patients and non-patients. However, it did not fare so well in terms of specificity resulting in no report of an AUC. The most common genomic alteration in prostate cancer, occurring in up to 50% of tumors, is a fusion between the ERG proto-oncogene and the prostate specific, androgen related gene TMPRSS2.[8] Of all contemporary assays being investigated, a TMPRSS2:ERG PCA3 combination urine test is the most likely to become clinically relevant in the near future and it boasts diagnostic potential comparable to the PSA blood test and an AUC of 0.66.[37]

As our results demonstrate, our miRNA assay has superior attributes in all categories to contemporary assays. However, I also believe that miRNA panels have the most potential for improvement. Utilizing a panel of body fluid biomarkers in combination with other diagnostic factors is the most likely approach to become clinically relevant, as no single biomarker candidate has been identified with acceptable qualities for use a single factor biomarker for any disease.[19, 20] A multivariate approach is the only way that a circulating biomarker will ever have the specificity to differentiate between the different prostate pathologies, different stages of prostate cancer, cancers of different origins, and account for outliers. The advantage to exploring miRNAs as relevant biomarkers comes from their large numbers and superior association with the cell state.

The Urinary Panel

The follow is a summary of the possible roles that the members of the urinary panel might play in prostate cancer. Information on the expression of these miRNAs in the prostate cancer cell line progression model and the tumor versus match normal epithelium (TGCA) analysis as described in chapter two have been incorporated for the sake of interpretation.

Hsa-miR-204-5p

The analysis of NGS sequencing data demonstrated that this miRNA was downregulated in the urine of patients as opposed to controls by -2.29 fold with a P value of 0.017. This expression trend was validated by qRT PCR analysis and was found to be the most powerful, individual diagnostic factor identified in this study. This miRNA was also found to be downregulated in tumors as opposed to matched “normal” stroma by -0.82 fold with a P value of 0.00093 in the TGCA analysis. However, this miRNA was not found to be significantly different

in the comparative P69 vs. M12 sequencing analysis described in Chapter 2. Microarray profiling of gastric tumors and surrounding stroma identified miR-204-5p to be the most powerfully under-expressed of all the miRNAs tested. Its absence was demonstrated to support anti-apoptotic pathways by allowing the overexpression of bcl-2, one of its direct targets. Ectopic expression of miR-204-5p inhibited colony forming ability, migration, and tumorigenicity of gastric cancer cells as well as making them more susceptible to the effects of apoptosis inducing chemicals.[106] Another study demonstrated that miR-204-5p had a tumor suppressor effect on four prostate tumor cell lines, LNCaP, PC3, VCaP, and NCI H660 via its ability to target the classical oncogene c-MYC.[105]

Hsa-miR-205-5p

The analysis of the NGS data demonstrated that this miRNA was upregulated in the urine of patients as compared to controls by 2.80 fold with a P value of 0.011. However, this miRNA was found to be downregulated in tumors as opposed to matched normal stroma by -1.93 fold with a P value of 1.87E-15 in the TGCA analysis. In the cell progression model, the expression of miR-205-5p mirrors that of the miR-200 family, supporting the many existing reports that these miRNAs directly coordinate their effects on the EMT transition and the expansion of tissue stem cell populations via the suppression of N-cadherin, and the SNAI1/2 and ZEB1/2 transcription factors.[9] This miRNA's well established role as a tumor suppressor suggests that its increased presence in the urine could be a result of an effort of tumor cells to suppress miR-205-5p by dumping it into the surrounding extracellular matrix with eventual exclusion into the urine. Some of its other validated targets include, C-epsilon, MED1, and SHIP2, the last of which plays a critical role in Akt mediated survival, a pathway central to prostate cancer progression.[97]

Hsa-miR-223-3p and hsa-miR-223-5p

The expression of miR-223 was originally discovered as part of the myeloid differentiation pathway where its expression was found to be activated by the myeloid transcription factors NFIA, PU.1, and C/EBPalpha.[98] The overexpression of miR-223 has been observed in blood as well as the T-lymphocytes of people suffering from pathological immune disorders such as systemic lupus and rheumatoid arthritis.[104] miR-223 overexpression has been demonstrated to play a role in multiple solid tumors and leukemias including hepatocellular carcinoma, ovarian cancer, prostate cancer, CLL, ALL, and AML, although its roles in solid tumors and leukemias are likely to be different.

The tumorigenic effects of inflammation have long been recognized.[4] Due to its critical role in hematopoiesis, the overexpression of this miRNA in solid tumors is likely to reflect a recruitment of immune cells to the pro-tumorigenic microenvironment. The analysis of the NGS data demonstrated that miR-223-3p was upregulated in the urine of patients as opposed to controls by 5.94 fold with a P value of 5.58E-05 and that miR-223-5p was upregulated in the urine of patient as opposed to controls by 5.96 fold with a P value of 0.000245. However, neither arm of this miRNA was found to be significantly different in the TGCA analysis or in our cancer cell line progression model. This suggests that the presence of this miRNA has something to do with the presence of tumor associated immune cells, in agreement with the studies reported above.

Some specific targets of miR-223-5p includes mRNA transcripts that contain AU-rich elements such as those encoding RhoB and the FBXW7 protein, which normally represses cyclin E activity.[98] Also, before invading other tissues, prostate cancer almost always metastasizes to

bone, and when it does so, it adopts an osteomimetic phenotype. It is worth noting that miR-223-5p expression represses the differentiation of osteoclast precursors and is thought to be a potential systemic target for bone metastatic disorders.[98] One study has found that miR-223-3p was significantly overexpressed in other prostate cancer cell lines where it was found to support anti-apoptotic pathways, migration, and invasion by targeting the tumor suppressor SEPT6.[104]

Hsa-miR-199a-3p

The analysis of the NGS sequencing data demonstrated that this miRNA was upregulated in the urine of patients as opposed to controls by 4.88 fold with a P value of 0.00063. This miRNA was also found to be significantly upregulated by a fold change of 3.08 with a p-value of 0.00281 in the M12 cells compared to the P69 cells, despite the fact that one of its two loci lies on the short arm of chromosome 19, a chromosomal area lost in the M12 cell line. It is also upregulated 6.24 fold in the miR array screen of M12s compared to p69s. Perhaps this upregulation is the result of the loss of some trans regulation between the two copies of miR-199a and other members of its cluster. miRNA microarray expression profiling has shown miR-199a-3p to be one of the most significantly overexpressed miRNAs in invasive squamous cell carcinomas and cervical cancer cell lines, along with 199a-5p, 199b-3p, and 199b-5p.[99] miR-199a-3p is of particular interest to prostate cancer due to prostate cancer's propensity for invading bone tissue. This miRNA is specifically expressed in the skeletal system where it is known to inhibit chondrogenesis in response to activation by Twist-1 by targeting Smad1, a central regulator of bone and cartilage formation.[99] NKX3.1, one of the central proteins governing prostate differentiation and growth, acts as a haplo-insufficient tumor suppressor

targeting twist and is seen to be down-regulated early in prostate cancer progression.[28] It's loss could result in increased levels of Twist, which leads to the increased activation of this locus.

Hsa-miR-126-3p

The potential targets of this miRNA were discussed previously. However, it is worth noting that miR-126-3p was found to be upregulated in the metastatic M12 cell line by 1.792786 fold with a p-value of 0.0065. Similarly, another group recorded the over expression of this miRNA in another metastatic cell line, but not in the non-metastatic cell lines that it investigated.[104] In the future, this miRNA could help investigators differentiate between metastatic and localized prostate cancer. However, this miRNA was not found to be significantly dysregulated in the TGCA sequencing analyses.

Hsa-miR-143-3p

The analysis of the NGS sequencing data demonstrated that this miRNA was upregulated in the urine of patients as opposed to controls by 3.96 fold with a P value of 0.0036. It has been established that miR-143 originating from normal prostate epithelia actively inhibits nearby prostate cancer cell proliferation.[11] However, differences in expression of this miRNA were not found to be significant in the TGCA analysis or in our cell line progression model. Although its tumor suppressor effects remain a mystery, miR-143-3p is known to be a central player in the determination of cardiac progenitor cells and smooth muscle cells through the targeting of various transcription factors including nkx2-5, klf4, and elk-1. Perhaps underexpression of miR-143-3p functions to facilitate dedifferentiation.

Hsa-miR-184-5p

The analysis of the NGS sequencing data demonstrated that this miRNA was upregulated in the urine of patients as opposed to controls by 5.86 with a P value of 0.005. It was similarly upregulated in the M12 cells by 3.09 fold with a p-value of 0.0014 and 3.077-fold in the miR array screens, but interestingly was not found to be significantly different in the TGCA analysis. Several targets of miR-184-5p have been validated including the regulators of neurological development and apoptosis, perhaps explaining its tumor suppressor-like behavior in ectopic expression experiments involving cell lines. One of miR-184-5p's targets of particular interest to prostate cancer is Akt2, a central effector of the PI3K pathway. Since this pathway is critical to prostate cancer progression, it would make more sense to see this miRNA suppressed rather than upregulated in our cell lines and urine analysis. Perhaps its presence in the urine reflects an effort of tumor cells to actively pump this miRNA out of their cytoplasm or an attempt by the surrounding normal prostate tissue to maintain tissue architecture. It's over expression in the M12 cell line, our most aggressive and fastest growing cell line, can be explained by the fact that this miRNA's locus is directly activated by the classic oncogene cMYC.[102] Given the established tumor suppressive activity of miR-184-3p, it is likely that its presence is the unintended result of activation of this oncogenic pathway in the M12 cell line.

The Question of Normalization for a Clinical Assay

The problem of proper normalization across various urine samples extends to any potential clinical biomarker assay that may arise from this type of work. This could make developing an inexpensive and quick assay difficult. One way in which this hurdle could be overcome is with the concept of in situ normalization as developed by Stahlberg et al. In this

method, in place of a classical endogenous control, a gene is chosen that is known to be either correlated or anti-correlated with the gene of interest for normalization. While this does not really allow for the comparison between samples, it is a powerful method for the detection of diseases where the ratio between multiple factors is a significant marker.[41] This technique is perfect for the application of microRNA expression data. One such relationship has already been reported in a previous study: the inverse relationship of miR-141-5p and 21-5p. Due to our use of endogenous controls, we have inadvertently demonstrated that the ratio between the members of the biomarker panel that we have identified and the endogenous controls used for normalization correlates very powerfully with the presence of prostate cancer. A modified version of our normalization protocol may serve as a quick and effective normalization method for a usable clinical assay.

How miRNAs might get into the Urine and the Potential for Outliers.

In developing a highly specific and sensitive assay, all possible sources of miRNAs, prostate derived or otherwise, need to be thoroughly considered in order to accurately interpret the urinary miRNA profile and to account for possible patient outliers.

Firstly, it has been established that there is a natural level of leakage from the healthy prostate into the urine via the ducts of the prostatic urethra. Prostate epithelium and cellular materials are constantly being shed into this compartment, especially in response to physical manipulation by the physician.[37] Under pathological conditions, this contribution might be increased. For instance, the distensible nature of the glandular system of the prostate is what allows for it to store seminal fluid for later ejaculation.[5] The growth of a solid tumor within the

confines of the prostate could compromise the tissue's ability to store seminal fluid and could result in an enhanced leakage of prostatic materials into the urethra, which is then swept away by the urine as it passes. In the later stages of disease, as the tumor becomes more advanced, it may deteriorate the integrity of the glandular structure entirely. Different levels of structural integrity between advanced and early stage patients could stratify patients into different overall strata of profiles.

Secondly, It has been established that circulating miRNAs bound to proteins or sequestered within exosomes can be delivered to the kidneys and excreted via the urine, although the portion of these present in the urine of either healthy or diseased persons has yet to be analyzed.[31] It also has yet to be investigated whether some miRNAs are transported more easily than others, either based on sequence or type of packaging. One source of outliers could be a decrease in kidney function related with age. Since there is a high concentration of miRNAs in the blood, it is possible that age related leakage of miRNAs into the urine from the blood could confound a urinary assay if not properly considered. Thirdly, if a patient's tumor has invaded the bladder or urethra through the smooth muscle of the urethral sphincter, his miRNA profile will be drastically different from a localized cancer that is restrained to the prostate. Although this is rare and requires a tumor to be advanced, it has been observed clinically.[5] Small penetrations of carcinoma through the adipose and fibrous tissue and into the capsule of the neurovascular bundle of the prostate are more common however.

Lastly, the largest source of miRNAs present in the healthy urine is from dying renal and urethral cells.[31] One potential source of outliers could be the existence of urinary tract infections, more common to catheterized men. This could affect the miRNA profile through the activation of an immune response or through an alteration of desquamation in urinary tract cells. It is also

hypothesized that the presence of a catheter itself could alter the normal microflora of the distal urethra or that some men are just naturally predisposed to the presence or absence of specific bacterial species that cause different immune phenomena, like what is seen in the gastrointestinal tract. Both of these could affect the standing equilibrium of the mucosal immune response, which could in turn affect the miRNA content of the urine. The decision by our group to analyze the cell free compartment of the urine should, in theory, reduce the extremity of any outliers produced in this way by removing a large portion of miRNAs contributed by activated whole cells.

Thoughts for the Future

Indolent vs. Aggressive forms of Disease

Most often, prostate cancer is present in aged men in an indolent, latent form. Due to the slow growing nature of these tumors, they are not usually the cause of death for these patients. Because almost all positive diagnoses are followed by aggressive treatment, the inability to distinguish latent and aggressive disease has led to over diagnosis and over treatment of non-threatening prostate cancers.[12] Over-diagnosis is defined by many studies as the detection of a cancer that would otherwise go undetected throughout the lifetime of the patient. One of these studies estimated that over-diagnosis could be as high as 66% in the United States.[67] Identifying a microRNA signature that could help differentiate between these forms of the disease could help identify cancers that are likely to stay slow growing and localized and cancers that are likely to become a threat to life. An advancement in this area could help improve quality of life for patients who receive a positive diagnosis in their 70s or later.

As a primitive example, it has been previously described that in the serum of early prostate cancer patients, levels of circulating miR-21 are elevated while levels of circulating miR-141 are comparable to those of controls. In advanced stage disease the situation is the opposite, where levels of circulating miR-21 are comparable to controls and levels of miR-141 are high. Although this model has too low of a sensitivity to be adopted in the clinic, it gives us a good concept to aim for when considering the diagnostic value of microRNA expression patterns.[18]

Metastasis

Prostate cancer may metastasize to the lungs, liver, and pleura but if it becomes metastatic, it will most certainly form osteoblastic lesions in the bone.[8] Hormone ablation therapy, radiation, and surgery are effective treatments for localized prostate cancer, but the options for metastatic disease are essentially limited to chemotherapy.[2] However, due to the occult nature of the micro-metastases associated with advanced disease, techniques such as MRI and radionucleotide bone scans have a high false negative rate.[12] Because of this, the decision to move forward with chemotherapy is often made liberally, the thinking being that it is better to err on the side of safety. However, considering its side effects, being able to spare an elderly man the pain and cost of chemotherapy would be a significant clinical advancement.

Many studies have demonstrated differential miRNA signatures for metastases and primary tumors. The bulk of these characteristic metastases signatures are unique to each cancer type but some miRNAs do seem to overlap, such as miR-21-5p and miR-10b-5p.[17]Also, as opposed to primary prostate tumors which are multifocal and frustratingly heterogeneous, metastases are almost always monoclonal.[8] The emergence of a sharp profile from a more diffuse and general dysregulation may be a sign of an expansion of metastatic tissue. However when

accomplished, an accurate and sensitive miRNA assay for metastasis would make a huge difference in the lives of patients with advanced disease.

The Androgen receptor and CRPC

Androgens play an important role in early tumorigenesis, interacting with aberrant or over expressed forms of the androgen receptor to stimulate growth.[2] Even when the androgen pathway is not aberrant, tumor growth is still androgen dependent as evidenced by the fact that androgen starvation is an effective strategy for de-bulking tumors. This is because, in prostate tissue, many central cellular processes such as proliferation and growth are directly or indirectly under the control of the androgen pathway's effectors. One interesting example is the hTERT gene which is, in fact, directly controlled by androgens in the human prostate.[16] Also, P68, described in Chapter 1 for its ability to influence the interaction between large groups or pri-miRNAs and the Drosha/DGCR8 complex, has been demonstrated to interact with the androgen receptor, suggesting that it may be involved in propagating an AR driven miRNA profile.[66]

Androgen starvation is an effective way to de-bulk large tumors and is usually a part of combined therapeutics. However, androgen starvation will eventually result in the emergence of castrate resistant prostate cancer (CRPC) for which treatment options are very limited. When pCa overcomes androgen starvation, it isn't because the tumor tissue has abandoned its reliance on the androgen pathway for proliferation, but instead because it has found a way to circumvent the need for exogenous androgen stimulation. This is demonstrated by the observation that castration resistant cells often demonstrate AR over expression, AR gene mutations, AR corepressor or coactivator mutations, and amplification of the AR locus.[6] Of specific importance to those hunting for miRNA biomarkers, it has also been demonstrated that an increase in AR mRNA is all that is required to make the transition between androgen sensitivity to androgen

independence.[52] Being able to monitor the expression of a group of miRNAs associated with the AR in the urine could provide clinicians with an alternative method to circulating tumor cell count for the emergence of CRPC and relapse which would allow patients and their physicians more time to make decisions about treatment.

As treatment options for advanced disease expand in the coming years, late staging and prognosis will only become more relevant. This is especially true for one category of patient in particular, the post failure of androgen deprivation therapy CRPC patients. However, for this stage of disease, the only prognostic marker sanctioned by the US FDA is the circulating tumor cell count which is expensive, technically challenging, and of limited and complicated prognostic value to patients who fall into certain categories.[22] As a proof of concept, miR-32-5p and miR-148a-5p were demonstrated by one group to be downstream of AR binding sites and to be overexpressed in CRPC tissue samples compared to PC.[79] Another researcher in our laboratory has demonstrated that an upregulation of miR-32 is detectable in the blood of prostate cancer patients compared to controls (unpublished results). After androgen deprivation therapy, a return to pretreatment miR-32 levels or above might be good evidence of androgen independence.

The Big Data Problem

There is a lot of profiling information out there with no consensus as to how to interpret it. The variability and complexity inherent to miRNA profiling may seem overwhelming to the point of uselessness, but if the past few years of advancements in the fields of computational factoring and machine learning are any indication of the future, our ability to process vast quantities of data is poised to jump exponentially. [20] It could be that the vast amount of information provided by circulating miRNA profiles could be the source of the most sophisticated diagnostic information available to future diagnosticians.

Prostate Cancer Subgroups

At the genetic and histological level, prostate cancers from different patients have yet to be classified into distinguishable subgroups that correlate with patient outcomes.[8] This is in contrast to breast cancers which are grouped into subtypes based on expression of the estrogen, progesterone, and epidermal growth factor receptors. One contributing factor is that prostate cancer is highly multifocal. That is, it is often made up of genetically distinct, histological foci of cancer.[8] In breast cancers, miRNA profiling has been demonstrated to correlate with tumor subtype.[19] This observation lends itself to the idea that miRNA profiling of tissues could be used to help distinguish prostate cancers into similar subtypes with specific prognoses. As a proof of concept, miRNA profiles have already proved useful in the prediction of response to chemotherapy[3] and there is some convincing evidence that members of the miR-200 family correlate to the established breast cancer subgroups.[84]

Tissue Specific miRNA Modifications

There are many different interesting post-transcriptional modifications (excellently reviewed in reference 66) including uridylation, 5'-methylation, favoring of isomiRs,[35] arm switching and many more.[66] Many of these demonstrate tissue specificity and could affect the profiles of body fluids in such a way as to yield diagnostic information. As an example, RNA specific adenosine deaminases also act on pre-miRNA transcripts (ADARs) to change either their expression or their specificity by changing an adenosine to an inosine within the seed sequence.[7] In one striking example, an ADAR acts on pre-miR-151 which then proceeds to block targets involved in Dicer processing of other pre-miRs leading to their accumulation in the cytoplasm.[1] This demonstrates that ADARs have some important implications for cancer development, in their own right. Since ADARs are tissue specific, quantitating the amount of

circulating miRNAs with tell-tale signs that they have been processed by specific ADARs could give clues as to where a pathology is located in the body.

Detecting the expansion of specific miRNA profiles.

Most miRNA expression profiles that have been established are extremely specific to cell type and differentiation status.[13] Detecting the expansion of a miRNA profile associated with a specific type of cell known to be associated with aggressive or indolent disease may help differentiate aggressive from indolent disease. The first cell type to be investigated for this purpose was the putative prostate tissue stem cell and there are many active studies pursuing this exact concept.[13] However, two hypothetical candidate cell types include the basal cells and neuroendocrine cells of the prostate.

The epithelium is mostly made up of simple cuboidal or columnar epithelial "luminal" cells. Luminal cells are terminally differentiated, have a low proliferative index, contain secretory granules, express cytokeratins 8 and 18, and stain positive for PSA, acid phosphatase, and the androgen receptor. They are anchored to the basement membrane by integrins. Wedged between the epithelium and the basement membrane is a ring of flat "basal" cells with a high nucleus to cytoplasm ratio that express cytokeratins 4, 14, and 15 and stain negative for PSA and the androgen receptor. They make up less than 10% of the glandular epithelium in the healthy prostate.[5] The basal cell population is thought to be the originator of the luminal epithelium and is also thought to contain the proposed prostate stem cells, defined as single cells that have the ability to reconstitute the entire gland. These are also the cells most predicted to be the origin of prostate cancer stem cells and prostate cancer in general.[5] PIN is widely regarded as a precursor

to prostate cancer and so differentiating it from true malignancy could be a challenge. One key difference between them is that in PIN, basal cells are reduced in number compared to normal prostate while in the case of cancer, the reverse is true.[8] Characterization of the miRNA profile associated with the basal phenotype may be a good place to start looking for a way to distinguish between these two conditions.

Scattered among the epithelial cells of the prostate are neuroendocrine (NE) cells that stain positive for chromogranin A, neuron-specific enolase, and synaptophysin, as well as other neuronal markers. They have a paracrine function on the growth, differentiation, and secretory effect of the epithelium.[5] While tumors derived from NE cells are rare, mouse experiments have demonstrated that NE cells themselves do have an effect on alveolar carcinoma growth and aggressiveness. This effect is still appreciable when NE cells are transplanted to parts of the body distant from the prostate, indicating that they could act in an autocrine manner.[16] A tumor's microenvironment is critical to its survival. It is possible that as a prostate tumor develops, it recruits resident NE cells and causes them to proliferate. If this were the case, then an expansion of the miRNA expression profile of NE cells could correlate with tumor aggressiveness.

Delivery to the Vagina

The prostate is first and foremost, an exocrine organ. It secrets a thick alkaline fluid composed of materials designed to increase the viability of spermatozoa inside the hostile environment of the vagina. This fluid is ejected with the spermatozoa and contributes 50-70% of the seminal fluid. I propose that the epithelial tissue of the prostate packages miRNAs for extracellular delivery to the vagina for the purpose of mitigating its hostile environment. The following is an original example for a proposal for how this might be accomplished. In 2013, a team of researchers established that norepinephrine potentiates the pro-inflammatory response of

human vaginal epithelial cells (HVEC) and that this response is dependent upon HVEC expression of the B-adrenergic receptor.[63] One miRNA that we found to be one of our most powerful biomarkers, 205-5p, was found to potentially target ADRB2, the gene that encodes the B-adrenergic receptor. I think that it is possible that the presence of this miRNA in the urine is derived directly from the prostate and that one of its natural functions there is as an intended component of the seminal fluid. Repeated exposures to seminal fluid may increase fertility by lowering the expression of the beta adrenergic receptor in the HVECs lining the vagina, which would in turn lower HVECs' responsiveness to NE, which would reduce the production of IFN-gamma by these cells, which would mitigate the spermatocidal, pro-inflammatory environment of the vagina. Being more fertile in a situation where sex is a more frequent event might have made our female ancestors more likely to conceive a child with an established partner as opposed to as the result of a chance encounter. This would have made her more likely to conceive while she could make use of social advantages such as a long term partner, a familial community, or some primitive equivalent. This would have been important since caring for an infant demands resources and attention that would be difficult for an individual parent to provide in ancient times.

More in depth small RNA analyses of semen of different men could give us information regarding which, if any, miRNAs originate in the prostate with the direct intention of delivery into the vagina along with the sperm.

Chapter 2- miRNA NGS of the Cancer Cell Line Progression Model

Specific Aims

The P69 cell line and its derivatives are a unique prostate cancer progression model. They were derived from normal prostate epithelium, immortalized with SV40 large T antigen, and allowed to become tumorigenic via multiple rounds of in vivo selection in nude mice.[30] From this approach, a family of related cell lines was produced, each representing a different stage of tumor progression. The P69 parental cell line is poorly tumorigenic, non-metastatic, and has a lower chromosomal modal number than other more established prostate cancer cell lines. Three rounds of subcutaneous injections produced the M12 daughter cell line which is highly tumorigenic and metastatic and harbors a chromosome 16:19 translocation resulting in the deletion of one copy of chromosome 19p-q13.1. Restoration of chromosome 19 to the M12's produced the F6 cell line which is less tumorigenic and not metastatic.[30] It has long been known that chromosome 19 contains one of the highest concentrations of miRNAs[32] leading to the hypothesis that an alteration in miRNA expression might be responsible for the M12 cell line's powerful metastatic character. To investigate this, deep sequencing was performed on RNA extracted from each of the cell lines. Recent genome wide association studies have established an association between a risk for prostate cancer and a panel of inheritable mutations. A single nucleotide polymorphism (SNP) analysis was performed on all participating cell lines, partly to investigate the mystery of P69 cell line's tumorigenicity and partly to establish that none of these SNPs were acquired by the M12 cell line during in vivo passaging, thereby explaining its character.

History and Character of the Cell Lines

The P69 cell line was derived from prostate epithelial cells isolated from the tissue obtained from a 63 year old African American man during a transurethral resection and

transfected with SV40 large T antigen via the pcc5 plasmid. It is important to point out that these cells are immortalized but not transformed by ectopic expression of any other oncogenic factor such as cMYC. Most cell lines immortalized by SV40 large T antigen are not tumorigenic and therefore, are not considered to be cancer cell lines. In contrast, the P69 cell line is weakly tumorigenic in athymic nude mice which allowed for serial passaging to move forward without any other unnatural modifications.[39] Histologically, P69 cells demonstrate a homogeneous flat, cobblestone appearance consistent with their epithelial character. These cells demonstrated acini-like morphology complete with basement membrane and basal polarity of alpha 6 and beta 1 integrin expression, when grown in embedded in lamimin rich extracellular matrix (lrECM) gel (3D) cultures.[49] Co-expression of keratin 5/6, keratin 8, and p63 suggest that the p69 cell line was derived from a prostate basal cell.[49] Although these cells have a number of characteristic translocations, none result in chromosomal loss and these cells retain both X and Y chromosomes. The most prominent cytogenetic event present in this cell line is a t(5;7) translocation that is retained in all of its derivative cell lines. P69 cells were injected subcutaneously and produced tumors in 2/18 athymic nude mice after 180 days. Cells from these two tumors were immediately injected subcutaneously and after 25 days, the tumors that were isolated from these mice produced the daughter cell lines M2182 and M2055.

The morphology of M2182 cells, differs markedly from that of the P69 parent. While the P69 cells show consistent epithelial character, these cells are extremely heterogeneous. Histological analysis of the tumor from which these cells were derived showed a poorly differentiated tissue.[39] Interestingly, the modal chromosome number for these cells was 46, demonstrating consistent pseudodiploidy after 2 rounds of in vivo selection. This pseudodiploid character is a characteristic unique to this prostate cancer cell model as it demonstrates that, in

this case, tumorigenesis precedes chromosomal instability. This sets this family of cell lines apart from the PC-3, DU-145, LNCap, and PC-82 cell lines which are all characterized by high chromosome numbers. The M2182 cell line was passaged via subcutaneous injection one additional time, producing tumors in 2/3 athymic nude mice, one of which resulted in the M12 cell line.

The M12 cells metastasized aggressively to the diaphragm and lung and were highly tumorigenic, producing tumors in 13/13 mice after 9-15 days. In contrast to its grandparent parent cell line, p69, the M12 subline demonstrated an unstructured spheroid morphology with no polarity when grown in lrECM 3D cultures.[49] It was also observed that early on the M12 cells quickly migrate out of these spheroid balls and penetrate the entire lrECM gel. In addition they have lost the Y chromosome and chromosome 19p-q13.1 as a result of an unbalanced translocation with chromosome 16.[40] The loss of chromosome Y is one of the most common cytogenetic phenomena detected in prostate cancers alongside aberrations involving chromosomes 7, 8, 10, and 16. Loss of chromosome 19 is less common, but is often lost in prostate tumors that have reached an advanced stage.[40] These regions harbor few known classical tumor suppressor genes relevant to prostate cancer. In order to investigate the role that this deletion has on the aggressiveness of the M12 cell line, a new copy of chromosome 19 was introduced via microcell mediated chromosome transfer (MMCT) using A9neo19 donor cells.

The resulting cell line (F6) demonstrated significantly reduced in vitro doubling time, anchorage independent growth, and tumorigenicity compared to the M12 cell lines.[40] It was also observed that these cells revert back to the acini-like morphology of the p69 cells, complete with basement membrane and basal polarity, when grown in lrECM 3D cultures.[49] F6 cells have an additional chromosomal aberration resulting in the acquisition of an additional copy of both the

long arms of chromosome 22 (from q13 on) and the X chromosome (also from q13 on). These hybrid cells created microscopic tumors in 6/15 athymic nude mice after 120 days with no metastases. Analysis of tumors formed by subcutaneous injection of the F6 cells revealed new chromosomal aberrations in all cells including an additional loss of chromosome 19 in 40% of the cells. Within the same MMCT experiment that produced the F6 cell line, another daughter cell line was produced that failed to obtain a new copy of chromosome 19, but did acquire other chromosomal aberrations and demonstrated comparable tumorigenicity to the M12 parent, demonstrating that the MMCT method does not itself drastically inhibit tumorigenesis.[40]

Materials and Methods

Cell Line RNA Extraction and Sequencing

Small RNA was extracted from duplicate P69 samples and one M2182, one M12, and one F6 sample using the miRVana microRNA extraction kit. The protocol was followed according to the manufacturer's specifications for the extraction of small RNA and RNA eluted in 200 ul. Sample concentration was normalized according to the miRNA concentration reported by the Agilent Bioanalyzer's small chip and samples were sent to the Nucleic Acids Research Facility at Virginia Commonwealth University for paired end sequencing on the Illumina platform. Normalization, trimming, and analysis was performed exactly as described in Chapter 1 and results are reported as comparisons between duplicate P69 samples and each of the M12, M2182, and F6 samples individually. Sequencing quality, trimmed reads, alignment, etc. are reported in Figure Y.

TCGA pCa tumor samples

Level 3 Illumina data from The Cancer Genome Atlas from 50 tumor samples and matched samples of normal tissue from the same patients was selected for analysis. Since the P69 cell line is immortalized epithelium, this comparison was thought to be especially appropriate. Normalization, trimming, and analysis was again performed exactly as described in Chapter 1.

SNP Analysis

The SNP analysis utilized in this study makes use of Ion Torrent DNA sequencing and emulsion PCR (emPCR). DNA was extracted from P69, M2182, M12, and F6 cell lines with the QIAamp DNA Mini Kit. Input DNA (10 ng) from each sample was used to generate DNA libraries using the Ion AmpliSeq Library Kit 2.0 and the Ion AmpliSeq Cancer Hotspot Panel v2. The Cancer Hotspot Panel is a pool of primers that specifies the amplification of 207 different amplicons covering over 2,800 different common mutations within the Catalogue of Somatic Mutations in Cancer (COSMIC) database, representing 50 different oncogenes and tumor suppressors important to prostate cancer. The COSMIC database catalogs more than two million coding sequence point mutations identified in different cancers. Individual samples were barcoded and ligated with the Ion Xpress Barcode Adapters 1-16 Kit and then attached to Agencourt AMPure XP magnetic beads. Sample libraries were then quantitated with a Qubit 2.0 Fluorometer and normalized to a concentration of 100 pM. emPCR was performed on the Ion OneTouch 2 Instrument. Samples enriched on the Ion OneTouch ES using the Ion PGM Template OT2 200 Kit and DynaBeads MyOne streptavidin C1 beads according to the manufacturer's protocols. The enriched ISPs were eluted off the MyOne streptavidin C1 beads using a sodium hydroxide and tween melt solution and then sequenced with an Ion Torrent Ion

318™ Chip. The Ion Torrent PGM was run with standardized Ion Torrent 200 Kit v2 modifications for 500 nucleotide flows, and the output was aligned to the HG19 as a reference. This sequencing was outsourced to American International Biotechnology, Richmond VA, and generously done by Katherine O'Hanlon overseen by Dr. William Budd.

Results

SNP Analysis

A next generation sequencing analysis was undertaken to identify potential nucleotide variations in genes associated with cancer progression. Over 200,000 reads were obtained for each cell subline with a mean read length of ~110 nts in length (Table 1). Although F6 is not shown in the table below, it produced similar results, demonstrating good coverage for all cell lines.

Table 10: SNP NGS Summary

Cell Line	Reads	Mean Length	Total Bases
P69	562,713	110	61,626,082
M2182	206,177	114	23,518,988
M12	448,016	114	50,956,206

There were three COSMIC hotspot gene mutations identified in all sublines (STK11-COSM29005, PGFRA- COSM22413 and APC-COSM19099 (Table 11). All of the COSMIC

hotspot mutations plus the other 11 novel mutations were consistent across all cell lines of the progression model (P69, M2182, M12, and F6), which implies that none of them are responsible for the aggressiveness demonstrated by the M12s. However, there was a single transition from a cytosine to a thymidine in the STK11* gene on chromosome 19 which is present in the P69 and M2182 cell lines but disappears in the M12 cell line, concomitant with the loss of one chromosome 19.

Table 11: SNP Summary

Gene Symbol	Chromosome	Position	Reference Nucleotide	Alternate Nucleotide	Cosmic ID
PIK3CA	chr3	178917005	A	G	---
MET	chr7	116340269	C	T	---
NOTCH1	chr9	139390853	C	T	---
RET	chr10	43613843	G	T	---
TP53	chr17	7579472	G	C	---
STK11*	chr19	1220321	T	C	---
STK11	**chr19**	**1221293**	**C**	**T**	**COSM29005**
PIK3CA	chr3	178927410	A	G	---
FGFR3	chr4	1807894	G	A	---
PDGFRA	chr4	55141055	A	G	---
PDGFRA	**chr4**	**55152040**	**C**	**T**	**COSM22413**
KDR	chr4	55955139	A	T	---
APC	**chr5**	**112175240**	**G**	**C**	**COSM19099**
APC	chr5	112175770	G	A	---
CSF1R	chr5	149433596	TG	GA	---

*Not present in M12 cell line.

By looking at each SNP analysis individually we can see an interesting timeline emerge. In the P69 and M2182 cell lines, there are two SNPs within different parts of the STK11 gene. They are one novel mutation and one cancer hotspot and they are each consistently expressed at an allelic ratio of about 50% in both parent and daughter cell lines. In the M12 cell line however, only the hotspot mutation is present and it enjoys an allelic ratio of 100%. Since the

M12s have lost a copy of the portion of chr19 where STK11 resides, the most obvious explanation for this is that the novel mutation was originally on the now missing copy of STK11. It is unclear whether or not this remaining mutation which does not produce a change in the amino acid sequence of the protein (Y272Y), has an effect on its activity. It is still likely that the mutation that we retain is fully functional. We can also see here that the allelic ratios in the F6 cell line deviate significantly from the previous norms of either 50% or 100%, possibly reflecting the increase in cytogenetic heterogeneity that we see in these cells.

Table 12: SNP Allelic Frequencies in the P69 Cell Line

Gene Symbol	Chromosome	Position	Reference Nucleotide	Alternate Nucleotide	Allele Ratio	Cosmic ID
PIK3CA	chr3	178917005	A	G	49.5	---
MET	chr7	116340269	C	T	51.4	---
NOTCH1	chr9	139390853	C	T	37.5	---
RET	chr10	43613843	G	T	100	---
TP53	chr17	7579472	G	C	44.8	---
STK11	**chr19**	**1220321**	**T**	**C**	**49.1**	**---**
STK11	**chr19**	**1221293**	**C**	**T**	**49.1**	**COSM29005**
PIK3CA	chr3	178927410	A	G	55.2	---
FGFR3	chr4	1807894	G	A	100	---
PDGFRA	chr4	55141055	A	G	100	---
PDGFRA	chr4	55152040	C	T	50.1	COSM22413
KDR	chr4	55955139	A	T	48.2	---
APC	chr5	112175240	G	C	64.8	COSM19099
APC	chr5	112175770	G	A	100	---
CSF1R	chr5	149433596	TG	GA	100	---

Table 13: SNP Allelic Frequencies in the M2182 Cell Line

Gene Symbol	Chromosome	Position	Reference Nucleotide	Alternate Nucleotide	Allele Ratio	Cosmic ID
PIK3CA	chr3	178917005	A	G	48.4	---
MET	chr7	116340269	C	T	54.3	---
NOTCH1	chr9	139390853	C	T	34.7	---
RET	chr10	43613843	G	T	100	---
TP53	chr17	7579472	G	C	62.1	---
STK11	**chr19**	**1220321**	**T**	**C**	**53.1**	**---**
STK11	**chr19**	**1221293**	**C**	**T**	**47.6**	**COSM29005**
PIK3CA	chr3	178927410	A	G	50.8	---
FGFR3	chr4	1807894	G	A	99.2	---
PDGFRA	chr4	55141055	A	G	100	---
PDGFRA	chr4	55152040	C	T	47.7	COSM22413
KDR	chr4	55955139	A	T	44.6	---
APC	chr5	112175240	G	C	32.9	COSM19099
APC	chr5	112175770	G	A	100	---
CSF1R	chr5	149433596	TG	GA	100	---

Table 14: SNP Allelic Frequencies in the M12 Cell Line

Gene Symbol	Chromosome	Position	Reference Nucleotide	Alternate Nucleotide	Allele Ratio	Cosmic ID
PIK3CA	chr3	178917005	A	G	62.4	---
MET	chr7	116340269	C	T	50.8	---
NOTCH1	chr9	139390853	C	T	28.6	---
RET	chr10	43613843	G	T	100	---
TP53	chr17	7579472	G	C	49	---
STK11	**chr19**	**1221293**	**C**	**T**	**100**	**COSM29005**
PIK3CA	chr3	178927410	A	G	65.9	---
FGFR3	chr4	1807894	G	A	100	---
PDGFRA	chr4	55141055	A	G	100	---
PDGFRA	chr4	55152040	C	T	51.5	COSM22413
KDR	chr4	55955139	A	T	44.6	---
APC	chr5	112175240	G	C	49.3	COSM19099
APC	chr5	112175770	G	A	100	---
CSF1R	chr5	149433596	TG	GA	100	---

Table 15: SNP Allelic Frequencies in the F6 Cell Line

Gene Symbol	Chromosome	Position	Reference Nucleotide	Alternate Nucleotide	Allele Ratio	Cosmic ID
PIK3CA	chr3	178917005	A	G	49.5	---
MET	chr7	116340269	C	T	90.3	---
SMO	chr7	128846355	C	T	10.1	---
NOTCH1	chr9	139390853	C	T	34.1	---
RET	chr10	43613843	G	T	100	---
TP53	chr17	7579472	G	C	52.7	---
STK11	**chr19**	**1220321**	**T**	**C**	**52.9**	---
STK11	**chr19**	**1221293**	**C**	**T**	**49.1**	**COSM29005**
PIK3CA	chr3	178927410	A	G	51.8	---
FGFR3	chr4	1807894	G	A	100	---
PDGFRA	chr4	55141055	A	G	100	---
PDGFRA	chr4	55152040	C	T	47.3	COSM22413
KDR	chr4	55955139	A	T	49.3	---
APC	chr5	112175240	G	C	50	COSM19099
APC	chr5	112175770	G	A	100	---
CSF1R	chr5	149433596	TG	GA	100	---

RNA Sequencing

Since SNP analysis could not define any known cancer genes that could account for the phenotypic differences between the p69, M2182, M12 and F6 cell lines, we initiated NGS to search for miRs whose dysregulation could contribute to the different tumorigenic and metastatic properties of this progression model. Previously, miR array screens were conducted in duplicate on the parental p69 cell and its M12 variant. Eventually, results from this previous analysis will be compared to NGS results in an effort to pin point relevant miRs driving tumor progression.

Table 16: miRNA NGS P69 vs M2182

Gene Name	Chromosome	logFC	logCPM	LR	PValue	FDR
hsa-miR-340-5p	chr5	-8.672291	10.063148	58.54637	1.99E-14	1.31E-11
hsa-miR-381-3p	chr14	-12.54818	9.7167823	55.34134	1.01E-13	3.35E-11
hsa-miR-429	chr14	-7.945767	10.869757	35.94044	2.03E-09	3.56E-07
hsa-miR-146a-5p	chr5	5.6748522	5.9314763	35.83435	2.15E-09	3.56E-07
hsa-miR-205-5p	chr1	-9.40322	12.729872	34.01031	5.48E-09	6.78E-07
hsa-miR-200c-3p	chr12	-8.976546	13.379708	33.78686	6.15E-09	6.78E-07
hsa-miR-370-3p	chr14	-11.43019	8.6030225	31.87443	1.64E-08	1.56E-06
hsa-miR-200a-3p	chr1	-8.931423	9.4067572	29.11996	6.80E-08	5.63E-06
hsa-miR-379-5p	chr14	-10.57524	7.7600633	27.68123	1.43E-07	9.65E-06
hsa-miR-411-5p	chr14	-10.5446	7.7298956	27.64473	1.46E-07	9.65E-06
hsa-miR-654-3p	chr14	-10.17118	7.3631675	27.41589	1.64E-07	9.87E-06
hsa-miR-409-3p	chr14	-10.06848	7.2616111	26.51293	2.62E-07	1.44E-05
hsa-miR-200b-3p	chr1	-7.306893	9.6681274	26.33481	2.87E-07	1.46E-05
hsa-miR-127-3p	chr14	-7.854096	8.3292901	26.14608	3.17E-07	1.50E-05
hsa-miR-934	chrX	-9.904999	7.1250306	25.82157	3.74E-07	1.65E-05
hsa-miR-543	chr14	-9.50421	6.7074089	23.09731	1.54E-06	6.37E-05
hsa-miR-493-5p	chr14	-9.767545	6.9630524	22.87422	1.73E-06	6.74E-05
hsa-miR-493-3p	chr14	-8.744402	5.989907	22.46514	2.14E-06	7.87E-05
hsa-miR-141-3p	chr12	-8.88349	6.1602202	19.94271	7.98E-06	0.000278
hsa-miR-200a-5p	chr1	-7.128074	8.5440246	18.79742	1.45E-05	0.000481
hsa-miR-200b-5p	chr1	-9.051804	6.3275499	17.10568	3.54E-05	0.001115
hsa-miR-134-5p	chr14	-5.291734	5.8575744	16.06363	6.12E-05	0.001843
hsa-miR-598-3p	chr8	-7.79695	5.130604	15.69745	7.43E-05	0.002074
hsa-miR-136-3p	chr14	-7.862185	5.1749528	15.66054	7.58E-05	0.002074
hsa-miR-382-5p	chr14	-8.001095	5.2856901	15.5985	7.83E-05	0.002074
hsa-miR-651-5p	chrX	-5.132838	5.7292055	15.49069	8.29E-05	0.002111
hsa-miR-129-5p	chr7, chr11	3.2518363	5.6992039	15.17975	9.77E-05	0.002397
hsa-miR-125b-2-3p	chr21	5.2439076	4.0085396	14.79464	0.0001199	0.002834
hsa-miR-708-3p	chr11	3.1357166	6.2904811	14.68159	0.0001273	0.002906
hsa-miR-758-3p	chr14	-7.722852	5.0327932	13.41604	0.0002495	0.005505
hsa-miR-9-5p	chr1, chr5, chr15	-7.625341	5.0040919	13.15851	0.0002862	0.006112
hsa-miR-1185-1-3p	chr14	-7.626848	4.9491223	13.0495	0.0003034	0.006276
hsa-miR-323a-3p	chr14	-7.706867	5.0110519	12.82824	0.0003414	0.006849
hsa-miR-889-3p	chr14	-7.657582	4.9656434	12.29348	0.0004545	0.00885
hsa-miR-30a-5p	chr6	2.0908475	11.791584	11.99622	0.0005331	0.010083
hsa-miR-935	chr19	-7.221246	4.6260864	11.91707	0.0005562	0.010228
hsa-miR-335-3p	chr7	-2.401886	10.534727	11.65372	0.0006407	0.011464

hsa-miR-708-5p	chr11	2.8279161	7.9699047	11.01502	0.0009038	0.015745
hsa-miR-582-5p	chr5	-4.663765	5.3218581	10.87422	0.0009751	0.016552
hsa-miR-654-5p	chr14	-7.078403	4.480912	10.64118	0.001106	0.018304
hsa-miR-148a-3p	chr7	-2.731018	11.115454	10.5735	0.0011472	0.018523
hsa-miR-369-3p	chr14	-7.087502	4.4846182	10.46925	0.0012138	0.019131
hsa-miR-411-3p	chr14	-7.069145	4.457903	9.893838	0.0016583	0.025531
hsa-miR-323b-3p	chr14	-6.990587	4.3909656	9.755046	0.0017883	0.026312
hsa-miR-369-5p	chr14	-6.783574	4.2410767	9.754758	0.0017886	0.026312
hsa-miR-495-3p	chr14	-6.931813	4.342174	9.656266	0.0018871	0.027157
hsa-miR-944	chr3	-7.3065	4.7528396	9.220271	0.0023935	0.033713
hsa-let-7g-3p	chr3	5.1814771	2.4933962	8.805469	0.0030033	0.04142
hsa-miR-629-5p	chr15	-3.354367	8.0147785	8.766761	0.0030677	0.041445
hsa-miR-299-3p	chr14	-6.792964	4.2203811	8.727155	0.0031351	0.041508
hsa-miR-744-5p	chr17	-2.034339	11.254919	8.653361	0.0032646	0.042376
hsa-miR-539-3p	chr14	-6.453826	3.9675278	8.123694	0.004369	0.054924
hsa-miR-1910-5p	chr16	-6.40306	3.9506157	8.112041	0.0043972	0.054924
hsa-miR-6501-5p	chr21	3.7145808	2.9815034	7.93164	0.0048578	0.059553
hsa-miR-129-1-3p	chr7	3.7147703	2.9815034	7.892704	0.0049635	0.059742
hsa-let-7d-5p	chr9	-2.117487	12.677702	7.697619	0.0055294	0.065365
hsa-miR-1294	chr5	-6.183616	3.785751	7.424735	0.0064333	0.073435
hsa-miR-141-5p	chr12	-4.338616	5.0556808	7.424577	0.0064339	0.073435
hsa-miR-221-5p	chrX	2.0848437	6.391886	7.267509	0.0070213	0.078408
hsa-miR-375	chr2	-3.484342	5.1221568	7.245865	0.0071064	0.078408
hsa-let-7i-5p	chr12	2.2957013	16.715867	7.15418	0.0074789	0.081165
hsa-miR-136-5p	chr14	-5.973259	3.6134911	7.000483	0.0081488	0.087008
hsa-miR-3664-5p	chr11	4.7796309	2.3392565	6.891529	0.0086605	0.088204
hsa-miR-4659a-3p	chr8	4.7796309	2.3392565	6.891529	0.0086605	0.088204
hsa-miR-4474-3p	chr9	4.7796309	2.3392565	6.891529	0.0086605	0.088204
hsa-miR-433-3p	chr14	-6.379645	3.8789678	6.847639	0.0088758	0.089027
hsa-miR-27b-5p	chr9	2.1553767	7.4831288	6.703051	0.0096248	0.095099
hsa-miR-4497	chr12	3.4964478	2.8726121	6.635261	0.009998	0.097044
hsa-miR-377-3p	chr14	-6.022918	3.6271826	6.614553	0.0101149	0.097044
hsa-miR-656-3p	chr14	-5.81706	3.486217	6.44361	0.0111352	0.105307
hsa-miR-148a-5p	chr7	-2.68988	6.2201689	6.34921	0.0117434	0.109494
hsa-miR-485-3p	chr14	-5.942797	3.5629937	6.262382	0.0123328	0.113393
hsa-miR-376c-3p	chr14	-5.580185	3.3305671	6.153677	0.0131139	0.118923
hsa-miR-409-5p	chr14	-5.599274	3.335382	6.021738	0.0141307	0.124565
hsa-miR-618	chr12	-5.713739	3.4582101	6.000672	0.0143004	0.124565
hsa-let-7i-3p	chr12	2.0009366	7.1859608	6.000656	0.0143006	0.124565
hsa-miR-329-3p	chr14	-5.529089	3.3161719	5.974179	0.0145168	0.124807
hsa-miR-556-3p	chr1	-5.287797	3.1518639	5.703965	0.0169266	0.14201

hsa-miR-23a-5p	chr19	-3.097498	4.7759874	5.701871	0.0169468	0.14201
hsa-miR-487b-3p	chr14	-5.395773	3.2316274	5.629107	0.0176646	0.146175
hsa-miR-582-3p	chr5	-2.54518	7.1206987	5.599272	0.0179679	0.146723
hsa-miR-16-5p	chr13	1.4235721	11.038119	5.579287	0.0181741	0.146723
hsa-miR-23b-3p	chr9	1.9573244	8.1018797	5.502409	0.0189903	0.151465
hsa-miR-3614-5p	chr17	2.531968	4.3894983	5.402201	0.0201114	0.158497
hsa-miR-410-3p	chr14	-5.90353	3.5050319	5.272944	0.0216594	0.168688
hsa-miR-203a-3p	chr14	-3.172983	7.09839	5.211115	0.0224429	0.172758
hsa-miR-382-3p	chr14	-5.184408	3.0717108	5.080347	0.0241985	0.184131
hsa-miR-193a-5p	chr17	1.740287	8.660351	5.042799	0.0247285	0.186026
hsa-miR-296-3p	chr20	-2.306024	7.6343258	4.976608	0.0256923	0.191105
hsa-miR-4521	chr17	-5.209988	3.0767387	4.881817	0.027141	0.199637
hsa-miR-4683	chr10	-5.222587	3.1371223	4.794656	0.0285482	0.202498
hsa-miR-181c-5p	chr19	2.4671956	3.9411375	4.747547	0.0293401	0.202498
hsa-miR-3127-3p	chr2	-4.989542	2.9651669	4.739435	0.0294787	0.202498
hsa-miR-17-3p	chr13	1.6773977	6.7237412	4.731572	0.0296138	0.202498
hsa-miR-1268b	chr17	4.2206945	2.1671304	4.720934	0.0297975	0.202498
hsa-miR-204-5p	chr9	4.2206945	2.1671304	4.720934	0.0297975	0.202498
hsa-let-7c-3p	chr9, chr22	4.2206945	2.1671304	4.720934	0.0297975	0.202498
hsa-miR-337-3p	chr14	-5.00872	2.9702526	4.698453	0.0301898	0.202498
hsa-miR-338-5p	chr17	-4.972073	2.9600919	4.691358	0.0303147	0.202498
hsa-miR-3929	chr18	-5.733861	3.5123903	4.675896	0.0305888	0.202498

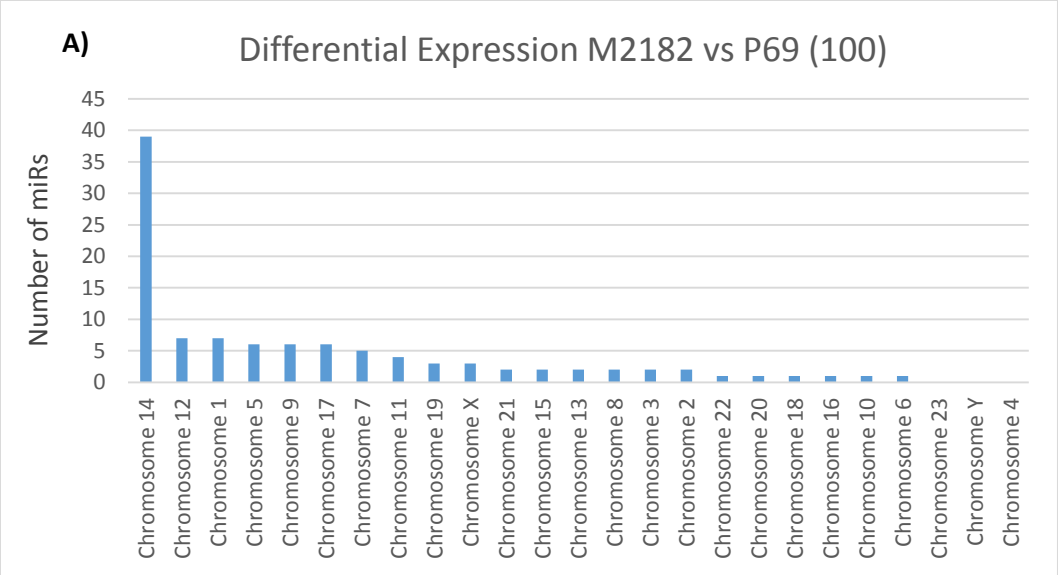

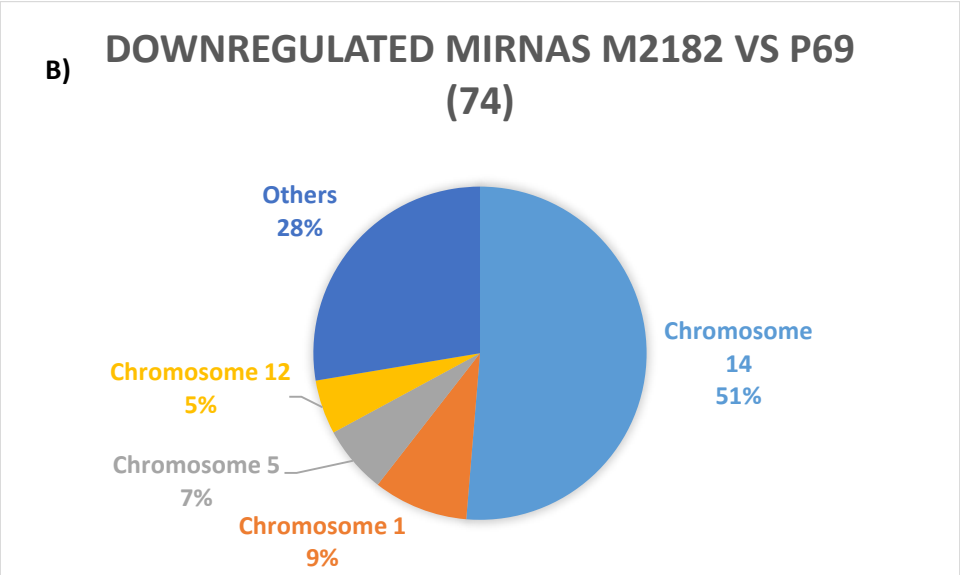

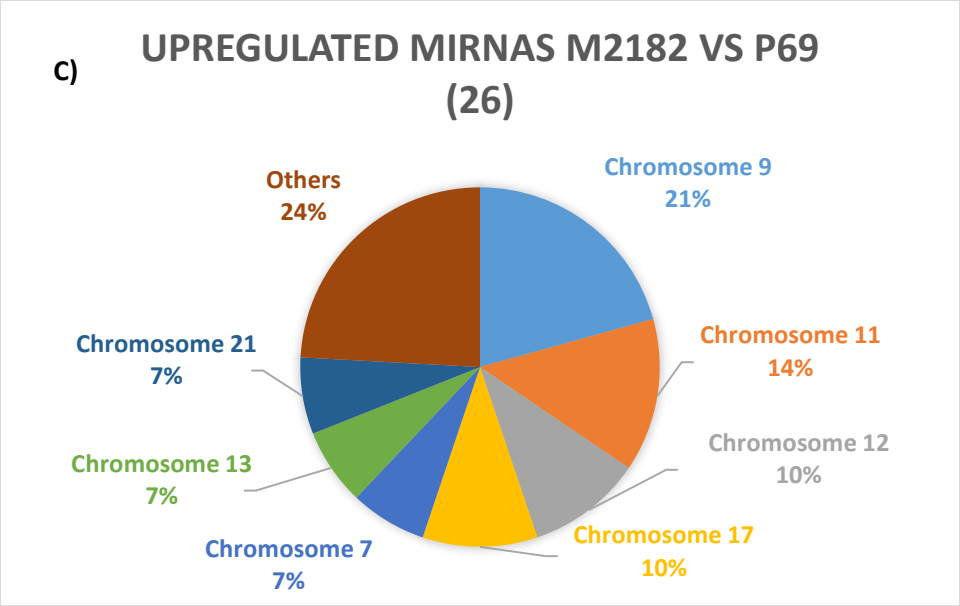

Figure 11: The chromosomal representation of dysregulated miRNAs between the P69 and M2182 cell lines. A) A bar graph representing the total numbers of dysregulated miRNAs (both upregulated and downregulated) between the P69 and M2182 cell lines segregated by the chromosomal location. It can immediately be seen that the vast majority of dysregulated miRNAs lie on chromosome 14. B) A pie graph of only downregulated miRNAs demonstrates that a majority lie on chromosome 14 (51%). C) A pie graph of only upregulated miRNAs demonstrates a much more even distribution of dysregulated miRNAs between chromosomes. Considering both B and C, we can see that overall there are almost 3 times as many downregulated miRNAs (74) as there are upregulated miRNAs (26).

By far the largest number of dysregulated miRNAs come from chromosome 14 (39) and it should be pointed out that not a single one of these is upregulated. This phenomenon persisted in all of the other cell lines.

Table 17: Sequencing Results M12

Gene Name	Chromosome	logFC	logCPM	LR	PValue	FDR
hsa-miR-675-5p	chr11	10.48098	6.3352868	56.85745	4.69E-14	3.10E-11
hsa-miR-34a-5p	chr1	5.888364	8.7589316	46.10263	1.12E-11	3.71E-09
hsa-miR-370-3p	chr14	-9.48895	8.659433	35.48923	2.56E-09	5.66E-07
hsa-miR-493-3p	chr14	-9.3606	5.9076875	32.8014	1.02E-08	1.35E-06
hsa-miR-127-3p	chr14	-8.33681	8.377626	32.79676	1.02E-08	1.35E-06
hsa-miR-493-5p	chr14	-10.3842	6.955522	32.16034	1.42E-08	1.57E-06
hsa-miR-598-3p	chr8	-8.4122	4.9548096	24.67561	6.78E-07	5.75E-05
hsa-miR-136-3p	chr14	-8.47713	5.0025315	24.63068	6.94E-07	5.75E-05
hsa-miR-654-3p	chr14	-5.64906	7.3934053	22.61502	1.98E-06	0.000146
hsa-miR-375	chr2	3.875028	8.0789744	20.23177	6.86E-06	0.000454
hsa-miR-1250-5p	chr17	5.621295	4.6057246	19.64089	9.34E-06	0.000562
hsa-miR-409-3p	chr14	-5.04411	7.2955072	18.90595	1.37E-05	0.000758
hsa-miR-654-5p	chr14	-7.69118	4.2170658	17.79949	2.45E-05	0.00125
hsa-miR-134-5p	chr14	-4.28	5.7937288	17.55702	2.79E-05	0.00126
hsa-miR-1257	chr20	4.664937	4.5637498	17.51255	2.85E-05	0.00126
hsa-miR-1269a	chr4	4.749274	4.630331	17.24964	3.28E-05	0.001356
hsa-miR-147b	chr15	3.55611	5.7494634	16.33096	5.32E-05	0.002071
hsa-miR-381-3p	chr14	-3.89591	9.838635	15.70913	7.39E-05	0.002717
hsa-miR-590-5p	chr7	7.001886	3.4677385	14.50294	0.00014	0.004876
hsa-miR-411-5p	chr14	-4.10567	7.8055164	14.29948	0.000156	0.005161
hsa-miR-95-3p	chr4	2.77126	6.3715901	14.09168	0.000174	0.005489
hsa-miR-9-5p	chr1, chr5, chr15	3.017321	7.3062746	13.10485	0.000295	0.008658
hsa-miR-136-5p	chr14	-6.58187	3.2398911	13.06526	0.000301	0.008658
hsa-miR-16-2-3p	chr3	-2.9334	11.075447	12.89995	0.000329	0.009064
hsa-miR-548ar-3p	chr13	6.476366	3.09203	12.52451	0.000402	0.010393
hsa-miR-4421	chr1	6.476366	3.09203	12.48961	0.000409	0.010393
hsa-miR-424-3p	chrX	-3.18094	10.243336	12.42388	0.000424	0.010393
hsa-miR-191-3p	chr3	-3.46682	5.4169411	12.23556	0.000469	0.011086
hsa-let-7f-1-3p	chr9	-3.99859	4.5650288	11.95661	0.000545	0.012308

hsa-miR-196a-5p	chr17	2.820411	8.1780643	11.91188	0.000558	0.012308
hsa-miR-656-3p	chr14	-6.42394	3.0954587	11.7599	0.000605	0.012604
hsa-miR-411-3p	chr14	-5.12293	4.2162943	11.74745	0.000609	0.012604
hsa-miR-433-3p	chr14	-6.9885	3.5322098	11.61041	0.000656	0.013156
hsa-miR-382-5p	chr14	-3.94655	5.1898311	11.36491	0.000748	0.014573
hsa-miR-485-3p	chr14	-6.54944	3.1794872	11.16467	0.000834	0.015769
hsa-miR-379-5p	chr14	-3.37206	7.8662884	11.08155	0.000872	0.016033
hsa-miR-301b-3p	chr22	3.474327	4.8391433	10.97718	0.000922	0.016504
hsa-miR-3065-5p	chr17	4.631569	3.6242743	10.86462	0.00098	0.017076
hsa-miR-487b-3p	chr14	-6.00228	2.8186083	10.75552	0.00104	0.017406
hsa-miR-369-3p	chr14	-4.26928	4.2734684	10.68631	0.001079	0.017406
hsa-miR-10a-5p	chr17	2.304609	13.258105	10.6622	0.001093	0.017406
hsa-miR-548ah-3p	chr4	3.349915	4.6115115	10.64398	0.001104	0.017406
hsa-miR-323b-3p	chr14	-4.83247	4.1473728	10.54316	0.001166	0.017954
hsa-miR-3664-5p	chr11	6.013099	2.7836886	10.37589	0.001277	0.019209
hsa-miR-184	chr15	3.087705	4.8152331	10.24206	0.001373	0.020195
hsa-miR-944	chr3	-5.36328	4.555844	10.04392	0.001529	0.021997
hsa-miR-152-3p	chr17	2.315802	9.1330732	9.628353	0.001916	0.02691
hsa-miR-382-3p	chr14	-5.78871	2.6370488	9.594902	0.001951	0.02691
hsa-miR-337-3p	chr14	-5.61139	2.5264609	9.041296	0.002639	0.03566
hsa-miR-576-3p	chr4	2.469907	5.29373	8.997121	0.002704	0.035779
hsa-miR-338-3p	chr17	-5.42373	2.4247609	8.958831	0.002761	0.035779
hsa-miR-199a-3p	chr19	3.081538	4.3007655	8.926641	0.00281	0.035779
hsa-miR-323a-3p	chr14	-3.70565	4.8942093	8.778075	0.003049	0.03808
hsa-miR-98-3p	chr8	-5.41038	2.4082323	8.648416	0.003273	0.04013
hsa-miR-2682-5p	chr1	2.407057	7.2944211	8.566853	0.003423	0.041205
hsa-let-7d-3p	chr9	-3.43439	7.5190379	8.393942	0.003765	0.044505
hsa-miR-122-5p	chr18	-4.44091	3.0241506	8.331172	0.003897	0.04526
hsa-miR-328-3p	chr16	-3.14837	5.5455648	8.291738	0.003983	0.045456
hsa-miR-597-3p	chr8	3.893616	3.3102441	8.251362	0.004072	0.045691
hsa-miR-548ao-3p	chr8	5.492478	2.4685463	8.212879	0.004159	0.045863
hsa-miR-372-3p	chr19	3.865788	3.2594223	8.175138	0.004247	0.045863
hsa-miR-4659a-3p	chr8	5.492478	2.4685463	8.154538	0.004295	0.045863
hsa-miR-3691-5p	chr16	5.492478	2.4685463	8.097273	0.004433	0.046177
hsa-miR-485-5p	chr14	-5.43541	2.4123409	8.084636	0.004464	0.046177
hsa-miR-369-5p	chr14	-3.42558	4.0415502	7.964503	0.00477	0.047314
hsa-miR-196a-3p	chr12	3.483345	3.6823701	7.958197	0.004787	0.047314
hsa-miR-187-3p	chr18	3.824204	3.2629259	7.957606	0.004789	0.047314
hsa-miR-548u	chr6	2.136299	6.0780429	7.863472	0.005044	0.048622
hsa-miR-548o-3p	chr7	2.632128	4.7902015	7.855073	0.005068	0.048622
hsa-miR-377-3p	chr14	-4.07126	3.3063933	7.670454	0.005613	0.052389

hsa-miR-573	chr4	2.533832	4.8411543	7.662799	0.005637	0.052389
hsa-miR-3127-5p	chr2	3.327382	3.5737832	7.643444	0.005698	0.052389
hsa-miR-490-3p	chr7	-5.16585	2.2770809	7.567163	0.005944	0.053257
hsa-miR-579-3p	chr5	3.715198	3.1590142	7.480956	0.006235	0.053257
hsa-miR-495-3p	chr14	-3.57425	4.1461033	7.430418	0.006413	0.053257
hsa-miR-543	chr14	-2.77738	6.8061615	7.419707	0.006451	0.053257
hsa-miR-126-3p	chr9	1.792786	12.074767	7.415971	0.006465	0.053257
hsa-miR-125b-5p	chr11, chr21	-2.11366	12.478931	7.412455	0.006477	0.053257
hsa-miR-127-5p	chr14	-5.20605	2.2852835	7.392657	0.006549	0.053257
hsa-miR-539-3p	chr14	-3.63397	3.7168493	7.387283	0.006569	0.053257
hsa-miR-23a-5p	chr19	-3.00936	4.6082631	7.385263	0.006576	0.053257
hsa-miR-10a-3p	chr17	2.230213	7.2016388	7.379602	0.006597	0.053257
hsa-let-7b-3p	chr9	-2.58209	5.2834221	7.30702	0.006869	0.054319
hsa-miR-296-3p	chr20	-2.67863	7.6420561	7.300799	0.006892	0.054319
hsa-miR-450b-5p	chrX	2.147228	7.6617199	7.251046	0.007086	0.055187
hsa-let-7f-2-3p	chrX	-2.46118	5.4015447	7.197493	0.007301	0.056197
hsa-miR-128-3p	chr2, chr3	-2.03285	11.215315	7.111267	0.00766	0.057844
hsa-miR-148b-3p	chr12	1.784121	10.907865	7.104476	0.007689	0.057844
hsa-miR-329-3p	chr14	-3.57835	2.979897	7.02224	0.00805	0.059505
hsa-miR-125b-2-3p	chr21	3.593308	3.1091984	7.013499	0.00809	0.059505
hsa-let-7a-3p	chr9, chr22	-2.21176	6.9095419	6.878635	0.008723	0.063459
hsa-miR-181a-2-3p	chr9	-2.13046	10.342785	6.852166	0.008853	0.063706
hsa-miR-2682-3p	chr1	3.336262	3.6144046	6.758249	0.009332	0.066424
hsa-miR-3129-3p	chr2	-4.93673	2.1479022	6.696228	0.009662	0.066532
hsa-miR-15b-5p	chr3	1.825168	10.230745	6.669626	0.009807	0.066532
hsa-miR-92a-1-5p	chr13	-2.438	8.2641077	6.654721	0.009889	0.066532
hsa-miR-758-3p	chr14	-2.84456	4.9815014	6.647138	0.009932	0.066532
hsa-miR-6866-5p	chr17	5.139035	2.2762212	6.646976	0.009932	0.066532
hsa-miR-642a-5p	chr19	5.139035	2.2762212	6.643882	0.00995	0.066532
hsa-miR-512-3p	chr19	5.139035	2.2762212	6.613384	0.010122	0.067004
hsa-miR-3116	chr1	5.139035	2.2762212	6.579103	0.010318	0.067631
hsa-miR-3200-3p	chr22	3.353912	2.9303525	6.443731	0.011134	0.072265
hsa-miR-33a-3p	chr22	2.766316	3.9288706	6.364888	0.01164	0.074813
hsa-miR-148a-3p	chr7	1.935925	12.639621	6.345345	0.011769	0.074914
hsa-miR-1185-1-3p	chr14	-2.74844	4.8972821	6.264789	0.012316	0.07765
hsa-miR-431-3p	chr14	-4.96702	2.1520145	6.236076	0.012517	0.078174
hsa-miR-548e-3p	chr10	1.857489	5.7167086	6.206615	0.012727	0.078743
hsa-miR-339-3p	chr7	-2.11746	9.259144	6.137829	0.013232	0.081107
hsa-miR-1910-5p	chr16	-3.04462	3.7401283	6.048531	0.013918	0.084529
hsa-miR-3940-5p	chr19	-5.52255	2.4205882	5.964598	0.014596	0.087295
hsa-miR-3139	chr4	4.923451	2.1681413	5.959638	0.014637	0.087295

hsa-miR-570-3p	chr3	4.923451	2.1681413	5.886894	0.015254	0.090162
hsa-miR-3170	chr13	4.923451	2.1681413	5.866616	0.015431	0.090399
hsa-miR-548k	chr11	1.894143	8.2768119	5.796123	0.016062	0.09327
hsa-miR-3677-3p	chr16	2.475676	4.2133491	5.723648	0.016738	0.096149
hsa-miR-889-3p	chr14	-2.7791	4.9132735	5.712154	0.016848	0.096149
hsa-miR-7-1-3p	chr9	1.764288	6.1247875	5.606257	0.017896	0.10126
hsa-miR-618	chr12	2.138383	4.9344568	5.476391	0.019275	0.107284
hsa-miR-224-5p	chrX	-1.94772	6.9168376	5.475387	0.019286	0.107284
hsa-miR-556-3p	chr1	2.211928	4.6062099	5.460845	0.019447	0.107284
hsa-miR-7-5p	chr9, chr15, chr19	1.743322	9.0592988	5.406258	0.020065	0.109775
hsa-miR-365a-5p	chr16	1.712045	6.8402291	5.371329	0.02047	0.110186
hsa-miR-1185-2-3p	chr14	-5.06289	2.1753721	5.371133	0.020473	0.110186
hsa-miR-643	chr19	3.135802	2.7983221	5.334908	0.020902	0.111592
hsa-miR-520g-3p	chr19	4.669893	2.0502485	5.202568	0.022554	0.119373
hsa-miR-3131	chr2	4.669893	2.0502485	5.166451	0.023027	0.119373
hsa-miR-597-5p	chr8	3.100262	2.8020182	5.16341	0.023068	0.119373
hsa-miR-195-5p	chr17	4.669893	2.0502485	5.159725	0.023117	0.119373
hsa-miR-9-3p	chr1, chr5, chr15	2.620518	3.5080849	5.148871	0.023261	0.119373
hsa-miR-34c-5p	chr11	-1.9367	5.545866	5.093011	0.024022	0.122091
hsa-miR-363-3p	chrX	-1.79728	6.3615813	5.083104	0.02416	0.122091
hsa-miR-374a-3p	chrX	1.696491	8.7016884	4.976214	0.025698	0.12888
hsa-miR-376c-3p	chr14	-2.75651	3.0566237	4.842516	0.027766	0.138205
hsa-miR-1303	chr5	2.000339	4.6920058	4.748333	0.029327	0.144883
hsa-miR-449c-5p	chr5	2.112273	4.3874344	4.731084	0.029622	0.145259
hsa-miR-299-3p	chr14	-2.73452	4.0777917	4.712507	0.029944	0.14528
hsa-miR-503-3p	chrX	-2.59151	3.727045	4.705543	0.030066	0.14528
hsa-miR-409-5p	chr14	-2.77587	3.0606133	4.605431	0.031871	0.152078
hsa-miR-30b-5p	chr8	1.513539	10.100684	4.602152	0.031932	0.152078
hsa-miR-1278	chr1	1.677183	7.1805861	4.587985	0.032197	0.152245
hsa-miR-580-3p	chr5	2.49057	3.4251131	4.5718	0.032502	0.1526
hsa-miR-1293	chr12	-2.64721	3.4468847	4.517648	0.033547	0.156395
hsa-miR-6511b-3p	chr16	-4.24142	1.8420774	4.436395	0.03518	0.159676
hsa-miR-148b-5p	chr12	1.663716	7.2717588	4.431588	0.03528	0.159676
hsa-miR-1268b	chr17	4.362065	1.920639	4.422736	0.035463	0.159676
hsa-miR-5000-3p	chr2	4.362065	1.920639	4.422736	0.035463	0.159676
hsa-miR-3136-5p	chr3	4.362065	1.920639	4.422736	0.035463	0.159676
hsa-miR-1294	chr5	-2.43317	3.6137166	4.411475	0.035698	0.159676
hsa-miR-4517	chr16	-4.21201	1.8338735	4.3789	0.036386	0.161663
hsa-miR-224-3p	chrX	-2.05186	4.832077	4.353778	0.036927	0.162147
hsa-miR-146a-3p	chr5	-4.19767	1.8297875	4.351093	0.036985	0.162147

hsa-miR-340-3p	chr5	1.569211	5.7601478	4.330719	0.03743	0.163019
hsa-miR-138-5p	chr3, chr16	-2.13388	6.5033582	4.267339	0.038852	0.168104
hsa-miR-26a-2-3p	chr12	-2.21646	4.1429851	4.207465	0.040246	0.173007
hsa-miR-590-3p	chr7	1.563978	7.111982	4.189975	0.040664	0.173673
hsa-miR-3935	chr16	-2.81498	2.4975099	4.151213	0.041605	0.176553
hsa-miR-151a-3p	chr8	1.430195	10.844449	4.116336	0.042471	0.178699
hsa-miR-138-1-3p	chr3	-2.79921	3.9424093	4.10921	0.04265	0.178699
hsa-miR-1272	chr15	2.478951	3.0055759	4.038241	0.04448	0.185194
hsa-miR-137	chr1	1.655684	6.9304506	3.971105	0.046287	0.191514
hsa-miR-374b-3p	chrX	1.506554	7.4790533	3.876637	0.048963	0.201324

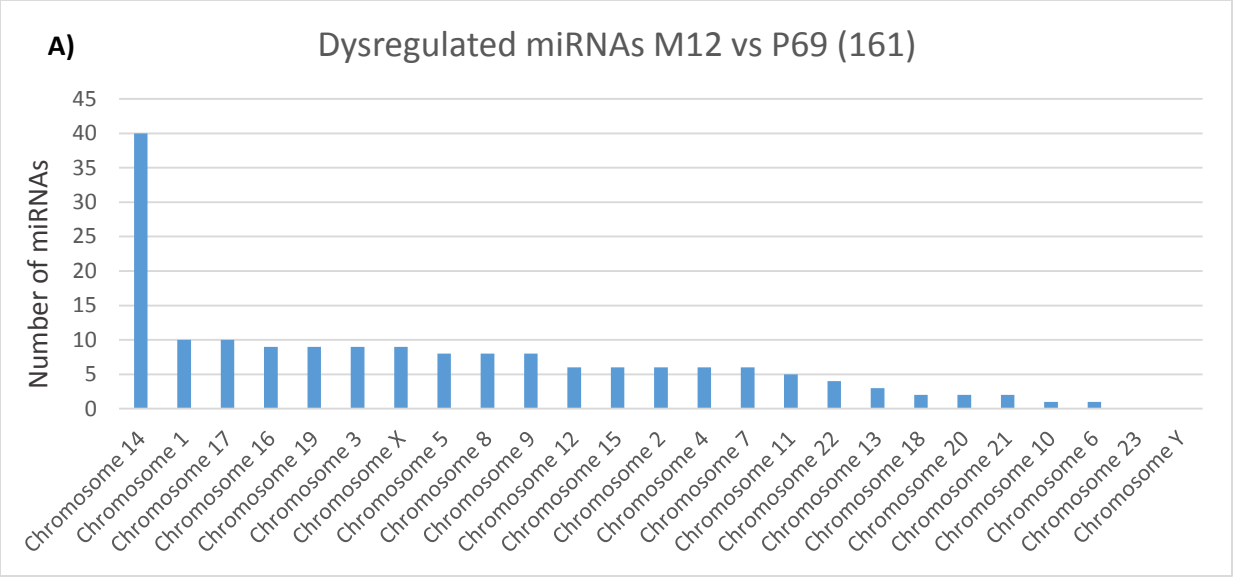

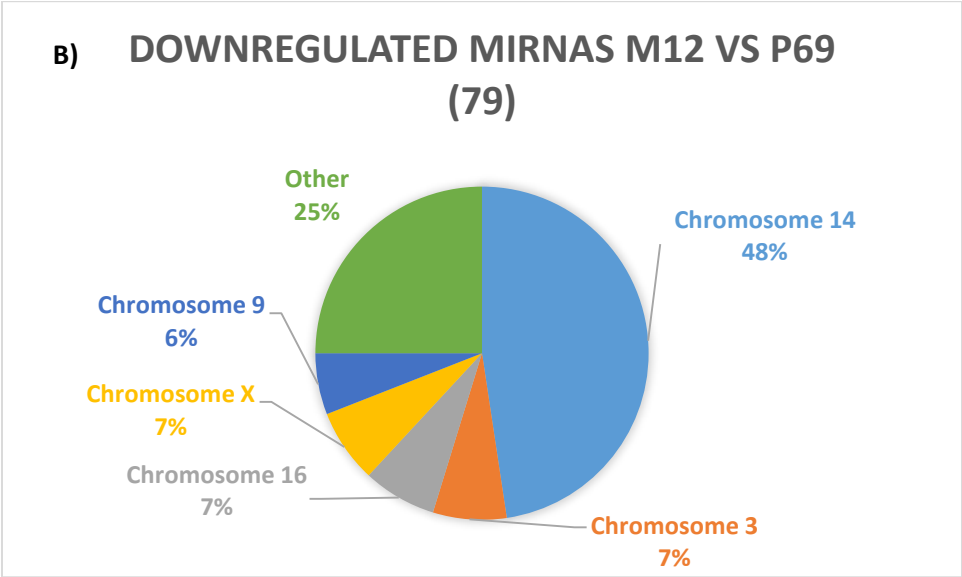

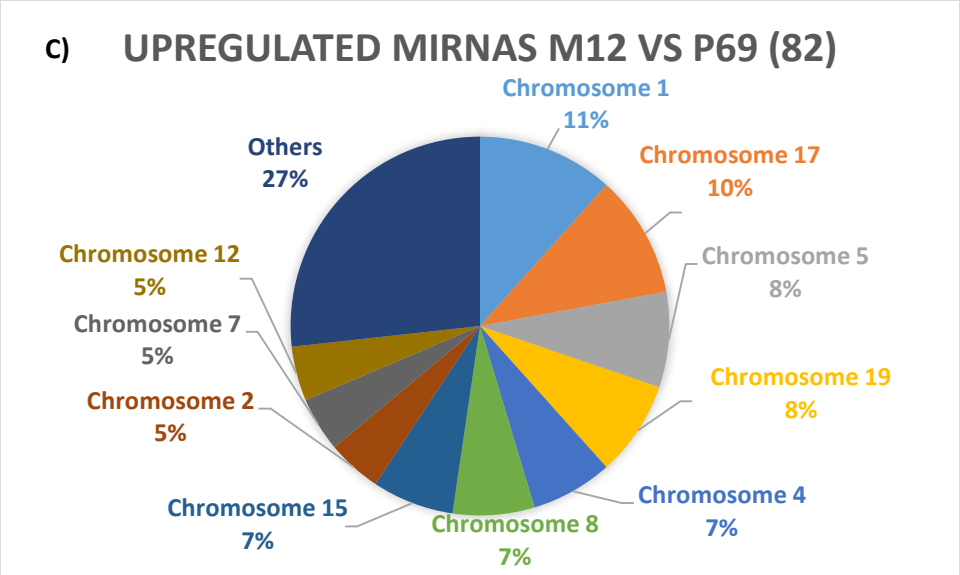

Figure 12: The chromosomal representation of dysregulated miRNAs between the P69 and M12 cell lines. A) A bar graph representing the total numbers of dysregulated miRNAs (both upregulated and downregulated) between the P69 and M12 cell lines segregated by the chromosomal location. The dysregulation of miRNAs on chromosome 14 can be seen to persist into this cell line from its immediate parent, the M2182 cell line. We can also see that the total number of dysregulated miRNAs in this cell line has increase by a 61% compared to its predecessor. B) A pie graph of only downregulated confirms that this trend. We can also see in B that the overall number of downregulated miRNAs in the M12 cell line is roughly the same as in the M2182 cell line (79 and 74 respectively). Despite losing a portion of chromosome 19, the number of dysregulated miRNAs encoded there is still comparable to M2182 levels. C) A pie graph of only upregulated miRNAs demonstrates that while distribution of dysregulated miRNAs between chromosomes is still relatively even, the overall number of upregulated miRNAs in the M12 (82) is more than 3 times the number of upregulated miRNAs in the M2182 cell line (26).

Here in the M12 cells we can see the number of downregulated miRNAs is comparable to the M2182 cell line (79 vs 74 respectively), and yet a there is a three-fold increase in upregulated miRNAs (82 vs 26 respectively). This is concomitant with the loss of chromosomes Y and 19p and with the acquisition of aggressiveness and the ability to form metastases.

It can be seen here that the downregulation of miRNAs on chromosome 14 persists into the M12 cells. Concomitant with the loss of chromosome 19p, the number of overall miRNAs on this chromosome has become slightly more significant, but there are as many upregulated as there are down regulated. This suggests that the loss of classical tumor suppressor genes encoded here may be of superior importance to prostate cancer progression than any putative tumor suppressor miRNAs. The number of miRNAs downregulated on chromosome Y is still zero, despite having lost this chromosome. This confirms that its established tumor suppressive effects on prostate cancer cell lines is not likely to have to do with any tumor suppressive miRNAs it might harbor.

Table 18: P69 vs F6

Gene Name	Chromosome	logFC	logCPM	LR	PValue	FDR
hsa-miR-34a-5p	chr1	5.28694	8.1245389	42.30434	7.81E-11	1.83E-08
hsa-miR-1269a	chr4	6.65214	6.1098223	42.19116	8.28E-11	1.83E-08
hsa-miR-675-5p	chr11	8.10835	4.4516836	23.98414	9.71E-07	4.59E-05
hsa-miR-505-3p	chrX	3.61660	6.2455042	19.62687	9.41E-06	0.000389
hsa-miR-125b-2-3p	chr21	5.33109	4.2350748	16.56261	4.71E-05	0.001558
hsa-miR-10b-5p	chr2	3.04822	11.270945	16.41801	5.08E-05	0.001601
hsa-miR-199a-3p	chr19	4.17014	4.969716	16.26473	5.51E-05	0.001657
hsa-miR-196a-5p	chr17	3.23062	8.4314117	16.07379	6.09E-05	0.001753
hsa-miR-10a-5p	chr17	2.41095	13.282397	14.04539	0.000178	0.004219
hsa-let-7i-5p	chr12	1.85346	16.45271	13.74265	0.00021	0.004786
hsa-miR-361-3p	chrX	2.80688	8.5085082	13.1887	0.000282	0.005826
hsa-miR-1250-5p	chr17	4.87268	3.8831863	12.97187	0.000316	0.006342
hsa-miR-139-5p	chr11	3.39115	5.1520331	12.91645	0.000326	0.006342
hsa-miR-642a-5p	chr19	6.08884	2.9559976	12.67369	0.000371	0.007014
hsa-miR-195-5p	chr17	6.08884	2.9559976	12.60353	0.000385	0.00708

hsa-miR-99a-5p	chr21	2.54264	7.1774488	11.59852	0.00066	0.010162
hsa-miR-664a-3p	chr1	2.88991	5.7458885	11.40007	0.000734	0.01105
hsa-miR-30a-5p	chr6	2.07473	11.818727	10.46181	0.001219	0.016135
hsa-miR-449c-5p	chr5	3.11206	4.9415651	10.01221	0.001555	0.019797
hsa-miR-221-5p	chrX	2.32529	6.6357527	9.819883	0.001726	0.021563
hsa-miR-1245a	chr2	5.58332	2.6647987	9.411507	0.002156	0.025954
hsa-miR-148a-3p	chr7	2.07778	12.681966	8.136702	0.004338	0.045033
hsa-miR-187-3p	chr18	3.88489	3.203581	8.130102	0.004354	0.045033
hsa-miR-181c-5p	chr19	2.91202	4.3529279	7.824303	0.005155	0.04875
hsa-miR-10a-3p	chr17	2.14456	7.0650517	7.670906	0.005612	0.050891
hsa-miR-130a-3p	chr11	2.00606	7.6840626	7.53043	0.006067	0.05334
hsa-miR-3200-3p	chr22	3.66418	3.0439327	7.490012	0.006204	0.05334
hsa-miR-152-3p	chr17	2.07854	8.9084374	7.447926	0.006351	0.053346
hsa-miR-590-5p	chr7	5.10988	2.4297758	7.443662	0.006366	0.053346
hsa-miR-548ao-3p	chr8	5.10988	2.4297758	7.418374	0.006456	0.053424
hsa-miR-509-3-5p	chrX	5.10988	2.4297758	7.392172	0.006551	0.053539
hsa-miR-4421	chr1	5.10988	2.4297758	7.344333	0.006727	0.054312
hsa-miR-10b-3p	chr2	3.07171	4.0258038	7.210032	0.00725	0.056463
hsa-miR-224-5p	chrX	1.97105	8.2978289	6.989162	0.0082	0.063125
hsa-miR-2682-5p	chr1	2.07079	6.9817644	6.873096	0.00875	0.065826
hsa-miR-196a-3p	chr12	3.26264	3.41058	6.851355	0.008857	0.065883
hsa-miR-16-5p	chr3, chr13	1.77086	11.285314	6.708965	0.009593	0.069786
hsa-miR-184	chr15	2.58788	4.3264753	6.239362	0.012494	0.087064
hsa-miR-195-3p	chr17	2.65931	4.1834736	6.214046	0.012674	0.087072
hsa-miR-2682-3p	chr1	3.21916	3.4147977	6.202327	0.012758	0.087072
hsa-miR-6500-3p	chr1	3.31461	2.8733581	6.144557	0.013182	0.088263
hsa-miR-597-3p	chr8	3.31459	2.8733581	6.142171	0.0132	0.088263
hsa-miR-3065-5p	chr17	3.38240	2.7541336	5.814981	0.01589	0.101855
hsa-miR-3127-5p	chr2	2.91935	3.2066061	5.636264	0.017593	0.109871
hsa-miR-452-5p	chrX	1.59653	11.241521	5.557691	0.0184	0.113097
hsa-miR-95-3p	chr4	1.95871	5.7080952	5.542424	0.018561	0.113097
hsa-miR-365a-5p	chr16	1.71798	6.7675464	5.473446	0.019308	0.113111
hsa-miR-374a-3p	chrX	1.77063	8.6879929	5.339528	0.020847	0.116626
hsa-miR-338-5p	chr17	2.33324	4.2922706	5.324789	0.021024	0.116626
hsa-miR-579-3p	chr5	3.15774	2.7721097	5.240973	0.022061	0.116626
hsa-miR-4691-3p	chr11	4.40050	2.1466227	5.202834	0.02255	0.116626
hsa-miR-3691-5p	chr16	4.40050	2.1466227	5.202834	0.02255	0.116626
hsa-miR-5000-3p	chr2	4.40050	2.1466227	5.202834	0.02255	0.116626
hsa-let-7g-3p	chr3	4.40050	2.1466227	5.202834	0.02255	0.116626
hsa-miR-943	chr4	4.40050	2.1466227	5.202834	0.02255	0.116626
hsa-miR-96-3p	chr7	4.40050	2.1466227	5.202834	0.02255	0.116626

hsa-miR-4474-3p	chr9	4.40050	2.1466227	5.202834	0.02255	0.116626
hsa-miR-1298-5p	chrX	4.40050	2.1466227	5.202834	0.02255	0.116626
hsa-miR-374c-5p	chrX	1.73857	8.7752367	5.129653	0.02352	0.119773
hsa-miR-548a-3p	chr6, chr8	3.12410	2.7767159	5.109919	0.023789	0.120218
hsa-miR-618	chr12	2.18522	4.8465448	4.956013	0.026	0.126295
hsa-miR-15b-5p	chr3	1.61895	10.047672	4.801022	0.028443	0.136443
hsa-miR-664b-3p	chrX	2.63479	3.0514968	4.765006	0.029044	0.138191
hsa-miR-126-3p	chr9	1.40233	11.787279	4.74413	0.029398	0.138191
hsa-miR-1257	chr20	2.63470	3.0514968	4.742083	0.029433	0.138191
hsa-let-7c-5p	chr21	1.55967	9.2199826	4.572925	0.032481	0.149323
hsa-miR-374a-5p	chrX	1.60071	8.875408	4.493051	0.034033	0.155378
hsa-let-7g-5p	chr3	1.13731	15.427259	4.292813	0.038274	0.165603
hsa-miR-454-3p	chr17	1.75129	5.1928679	4.120601	0.042364	0.18211
hsa-miR-4664-3p	chr8	2.36334	4.2477801	4.095113	0.043007	0.183683
hsa-miR-548ah-3p	chr4	2.28859	3.7609821	4.058521	0.043949	0.184141
hsa-miR-137	chr1	1.63693	6.8443564	3.993441	0.045678	0.188991

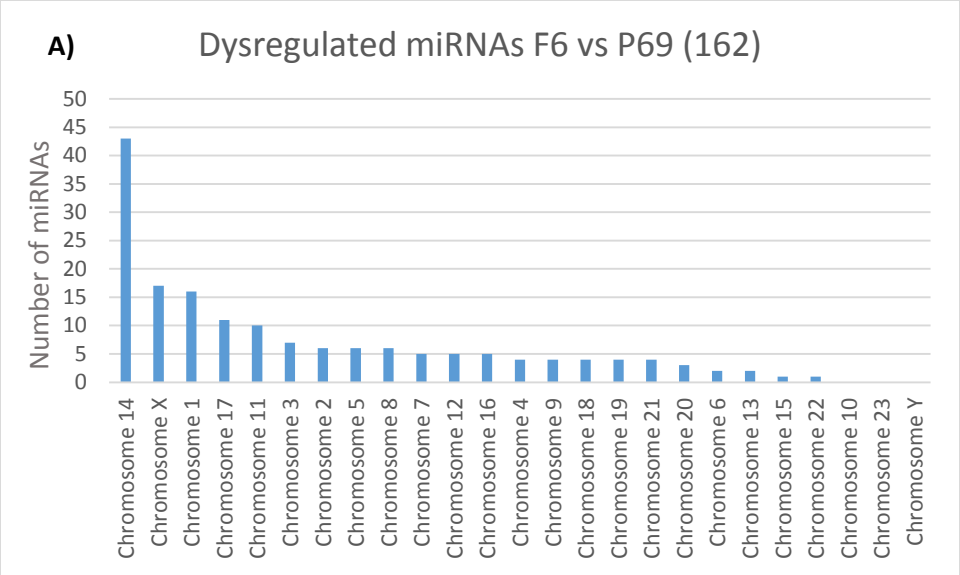

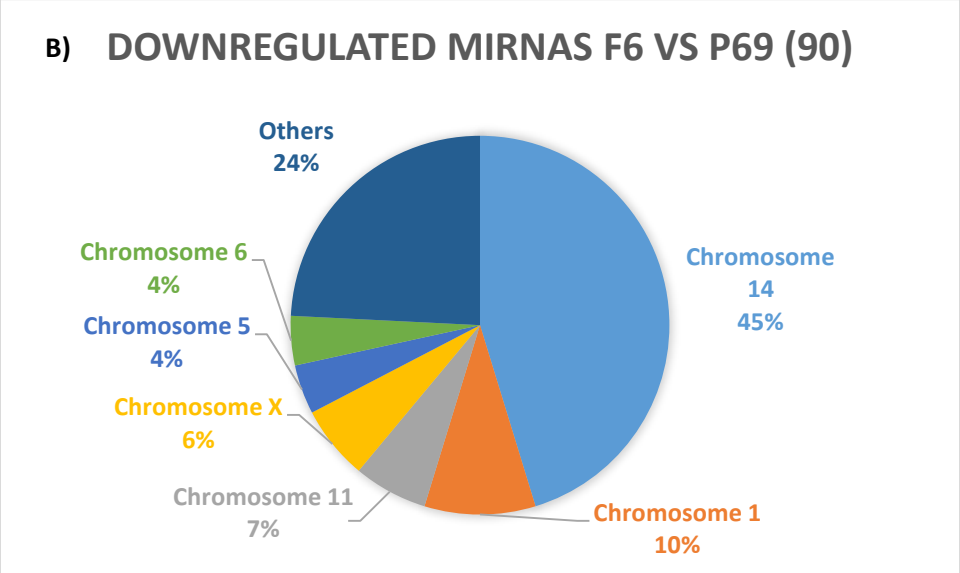

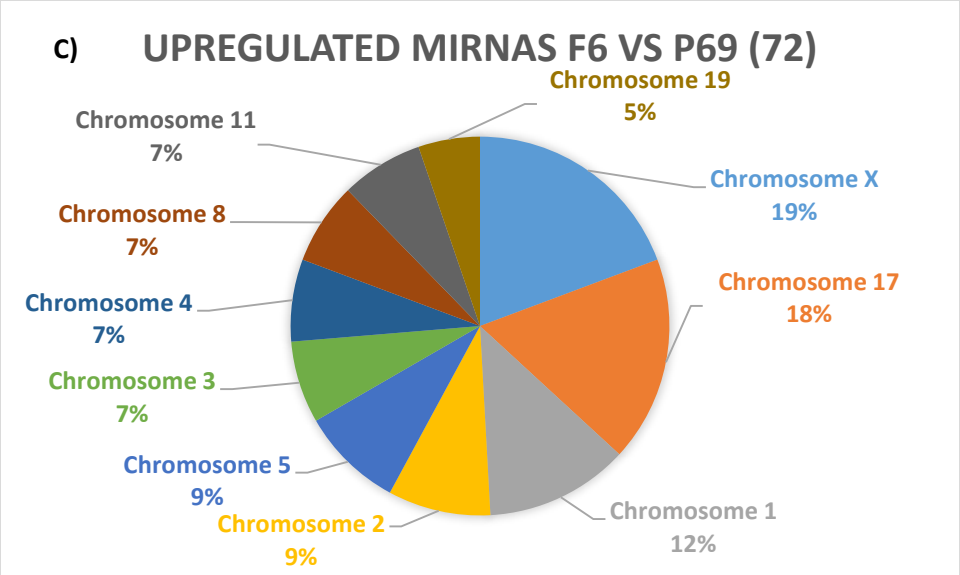

Figure 13: The chromosomal representation of dysregulated miRNAs between the P69 and F6 cell lines. A) A bar graph representing the total numbers of dysregulated miRNAs (both upregulated and downregulated) between the P69 and F6 cell lines segregated by the chromosomal location. The dysregulation of miRNAs on chromosome 14 can be seen to persist into this cell line as is has in both the M2182 and M12 cell lines. We can also see that the total number of dysregulated miRNAs in this cell line is almost the same as its immediate predecessor the M12 cell line (162 and 161 respectively). B) A pie graph of only downregulated miRNAs confirms that the suppression of miRNAs on chromosome 14 persists. We can also see in B that the overall number of downregulated miRNAs in the F6 cell line has increase to 90 from the 79 exhibited by the M12 cell line, despite the addition of a new chromosome 19. C) A pie graph of only upregulated miRNAs demonstrates that while distribution of dysregulated miRNAs between chromosomes is still relatively even, the overall number of upregulated miRNAs in the F6 (72) is slightly decreased compared to the M12 cell line (82).

Chromosome 19 harbors the largest cluster of miRNAs encoded in the human genome at 19q13.41. The Chromosome 19 megacluster (C19MC) harbors 46 miRNA genes whose expression is largely restricted to the placenta. Eight of these miRNAs have been demonstrated to target p21, a positive regulator of the cell cycle. It was also demonstrated that ectopic expression of a handful of these miRs resulted in G1 accumulation.[51] The portion of chromosome 19 that is lost in the M12 cell line does not include this area which therefore remains diploid. When a whole chromosome 19 is introduced to produce the F6 cell lines, this area becomes triploid. It is tempting to assume that the increased presence of this tumor suppressor encoding DNA accounts for the decreased tumorigenicity of the F6 compared to the M12 cell line, but the above F6 profile demonstrates that this is not the case as no large influx of expression on chromosome 19 is observed. It seems that in both this cell line and in the chr19 donor cell line, this giant miRNA cluster is effectively permanently silenced.

Table 19: Overall Sequencing Summary of miR expression in the parental p69 Cells compared to its subsequent variants

Cell Line (vs P69)	M2182	M12	F6
Upregulated	26	82	72
Downregulated	-74	-79	-90
Ratio	0.35	1.04	0.80
Tumors formed in mice[39.40]	2/3	13/13	6/15

One long recognized maxim of tumor biology is that tumor suppressors are more important to lose than oncogenes are to gain. This table illustrates that in the first step of this tumor progression model, tumorigenesis begins with a lasting knockdown of a large number of miRNAs. One of the most inscrutable things about prostate cancer is that, where in other cancers,

Dicer1 is usually downregulated, in prostate cancer Dicer1 is upregulated and the degree of this upregulation correlates with Gleason score.[80] In this case we detect a large number of miRs that are downregulated between M2182 and M12 compared to parental p69. On the other hand, there is a tremendous increase in the number of miRNAs that are upreguated (82) in the M12 cell line and only 26 in its immediate precursor M2181 with a slight decrease of only 10 in the F6 cell line. There results demonstrate that the acquisition of aggressiveness and metastasis in the late stage of a prostate cancer progression model is concomitant with massive upregulation of a select group of miRNAs that may function as oncomiRs.

Discussion

SNP Analysis

Since most seminal mutations that lead to prostate cancer later in life are actually acquired during the rapid expansion of this tissue during puberty, it cannot be assumed with certainty that each of the above SNPs were with this patient from birth. However, these are the SNPs present in the "normal" prostate epithelium taken from the patient before immortalization. After an exhaustive search in the literature, it was determined that the specific base changes reported by the SNP analysis were not likely to have effected tumorigenesis in a meaningful way.

The Early Downregulated miRs

The Chromosome 14 Cluster

Upon investigation, it was discovered that all of the miRNAs from chromosome 14 that are suppressed in the M2182, M12, and F6 cell lines are all located within the same paternally imprinted region of chromosome 14 referred to in humans as the Dlk-Dio3 area.[93] This area is a highly conserved region important to the development of mice and humans as demonstrated by the extreme phenotypes of altered gene dosages. This cluster also been dubbed the largest miRNA tumor suppressor cluster in mammals, the dysregulation of which plays an important role on the acquisition and maintenance of stemness, the EMT, and on metastasis to bone in prostate cancer.[24] Other cancers in which this entire cluster has been demonstrated to be silenced include gastrointestinal tumors, gliomas, neuroblastomas, ovarian cancer, and melanomas.[93] Our TGCA analysis confirms that on average, every single miRNA in this cluster is downregulated in tumors vs. normal epithelium. However the degree of this downregulation is variable between miRNAs, suggesting that some are suppressed more often than others. In fact, one miRNA, 544b-5p, seems to be upregulated, but this effect does not reach significance.

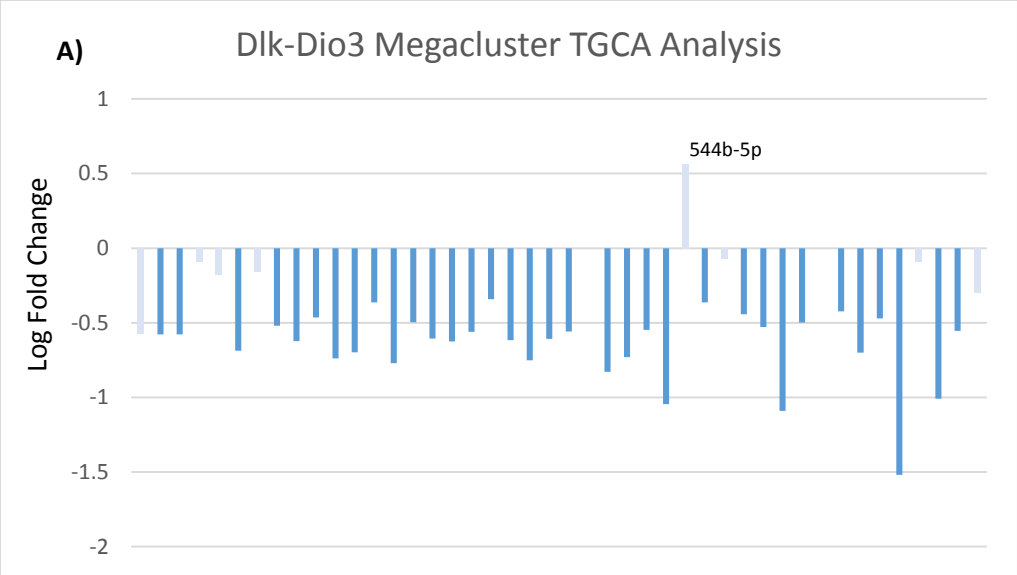

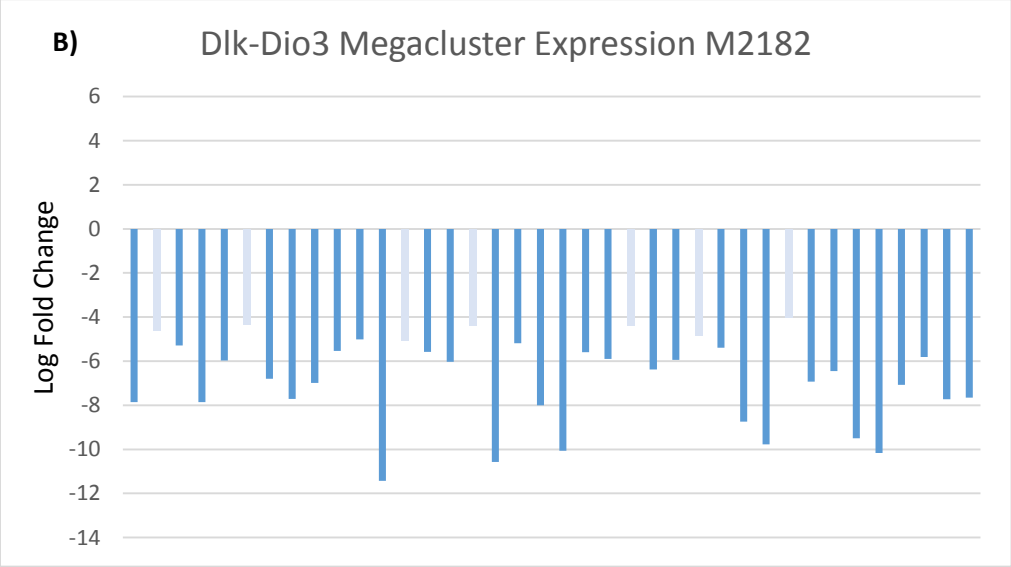

Figure 14: Suppression of the Dlk-Dio3 megacluster in prostate cancer. A) Dlk-Dio3 Megacluster Expression in Tumors vs Matched Normal Epithelium. B) Dlk-Dio3 Megacluster Expression in the P69 cell line vs the M2182 cell line. See tables 25 and 26 in the appendix for detailed legends. It should be noted that in the TGCA analysis (A), both arms of each miRNA are combined and reported as a single value while our sequencing data (B) reports on them separately. Light coloring implies a lack of statistical significance.

The regulation of imprinting for these genes is maintained by the maternal copy of an intergenic differentially methylated region (IG-DMR) centromeric to the cluster and to a lesser extent by a similar region telomeric to the cluster called MEG3-DMR. Uniparental disomy studies have demonstrated that these two regions alternatively control imprinting of the cluster in different parts to the body, with the IG-DMR being vastly dominant.[93] Interestingly, deletion of the maternal copy of the IG-DMR resulted in a loss of gene expression from the maternal copy, resulting in a paternal-like expression pattern resulting in miRNA silencing.

It has been demonstrated by previous studies involving small molecule inhibitors of histone acetylation and chromatin methylation that many of the members of the 14.32 megacluster are independently regulated and exhibit different expression patterns in different tumor types.[50] Many studies have also shown that a few of the miRNAs encoded here rise in expression in some cancers, ostensibly acting as oncogenes.[93] One explanation for the suppression that we see is that the members of this large cluster are simply silenced by methylation, and the presence of only one functional gene under normal circumstances makes this effect much more impactful. However, this doesn't explain why 100% of the members of this family that we do see are silenced and none of them seem capable of regaining expression at any stage of the cell line progression model. The apparent permanence and unanimous nature of the silencing of this cluster suggests that it is a result of a LOH event. Since the megacluster spans only 44.7 kbs, it is possible that a deletion of this area on the maternally inherited copy of the chromosome could have occurred without having been discovered by previous cytogenetic analyses. However, there are also other possibilities such as a classical somatic crossing over event[4] or aberrant regulation of imprinting caused by mutation.[93]

P53 degradation is primarily degraded by the mouse double minute 2 homolog (MDM2). While in other cancers, p53 deletion or mutation is usually required for tumor progression, it is almost never lost in prostate cancers which prefer to attenuate its action by over expressing MDM2.[2] Our SNP analysis demonstrates that there are two copies of p53 present in each of our cells lines and that neither of them harbor known inactivating mutations. Ectopic expression of Meg3, one of the genes expressed on the *paternal* allele opposite the active maternal miRNA megacluster, has been shown to increase the levels of p53 in a prostate cancer cell line by directly inhibiting MDM2.[96] A classical LOH event derived from somatic crossing over that would result in silencing of the maternally expressed megacluster would also result in a doubling of expression for the paternally expressed genes including Meg3. This would antagonize the suppression of p53 via MDM2 overexpression. While it is still possible that this is the case, it would be more beneficial to the budding prostate cancer cell to knock out the maternally expressed miRNAs via the deletion of the locus that encodes them or by deletion of the maternal copy of the centromeric IG-DMR.

The miR-200 Family

The miR-200 family is an evolutionarily conserved group of 8 miRNAs specific to epithelial tissues.[23] Its members include 141-5p, 141-3p, 200a-5p, 200a-3p, 200b-5p, 200b-3p, 200c-3p, 429-5p. Interestingly, although this family experiences coordinated expression, they are encoded on two separate transcripts: miR-200a, miR-200b, and miR-429 are generated from a single transcript on chromosome 1 while miR-200c and miR-141 are generated from a single transcript on chromosome 12.[86] Expression of this family is one the most potent inducers of epithelial differentiation, known to target ZEB1/2 via highly conserved targets on their 3' UTRs. The members of this conserved family are highly related in sequence and regulate many

processes related to cancer, including the EMT.[86] The miR-200 family participates in a negative feedback look with the transcription factors ZEB1 and ZEB2 to enforce either an epithelial or a mesenchymal phenotype in a mutually exclusive manner.[86] 200b also targets SNAIL1/2, another EMT factor that also must be repressed before the acquisition of pluripotency in IPCs.[86] All in all, the expression of this family is one the most potent inducers of epithelial differentiation that have been discovered.

miR-141 and miR-200c have been shown to attenuate Notch signaling in prostate cancer cells by directly targeting Jagged1, which led to impaired proliferation.[88] Notch signaling is critical for the growth of various tissues, including the prostate, and is often aberrantly expressed in late stage tumors, correlating with their acquisition of stem cell characteristics.

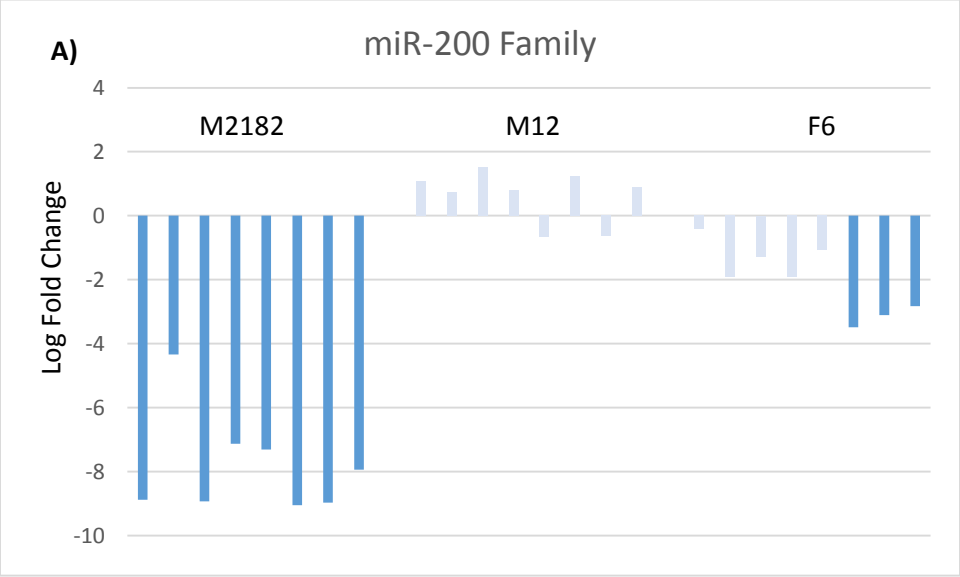

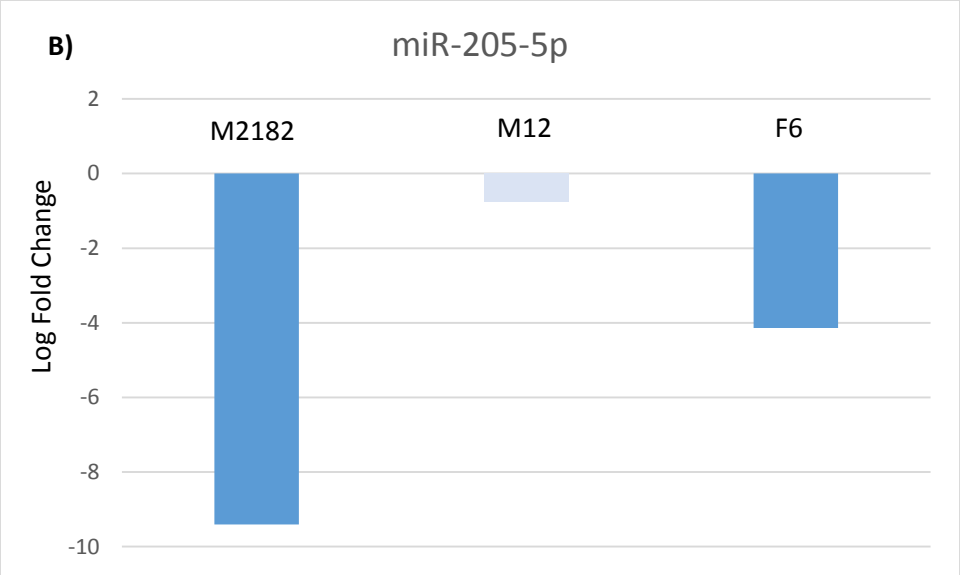

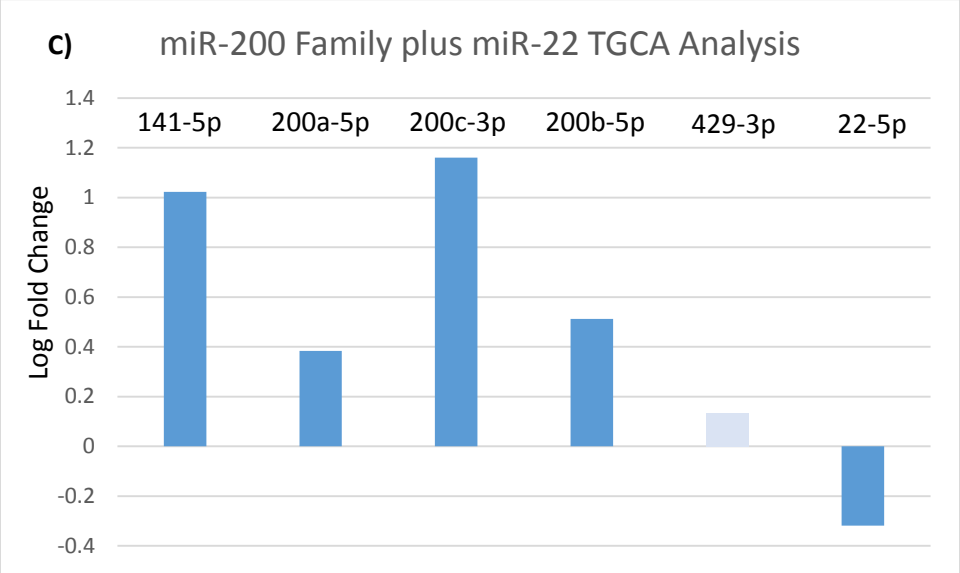

Figure 15: The Expression of the miR-200 Family and associated miRNAs over the Cancer Progression Model. A) The Expression of the miR-200 Family over the Cancer Progression Model. Here we can see a clear suppression early in the M2182 cell line, a return to P69 expression levels in the M12 cell line and a muted return of suppression in the F6 cell line. B) The expression of miR-205-5p, commonly reported to be correlated to the expression of the miR-200 family, mirrors their expression over the course of the progression model. C) The

expression of miR-22-5p in inversely correlated with miR-200 family expression in prostate tumor vs. matched normal epithelium. Light coloring implies a lack of statistical significance.

All eight members of this family display powerful suppression in the M2182 cell line. However, this repression disappears in the M12 cells where the expression of each one of these miRs is conspicuously similar to the P69 cell line. Then, in the F6 cell line, repression seem to resume for all of the members of the family, although only 3 of these reach statistical significance: miR-200b-3p, miR-200c-3p, and miR-429-5p. As described in the previous chapter, miR-205-5p shares multiple transcription factor targets with the miR-200 family and plays an equal part in the regulation of the EMT and MET as well as tissue stem cell proliferation. This miRNA shows the exact same expression pattern in our progression model as the miR-200 family members. They are all powerfully suppressed in the M2182 cell line, return to P69 expression levels in the M12 cell line, and then experience a muted return of suppression in the F6 cell line. This coordination of expression for multiple miRNAs transcribed on multiple transcripts suggests pathway activation/repression as opposed to a coincidence of random events such as an aberrant epigenetic mechanism or mutational promoter silencing.

The data from mature tumors demonstrates that the members of this family may actually be upregulated once tumorigenesis is achieved. It is important to point out that as the expression of the miR-200 family increases, the expression of miR-22-5p decreases by a -0.32 fold with a p-value of 1.25E-05. Collectively, these data suggest that a previously unidentified, transient suppression of the miR-200 family of miRNAs may play a role in prostate cancer progression.

It is known from studies on the rates of induction of pluripotency in adult somatic cells that a candidate cell's general expression profile at the time of application of the Yamanaka factors is the crucial determinate of its chance of successfully undergoing dedifferentiation. The miR-200 family of miRNAs powerfully enforce differentiation to the epithelial phenotype. The fact that we see a return to P69 levels of expression in the M12 cells seems counter intuitive to

the maxim that as a cancer progresses, it becomes more stem cell like.[4] Instead of thinking of the acquisition of stem cell characteristics as a general dedifferentiation process that extends to all of the cells of a tumor, we might try thinking of it as an expansion of the population of functional cancer stem cells present in the malignant tissue. In this case, the transient decrease in miR-200 family members could represent an opportunity for the developing cancer to expand its population of cancer stem cells by allowing all of the cells in the population to adopt a more stem cell like expression pattern and increasing activity of the Notch signaling pathway. This would increase the perpetually slim chance that a handful of them would successfully undergo dedifferentiation to pluripotency. This is supported by the observation made by another researcher that the tumor from which this cell line was derived was poorly differentiated.[39] The apparent return of expression in the M12 cells and in the mature tumors reported on in the TGCA analysis could represent a subsequent overall increase in the number of cells undergoing differentiation, which we could interpret as an expansion of transit amplification cause by the higher number of cancer stem cells.

One study demonstrated that an increase in miR-22 was partly responsible for expanding the mammary stem cell population by targeting the methylcytosine dioxygenase TET which is responsible for demethylating the miR-200 promoters.[58] Although the difference in expression of miR-22 between the M2182 and P69 does not reach statistical significance, there is a two-fold decrease in expression between the M2182 and M12 cell lines concomitant with relief of suppression of the miR-200 family in the M12 cells. Previous work in our laboratory has demonstrated that this miRNA plays an active role in the phenotype of these cells lines.[69] A high count per million (CPM) for miR-22-5p in both the M2182 and P69 cell lines suggest the reason that this miRNA does not change significantly is because it is already overexpressed in the P69

cell line. It could be that suppression of these promoters was made possible by overexpression of miR-22 (an absence of the on-switch TET) in the P69 cell line but that it took two rounds of in vivo selection for these genes to be silenced by other epigenetic phenomena (the off-switch).

The Late Upregulated miRNAs

miR10a and miR-196a

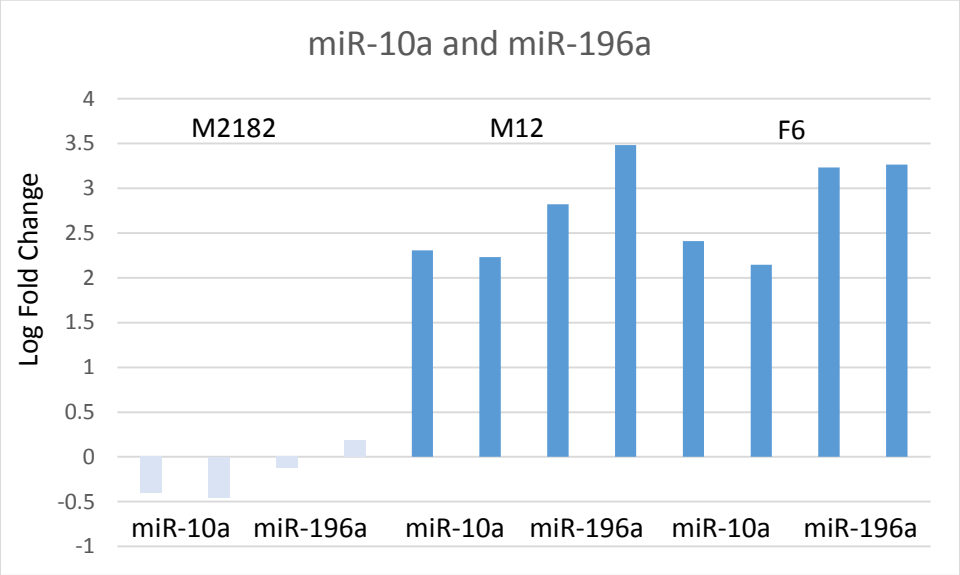

Figure 16: The Expression of miR-10a and miR196a (3p and 5p) in the Cancer Cell Line Progression Model. Strangely, it can be seen that the copy numbers of both the 3p and 5p arms of both miRNAs are roughly equal. Light coloring implies a lack of statistical significance.

miR-10 and miR-196 are both highly conserved miRNA families exclusive to vertebrates. They are both encoded in the intergenic regions between HOX genes and play important roles in developments. miR-10a is encoded on chromosome 17 in the region between HOXB4 and HOXB5, Two copies of 196a exist, one on chromosome 17 between HOXB9 and HOXB10 and one on chromosome 12 between HOXC9 and HOXC10.[89] The presence of these miRNA in the M12 cell line could reflect a higher degree of permissive chromatin structures facilitated by the loss of one copy of BRG1, possibly explaining the acquisition of upregulated miRNAs.

Important HOX gene targets of 196a include HOXB8, HOXC8, HOXD8, and HOXA7. 196a also regulates the HMGA family members and HMGA2 especially. The high mobility group AT-hook (HMGA) family part of the non-histone chromosomal high-mobility group is comprised of 2 proteins, HMGA1 and HMGA2. While not specifically altering the expression of any genes in particular, these proteins are a critical part of maintaining permissive and repressive chromatin structures. After embryogenesis, transcription of these proteins is tightly repressed by conserved targeting by the let-7 family of miRNAs such that expression of these two groups is mutually exclusive. In adults, the expression of these genes outside of embryogenesis is indicative of tumor formation. In ovo experiments in zebrafish have demonstrated that miR-196 regulates the axial skeleton through targeting components of the retinoic acid pathway, a pathway critical to prostate development.[89]

miR-10a has been demonstrated to work together with HOXB4 to repress expression of HOXA1, HOXA3, and HOXD10. Decreased expression of HOXD10 results in an increase in the expression of RhoA, RhoC, and Rho kinase which all facilitate tumor cell invasion. Some of its other targets include Ran and Pbp1 genes as well as the USF1/2 transcription factors. miR-10a binds directly downstream of the oligopyrimidine tract on the 5'-UTR of mRNAs encoding

ribosomal proteins, augmenting their translation. miR-10a overexpression has been observed in multiple solid cancer types.[90]

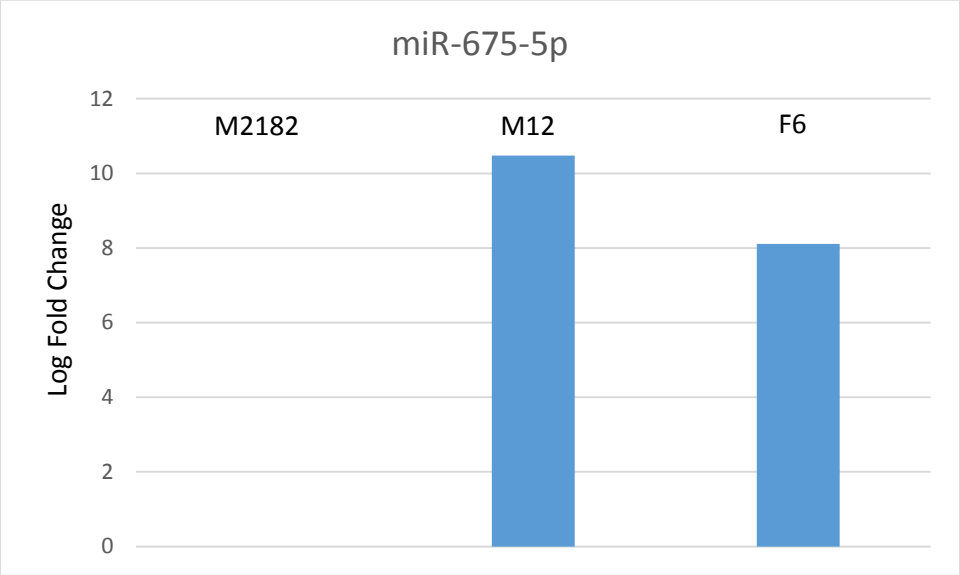

Figure 17: The Expression of miR-675 in the Cancer Cell Line Progression Model. Not a single read was recorded from the M2182, reflecting the extremely tight regulation of cleavage from H19. Light coloring implies a lack of statistical significance.

miR-675 is a tumor suppressor miRNA derived from the multifunctional lncRNA H19. H19, including the miR-675 stem loop, is one of the most highly expressed and conserved RNA transcripts in mammalian development.[94] In vivo, the liberation of 675 from H19 is tightly regulated, its only truly established role being the modulation of placental growth in the human embryo.

miR-675

miR-675 represses expression of p53 and pRB.[95] Overexpression can be caused by LOH at the imprinted region, a loss of p53, or through Myc activity. This has been demonstrated to lead to the activation of genes promoting proliferation, survival, and angiogenesis and has been implicated in multiple solid tumor types, usually correlating with severity of tumor grade.[92] This fits conceptually with its presence in the M12 cells as these would represent a very high tumor grade in our progression model. However it has been demonstrated to act as a tumor suppressor in multiple different cell line studies suggesting that it's action is complex.[94] Dual luciferase experiments have demonstrated that miR-675 targets the 3'-UTR of TGF-beta inducible protein, part of the TGF-beta pathway, which is well known to antagonize prostate cancer progression.[95]

Excision of miR-675 is regulated by the localization of the stress response RNA binding protein HuR from the nucleus to the cytoplasm. However it was also demonstrated through CHIP studies that 48 other proteins actively bound the H19 transcript in that area of the miR-675 stem loop. These included among others, Upfl, Zcchc11, and Luc71.[94]

H19

Although its expression is thought to be repressed in adult tissues, H19 itself has been reported to act as a both a tumor suppressor or an oncogene.[95] The presence of miR-675 in the

M12 and F6 cells demonstrates the presence of H19, although considering the tight regulation of miR-675 processing, it is unclear if it is the expression of H19 that is increasing or if it is just the processing of miR-675 that is increasing. It has been demonstrated that in the placenta, H19 functions as a vast reservoir of miR-675 precursor and that even at its peak miR-675 expression, only 1% of H19 is processed. However it has been demonstrated that ectopic expression of H19 in p69 cells and PC3 cells resulted in an increase in miR-675 expression.[95] Like miRNAs, lncRNAs have been well established contributors to the maintenance of the stem cell state, progenitor cell proliferation, mammalian development, differentiation, and cancer.[92] H19 is mediates allelic imprinting of many genes including the IGN locus, and is itself paternally imprinted along with the rest of the Igf2 locus. In adults, its expression is restricted to skeletal tissues after embryogenesis. H19 exerts its tumor suppressor action by coordinating with the methyl-CpG-binding domain harboring protein MBD1 to repress multiple genes including mesoderm-specific transcript homolog protein (MEST) and Igf2, the agonist for the IGFRs.[92] It is possible that H19 could have an oncogenic effect in the context of the M12 cells by acting as a molecular sponge for the let-7 miRNAs, which have been demonstrated to enforce the differentiated phenotype.[95]

The 548 Family

This extremely large and poorly conserved (only primates- like alu sequences) family of miRNAs is hypothesized to have expanded evolutionarily in connection to nearby transposable elements (TEs). In fact, a handful of these miRNAs have been demonstrated to be associated with active TEs in the body and it is possible that many more are as well. It has been proposed by others that the activation of TEs plays a part in aging and cancer progression. I propose that these miRNAs experience copy number increases as their nearby TEs become active.

miR-34a-5p

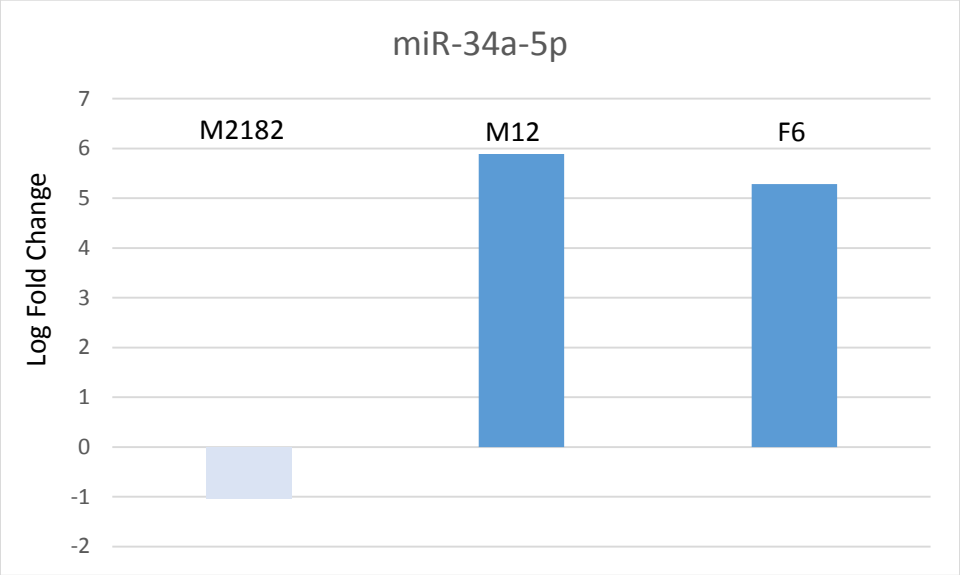

Figure 18: The Expression of miR-34a in the Cancer Cell Line Progression Model. miR-34a, an effector of p53, is a potent tumor suppressor and yet can be seen to be upregulated in the late stages of the model. Light coloring implies a lack of statistical significance.

Despite its well established tumor suppressor qualities, 34a is our second most significantly upregulated miRNA in the M12 cell line. 34a belongs to a family of evolutionarily conserved miRNA effectors of the tumor suppressor p53, augmenting apoptosis, senescence, and cell cycle arrest in many types of cancer.[91] It has also been demonstrated that miR-34a targets the 3-UTR of the AR receptor mRNA transcript in vivo.[52] Due to its tumor suppressive properties, it is usually seen to be downregulated in cancer but here we see that its mature form is the second most significantly upregulated miRs observed in the M12 cell line. It is important to note that p53 is rarely dysregulated in all but extremely late stage prostate cancers and that our SNP screen of these cell lines did not detect a DNA aberration of p53. It is likely that expression of this miRNA is activated by the low levels of p53 still active in our cells lines in response to the aberrant progression of the cell cycle. If a miRNA is found by sequencing in its mature form, it is likely that it is effectively bound by the RISC complex ready to perform its duties. This is because free mature miRs floating in the cytoplasm are usually degraded so fast that they cannot be significantly appreciated, and especially not in the concentration that is observed here for miR-34a. Considering our observation that this mature potent tumor suppressor miRNA is present in a 6 fold concentration in the M12 compared to the P69 and yet does not appear to be effecting its intended cell cycle arrest, it may be possible that its action is attenuated by a late actor such as a miRNA sponge like H19, RNA-binding proteins, circular RNAs (circRNAs), competitive pseudogenes, or many other possibilities.

The first anticancer miRNA mimic to reach phase 1 trials in April, 2013 was MRX34, a miR34a-5p mimic. The logic behind using miRNA mimics as cancer drugs is two-fold dependent on their large number of targets. It is thought that since miRNAs target entire pathways instead of just a single protein, their effect will be both more powerful and less susceptible to acquired

resistance by tumors. The fact that we see miR34a-5p specifically to be so powerfully upregulated in our most aggressive cell line, indicating an intact p53 pathway, suggests that this later point might not actually be the case. Apparently, there are more ways in which a cancerous cell can resist the effects of an ectopic miRNA rather than through somatic mutation of its targets binding sites.

The Rest

miR-9

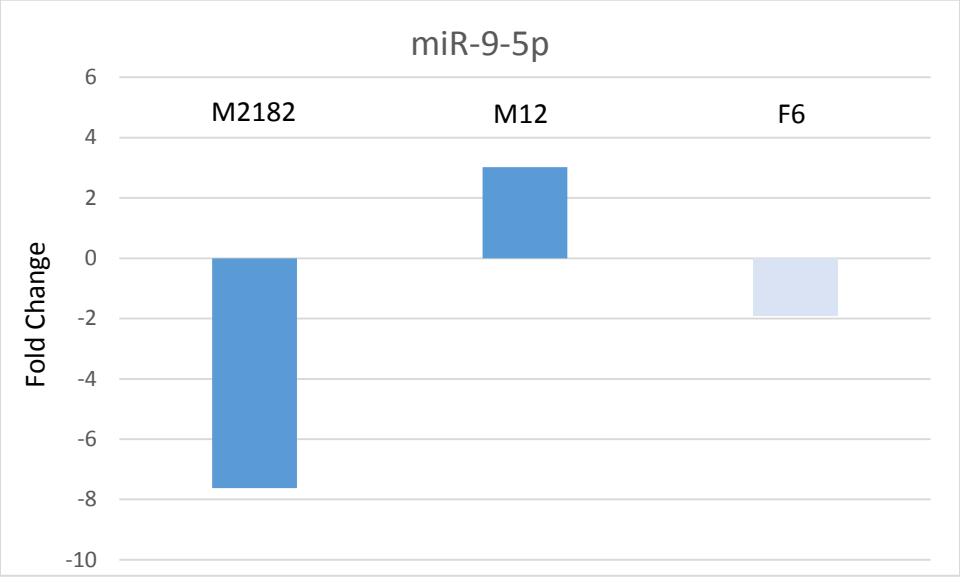

Figure 19: The Expression of miR-9 in the Cancer Cell Line Progression Model. miR-9-5p was found to be powerfully downregulated in the M2182s but powerfully upregulated in the M12s. Light coloring implies a lack of statistical significance.

Among its other functions, miR-9 has been found to target the 3'-UTR of the AR mRNA transcript.[52] However, previous work in our laboratory has demonstrated that miR-9 can also act as an oncomiR by repressing E-cadherin and SOCS5.[65] It could be that miR-9's biphasic expression is a result of its mixed effects on cancer progression, first being suppressed during the early, more androgen dependent stage of prostate cancer progression due to its targeting of the AR mRNA transcript, and then upregulated in the late, near-androgen independent stage of the progression model when AR expression is more robust.

miR146a-5p

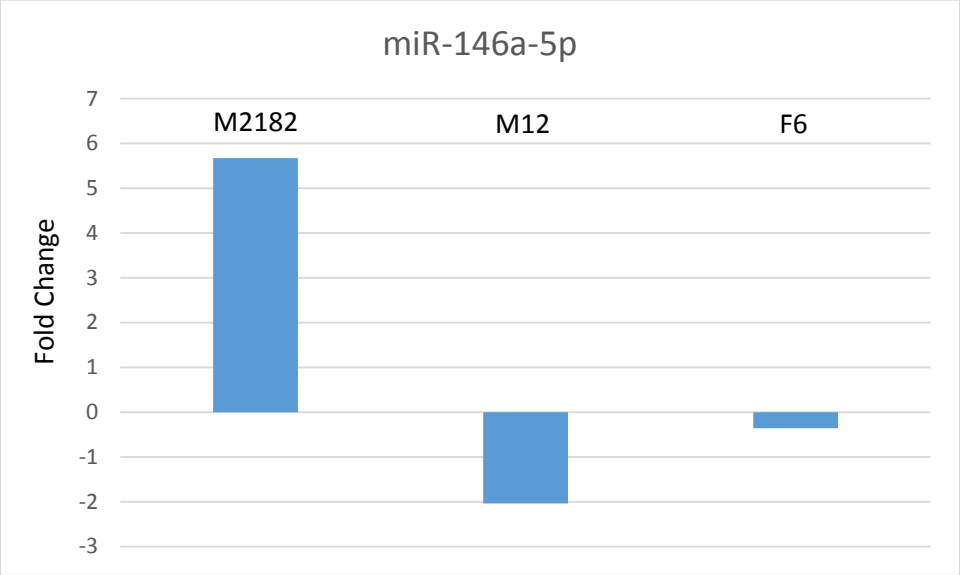

Figure 20: The Expression of miR-146a in the Cancer Cell Line Progression Model. The tumor suppressor miRNA 146a-5p demonstrates the exact opposite expression pattern as miR-9 above. Light coloring implies a lack of statistical significance.

One study found that miR-146a-5p was dramatically upregulated in an androgen dependent prostate cancer cells while it was dramatically down regulated in androgen independent prostate cancer cells.[80] Similarly, miR-146a is the #1 most upregulated miRNA in our M2182 cell line where it is expressed at almost 6 fold the levels of the p69 cell line. Yet it is significantly downregulated in the M12 cell line. The M12 cells, while not totally androgen dependent, need very little androgen compared to truly androgen dependent prostate cancer cell lines. Forced expression of 146a in the PC3 prostate cancer cell line resulted in inhibition of migration, proliferation, invasion, and metastasis via silencing of the HA/ROCK1 pathway.[80] It could be that miR-146a-5p is a tumor suppressor activated in early tumorigenesis as a response to the aberrant cell cycle progression and that this activation is eventually overcome.

Literature Search- Tumor suppressors lost with chromosome 19p

In an experiment involving MMCT of variable fragments of chromosome 19 into another cell line, one investigator came to the conclusion that there must be a tumor suppressor in the region of chr19p13.1-13.2.[39] Another study of 37 CRPC tumors demonstrated that a loss of chromosome 19 with a minimal overlap generally centered on 19p13.1 was the most common late stage chromosomal event.[40] There has been much investigation into possible tumor suppressors that may lie on the short arm of chromosome 19 since the creation of these cell lines. A literature search produced two convincing candidate tumor suppressors, STK11 and BRG1, that both coincidentally happen to lie close together on 19p13.2.

STK11 is a 433 amino acid serine-threonine kinase with a nuclear localization signal that functions in complex with the pseudokinase STE20-related adapter and the armadillo repeat scaffolding-like protein MO25.[82] It's most well studied activity is its regulation of the cellular energy checkpoint through the phosphorylation and activation of adenosine monophosphate

kinase (AMPK). When the ratio between AMP and ATP inside the cell reaches a critical threshold, this complex activates AMPK, which proceeds to modulate its downstream targets, arresting the cell cycle. It is postulated that deregulation of this checkpoint is important for tumorigenesis in that it allows for high energy processes such as DNA replication to proceed under conditions of energetic stress. Germline mutations in this gene cause the cancer prone disease Peutz-Jeghers syndrome in humans which, among other things, causes hamarrtomatous polyps of the gastrointestinal tract. Heterozygous mice survive to adulthood but also have gastrointestinal polyps similar to what happens in humans.[82]

It has been observed that STK11 mutations accumulate in less differentiated tumors of various cell types.[82] It has also been demonstrated that STK11 mutations occur in about half of all NSCLCs, by way of large deletions or nonsense mutations, and is the third most altered gene in lung adenocarcinomas after TP53 and KRAS.[82] STK11 alterations are found most often to be concomitant with alterations in KRAS, TP53, P16, MYC, PIK3CA, and BRG1 but almost never with alterations in EGFR.[82] Previous proteomic analysis in our lab demonstrated that EGFR plays an active role in growth signaling in the P69, M2182, and M12 cell lines. Also, as is common in prostate cancer, proteomic analysis demonstrated an upregulation of the PI3K pathway in M12's compared to parental p69 cells, which together with the loss of STK11 may further promote tumorigenesis in vivo.

STK11 has also been linked to the regulation of cell polarity. One study reported that STK11 expression induces complete polarization in intestinal epithelial cell cells in a cell-autonomous fashion. This is important because previous work in our laboratory has demonstrated that the loss of the ability of M12 cells to form acini in lrECM 3D cultures, as compared to their parental cell line, was concomitant with the loss of the polarization of alpha-

6/beta-1 integrins. This polarization and acini forming ability was restored by the return of chromosome 19 in the F6 cells. STK11 deficient mice have reduced TGF-Beta activity in endothelial cells which allows for a permissive environment for epithelial expansion. That the TGF-Beta pathway antagonizes prostate cancer progression is well documented. This may be exemplified by the fact that tissue specific knockout of STK11 has been demonstrated to lead to prostate intraepithelial neoplasia in mice, a condition thought to precede prostate cancer.[82]

STK11 also regulates the levels of cyclooxygenase-2 and the transcription factor Ets Variant 4 (ETV4).[82] ETV4 is a member of the winged helix-turn-helix superfamily associated with transcriptional misregulation and the upregulated expression of matrix metalloproteinases and other genes associated with invasion and metastasis.[83] This specific TF has been demonstrated to be commonly upregulated by a translocation that results in a fusion with TMPRSS2 (TMPRSS2:ETS fusion), the single most prominent molecular hallmark of prostate cancer. It is activated by sumoylation in response to MAPK/ERK pathway activity downstream of the ERbB2/ERbB3 heterodimer. Previous proteomic data in our laboratory has demonstrated the significant upregulation of both ErbB2/ErbB3 and the downstream MAPK/ERK pathway in M12 cells compared to P69 cells (See Table 20 below). Interacting proteins, as predicted by STRING UniProtKB I2D with a STRING value of 1 and reported in ETV4's genecard, includes HOX4D, possibly coordinating with the action of miR-10a-5p in the M12 cell line as described in the discussion section.[83]

Brahma/SWI2-related gene 1 (BRG1) is a critical component of the SWI/SNF chromatin remodeling complex. It features a bromodomain and Helicase/ATPase activity and can regulate transcriptional activation or repression by remodeling chromatin structure. This gene is also seen

to experience inhibiting point mutations and deletions in prostate cancer cell lines and in lung cancers that undergo LOH. BRG1 is also located at 19p13.2, only 10 Mb from STK11. One study demonstrated that inactivating mutations in this gene are common to one third of all NSCLC cell lines.[82] Although it is true that the protein Brahma (BRM) can partially substitute for BRG1 in the SWI/SNF complex, it has been observed that mice heterozygous for Brg1 are prone to developing epithelial tumors, despite full activity of BRM.[82] This may be due to the loss of BRG1 SWI/SNF's activity downstream of the retinoblastoma protein. It was also established that a tissue specific homozygous knockout of BRG1 in mice produced fewer tumors than their heterozygous littermates suggesting that retention of a single BRG1 allele (as is the case in the M12 cell line) may provide some anti-apoptotic protection. The auxiliary functions of the BRG1 containing SWI/SNF complex include regulation of cell growth, differentiation, and general DNA repair. It has also been demonstrated to interact with BRCA1 directly during homologous recombination after DNA damage.[82]

The SWI/SNF complex containing BRG1 is also involved in transcriptional modulation of hormone responsive promoters in response to hormone receptor activation, including the AR, through direct binding of hormone receptors and their target promoters.[82] One study reported that BRG1 and not BRM was required along with the rest of the SWI/SNF complex and the tumor suppressor Prohibitin to silence AR responsive genes during hormone ablation therapy of prostate cancer.[81] It could be that the loss of one copy of this gene in the M12s could facilitate their partial androgen independence.

Surprisingly, one study discovered that STK11 and BRG1 interact in the cell. That study demonstrated that STK11 had the capability to bind and regulate the chromatin remodeling activity of the BRG1 containing SWI/SNF in vivo and that the ATPase activity of BRG1 is

enhanced in its presence. The independent inactivation of these two genes often occurs concomitantly in many different types of cancers, including prostate cancer, through somatic mutation. This suggests that the effects of their simultaneous loss may cooperate in cancer progression.[82] Mouse studies have demonstrated that heterozygosity for either of these genes alone results in a tumor susceptibility syndrome making both of these haplo-insufficient tumor suppressors. Interestingly, our SNP analysis uncovered two STK11 mutations described below.

Low vs. High copy numbers

Due to the heterogeneous nature of microRNA function, it is difficult to draw conclusions about the relative impact of differential expression in high versus low copy number microRNAs. It is a good idea to evaluate differential expression in these two categories separately. Previous NGS studies have demonstrated that a handful of microRNAs (less than 20) represent the majority of cellular microRNA expression (more than 80%) in tissues.[57] In the case of neurons, the highest messenger RNA (mRNA) levels seen are below 2500 copies per cell with the vast majority of cells having a peak mRNA copy number for any particular gene being far below that. In the same cells, a high copy number miRNA, of which there are just a handful, could be present at 25,000 or more copy numbers.[60] A 10% increase in expression of one of these microRNAs might result in a 2500 copy number change, where as a 1000% increase in a low copy number microRNA originally expressed at 20 copies per cell would result in a an increase of only 180 copies. It seems logical to assume that changes in high copy number miRNAs will have a more physiological effect on the cell and this opinion is highly expressed in the current literature. However, it is this author's opinion that so little is known about the mechanisms of miRNA action that it is dangerous to discount them. Low expression miRNAs could easily be

part of amplification cascades, positive and negative loops with other miRNAs and transcription factors, or they could even be localized at more appreciable concentrations in a specific part of the cell where they act. That means that the concentration of one of these miRNAs could very well have a large impact on the cell state. It is for these reasons that particular attention was given to miRNA abundancy, as it directly informs any possible downstream hypotheses or conclusions about the roles of miRNAs described in our results.

Oncomirs and Tumor Suppressors miRs: The Reductionist's Approach

Since the expression of a particular miRNA and that of its target are inversely related, a miRNA that is upregulated in cancer, is assumed to target a classic tumor suppressor gene and is referred to as an oncomiR. Accordingly, a miRNA that is downregulated in cancer is assumed to target a classic oncogene and is known as a tumor suppressor miR. This classification is supported by the observation made by many that a number of miRNAs experience the same kind of selection pressures and genomic alterations as classical oncogenes and tumor suppressors such as amplifications, deletions, point mutations, translocations, and loss of heterozygosity. In fact, although miRNA's only represent less than 3% of the human genome[7,10], more than half of them are located in commonly amplified or deleted regions.[32] Certain human miRNAs have even been co-opted by cancer causing viruses, reminiscent of the very first oncogenes ever to be discovered, ras, myc and sarc.[4] A 2009 study determined that miR-127-5p was a central player in the development of Epstein Barr Virus positive Burkitt's Lymphoma possibly through its effect on the expression of the master regulators of B-cell differentiation, BLIMP-1 and XBP-1.[48] These and other examples demonstrate that miRNA expression is still powerfully selected for or against in a way that suggests oncogenic or tumor suppressive power. However, this concept is

complicated by the fact that miRNAs demonstrate both oncomiR and tumor suppressive activity in different tumor tissues.

Considering that miRNA expression profiles correlate with cell type and differentiation state better than any other type of biological molecule, it may be that there is more to the role of miRNAs in the biology of the cancer than can be adequately expressed with the "oncomiR" and "tumor suppressor miR" terminology. It may be more helpful to think of miRNAs in terms of their association with different cell states or modular programs. miRNAs commonly target hundreds of mRNAs at once and thinking of them only in terms of the specific tumor suppressors or oncogenes that they inhibit in a 1:1 ratio is unnecessarily laborious. For instance, members of the Let-7 family have been shown to negatively regulate the Myc, Ras, and HGMA2 proto-oncogenes,[21] leading to their initial classification as tumor suppressor miRs. However, something that is far more valuable to understand is the fact that the double negative nature of the relationship between the let7 family and the LIN28 RNA binding protein (RBP), which is activated by Myc,[66] creates a mutually exclusive expression pattern governing the exit of the stem cell state and entry into the differentiation program. It has been demonstrated that this shift in expression musts be reversed during the reprogramming of induced pluripotent stem cells (IPCs).[68] This could mean that let7 family expression must be reversed in order for the acquisition of stem cell characteristics by would be cancer cells.

Understanding how a particular miRNA or miRNA family affects the biology of the cell naturally involves the genes that they target, but adopting a reductionist's approach may lead us to miss the forest for the trees. I think that it is more important, at this point in our understanding of ncRNA biology, to focus on how and why miRNAs are associated with particular cell states and work backward from there.

Thoughts for the Future- Considering Proteomic Data

The most promising application of miRNA profiling information is its integration with corresponding genomic, proteomic, and metabolomic data. From this approach it may finally be possible to get a whole picture of the living cell. Below are a few examples of promising areas of investigation that come to light when considering the transcriptomic data presented in this study and proteomic data conducted on these cell lines previously.

Table 20: RPMA Analysis Shows Increased Protein Expression from the PI3K/RAS pathways in M12 versus p69 Cell Lines (original title).

Protein	Fold change
ErbB2	1.8
ErbB3	2.0
PI3K	1.4
p-BAD	1.7
MET	1.3
pERK	4.0

Table adapted from reference 69.

EGFR has been demonstrated to play a surprising role in miRNA biogenesis. As just one example of many, under hypoxic conditions, such as those which occur in the center of tumors pre-angiogenesis[4], EGFR is internalized in cells in association with late stage endosomes, where it phosphorylates human AGO2 at Y393, causing AGO2 to dissociate from Dicer1.[61] Through a poorly described mechanism, this leads to a decrease in activity for a specific set of tumor suppressor miRNAs with a characteristic long loop structure in their pri-miRNA.[66] This has been

demonstrated to increase cell survival and invasion in HeLa and MDA-MB-231 cell lines. It has been established that prostate epithelial cells require EGF in culture and that EGF is abundant in the prostate as a normal part of its growth and function. However, our cell lines exhibit interesting EGFR phenomena. As evidenced by previous research performed in our laboratory, both ErbB2 and ErbB3 are upregulated by two fold in the M12 cell line compared to the P69[69] cell line while the expression of EGFR itself was demonstrated to be downregulated 6 fold over all with a specific 4 fold decrease on the surface of the M2182 and M12 cells. This was all concomitant with a 3 fold increase in TGF-alpha expression, an EGF-like peptide, demonstrating a possible autocrine loop adopted by these cells.[39] In support of this, addition of a TGF-alpha neutralizing antibody arrested growth in this cell line. It could be that the observed decrease in EGFR expression is in response to the overexpression of TGF-alpha which is a common feature of autocrine loops of this kind.[4] However, why this does not lead to the decrease in ErbB2 and ErbB3 remains to be investigated. One explanation may be dysregulation of growth inhibitory miRNAs that usually play a large part in the negative feedback mechanism governing expression of these receptors. For instance, it was demonstrated previously in our lab that the 3'-UTR for ErbB2 contains two perfect match binding sites for miR-125b-5p, a miRNA that iscommonly reported to be downregulated in prostate cancer and lost in our M2182 and M12 cell lines.

A handful of let7 family miRNAs are significantly downregulated in the M12 cell line compared to the P69 cell line while others seem to be upregulated. A previous researcher in our laboratory identified an activation of the Ser/Thr kinase ERK (MAPK) in connection to an increase in miR-22-5p and a decrease in miR-125b-5p. ERK activation results in the inhibition of KSRB, an RBP that promotes the let7 family processing exactly antagonistic to LIN28 by binding to the same terminal loop in the pre-miRNA transcripts that produce them. ERK

activation also results in phosphorylation of TRBP at four different serine residues which leads to an increase in Drosha/DGCR8 stability and activity in the nucleus. However, while increasing the activity of a majority of mature miRNAs in this way, phosphorylation of TRBP simultaneously directly downregulates the let7 family of miRNAs through a separate but unidentified mechanism.[66] Apart from the those mentioned above, it is likely that there could be anywhere between tens to hundreds of analogous RBPs that effect the production of specific let-7 family members over others under different conditions. More research incorporating large proteomic data with high throughput RNA sequencing is needed to illuminate these subtle mechanisms.

Apo-AGO proteins and apo-Dicer are usually marked by polyubiquitination and degradation via autophagy involving the selective autophagy receptor NDP52.[66] A common hallmark of prostate cancer is a deficiency of autophagic processes through loss of beclin1 and overexpression of mTOR via PI3K/AKT activation.[8,16] This phenomenon could help explain why in prostate cancer, miRNA expression is generally downregulated, but Dicer1 expression is commonly seen to be upregulated. While previous work in our laboratory has centered on the increase in PI3K activity and expression mentioned above, we have yet to focus on how the activation of this pathway might affect miRNA processing in general.

Bibliography

Bibliography

1) Lawrie, Charles H. "MicroRNAs: A Brief Introduction." *MicroRNAs in Medicine*. 1st ed. N.p.: John Wiley & Sons, 2013. 1-15. Print.

2) Lawrie, Charles H. "MicroRNAs in Human Prostate Cancer: From Pathogenesis to Therapeutic Implications." *MicroRNAs in Medicine*. 1st ed. N.p.: John Wiley & Sons, 2013. 311-321. Print.

3) Berindan-Neagoe, I., and G. A. Calin. "Molecular Pathways: MicroRNAs, Cancer Cells, and Microenvironment." *Clinical Cancer Research* 20.24 (2014): 6247-253. Web.

4) Weinberg, Robert A. *Biology of Cancer*. S.l.: Garland Science, 2013. Print.

5) Costello, Anthony J., and Niall M. Corcoran. "Development, Applied, and Surgical Anatomy of the Prostate." *Prostate Cancer a Comprehensive Perspective*. By Ashutosh Tewari. Dordrecht: Springer, 2014. 3-17. Print.

6) Maitland, Norman J. "Stem Cells in the Normal and Malignant Prostate."*Prostate Cancer Biochemistry, Molecular Biology and Genetics*. By Donald J. Tindall. Dordrecht: Springer, 2013. 3-31. Print.

7) Bouyssou, Juliette M.c., Salomon Manier, Daisy Huynh, Samar Issa, Aldo M. Roccaro, and Irene M. Ghobrial. "Regulation of MicroRNAs in Cancer Metastasis." *Biochimica Et Biophysica Acta (BBA) - Reviews on Cancer*1845.2 (2014): 255-65. Web.

8) Merolla, Francesco. *Prostate Cancer: Shifting from Morphology to Biology*. By Stefania Staibano. Dordrecht: Springer Science, 2013. 57-69. Print.

9) Su, Yinghan, Xiaoya Li, Weidan Ji, Bin Sun, Can Xu, Zhaoshen Li, Guojun Qian, and Changqing Su. "Small Molecule with Big Role: MicroRNAs in Cancer Metastatic Microenvironments." *Cancer Letters* (2013): n. pag. Web.

10) Gordanpour, A., R. K. Nam, L. Sugar, and A. Seth. "MicroRNAs in Prostate Cancer: From Biomarkers to Molecularly-based Therapeutics." *Prostate Cancer and Prostatic Diseases* (2012): n. pag. Web.

11) Redzic, Jasmina S. "Extracellular RNA Mediates and Marks Cancer Progression." *Seminars in Cancer Biology* (n.d.): n. pag. Web.

12) Bryant, R. J., and F. C. Hamdy. "Changes in Circulating MicroRNA Levels Associated with Prostate Cancer." *British Journal of Cancer* 106 (2012): 768-74. Print.

13) Rane, Jayant K., Mauro Scaravilli, Antti Ylipää, Davide Pellacani, Vincent M. Mann, Matthew S. Simms, Matti Nykter, Anne T. Collins, Tapio Visakorpi, and Norman J. Maitland. "MicroRNA Expression Profile of Primary Prostate Cancer Stem Cells as a Source of Biomarkers and Therapeutic Targets." *European Urology* (2014): n. pag. Web.

14) Haj-Ahmad, Taha A., Moemen KA Abdalla, and Yousef Haj-Ahmad. "The National Cancer Institute's Cancer Information Service." *Journal of Cancer* 5 (2014): 182-5. Web.

15) Srivastava, Anvesha, Helle Goldberger, Alexander Dimtchev, Malathi Ramalinga, Juliet Chijioke, Catalin Marian, Eric K. Oermann, Sunghae Uhm, Joy S. Kim, Leonard N. Chen, Xin Li, Deborah L. Berry, Bhaskar V. S. Kallakury, Subhash C. Chauhan, Sean P. Collins, Simeng Suy, and Deepak Kumar. "MicroRNA Profiling in Prostate Cancer - The Diagnostic Potential of Urinary MiR-205 and MiR-214." Ed. Rakesh K. Srivastava. *PLoS ONE* 8.10 (2013): E76994. Web.

16) Shaw, Greg L., and David E. Neal. "Molecular Biology and Prostate Cancer."*Prostate Cancer a Comprehensive Perspective*. By Ashutosh Tewari. Dordrecht: Springer, 2014. N. pag. Print.

17) White, Nicole M. A., Eman Fatoohi, Maged Metias, Klaus Jung, Carsten Stephan, and George M. Yousef. "Metastamirs: A Stepping Stone towards Improved Cancer Management." *Nature Reviews Clinical Oncology* 8.2 (2010): 75-84. Web.

18) Hizir, Mustafa Salih, Mustafa Balcioglu, Muhit Rana, Neil M. Robertson, and Mehmet V. Yigit. "Simultaneous Detection of Circulating OncomiRs from Body Fluids for Prostate Cancer Staging Using Nanographene Oxide." *ACS Applied Materials & Interfaces* (2014): 140828081603005. Web.

19) McDermott, A. M., N. Miller, D. Wall, L. M. Martyn, G. Ball, K. J. Sweeney, and M. J. Karen. "Identification and Validation of Oncologic MiRNA Biomarkers for Luminal A-like Breast Cancer." *PLoS ONE* 9.1 (2014): E87032. Print.

20) Bermejo, Pablo, Alicia Vivo, Pedro J. Tarraga, and J. A. Rodriguez-Montes. "Development of Interpretable Predictive Models for BPH and Prostate Cancer." *Clinical Medical Insights: Oncology* 9 (2015): 15-23. Web.

21) Gao, Wen, Hua Shen, Lingxiang Liu, Jian Xu, Jing Xu, and Yongqian Shu. "MiR-21 Overexpression in Human Primary Squamous Cell Lung Carcinoma Is Associated with Poor Patient Prognosis." *Journal of Cancer Research and Clinical Oncology* 137.4 (2011): 557-66. Web.

22) Huang, X. "Exosomal MiR-1290 and MiR-375 as Prognostic Markers in Castration-resistant Prostate Cancer." *European Urology* 67.1 (2014): 33-41. Web.

23) Mitchell, P. S., R. K. Parkin, E. M. Kroh, B. R. Fritz, S. K. Wyman, E. L. Pogosova-Agadjanyan, A. Peterson, J. Noteboom, K. C. O'briant, A. Allen, D. W. Lin, N. Urban, C. W. Drescher, B. S. Knudsen, D. L. Stirewalt, R. Gentleman, R. L. Vessella, P. S. Nelson, D. B. Martin, and M. Tewari. "Circulating MicroRNAs as Stable Blood-based Markers for Cancer Detection." *Proceedings of the National Academy of Sciences* 105.30 (2008): 10513-0518. Web.

24) Gururajan, M., S. Josson, G. C.-Y. Chu, C.-L. Lu, Y.-T. Lu, C. L. Haga, H. E. Zhau, C. Liu, J. Lichterman, P. Duan, E. M. Posadas, and L. W. K. Chung. "MiR-154* and MiR-379 in the DLK1-DIO3 MicroRNA Mega-Cluster Regulate Epithelial to Mesenchymal Transition and Bone Metastasis of Prostate Cancer." *Clinical Cancer Research* 20.24 (2014): 6559-569. Web.

25) Priolo, C., S. Pyne, J. Rose, E. R. Regan, G. Zadra, C. Photopoulos, S. Cacciatore, D. Schultz, N. Scaglia, J. Mcdunn, A. M. De Marzo, and M. Loda. "AKT1 and MYC Induce Distinctive Metabolic Fingerprints in Human Prostate Cancer." *Cancer Research* 74.24 (2014): 7198-204. Web.

26) Yoon, Je-Hyun, Kotb Abdelmohson, and Myriam Gorospe. "Functional Interactions among MicroRNAs and Long Noncoding RNAs." *Seminars in Cell and Developmental Biology* 34 (2014): 9-14. Web.

27) Krol, Jacek, Inga Loedige, and Witold Filipowicz. "The Widespread Regulation of MicroRNA Biogenesis, Function and Decay." *Nature Reviews Genetics* (2010): n. pag. Web.

28) Katz, Betina, Sabrina T. Reis, Nayara I. Viana, Denis R. Morias, Caio M. Moura, Nelson Dip, Iran A. Silva, Alexandre Iscaife, Miguel Srougi, and Katia R. M. Leite. "Comprehensive Study of Gene and MicroRNA Expression Related to Epithelial-Mesenchymal Transition in Prostate Cancer." *PLoS ONE* 9.11 (2014): 1-10. Web.

29) Berezikov, Eugene. "Evolution of MicroRNA Diversity and Regulation in Animals." *Nature Reviews Genetics* 12.12 (2011): 846-60. Web.

30) Budd, William Thomas. "Combinatorial Analysis of Tumorigenic MicroRNAs Driving Prostate Cancer." Diss. Virginia Commonwealth U, 2012. Web.

31) Cheng, Lesley, Xin Sun, Benjamin J. Scicluna, Bradley M. Coleman, and Andrew F. Hill. "Characterization and Deep Sequencing Analysis of Exosomal and Non-exosomal MiRNA in Human Urine." *Kidney International* (2013): n. pag. Web.

32) Zhang, Xueping, Amy Ladd, Ema Dragoescu, William T. Budd, Joy L. Ware, and Zendra E. Zehner. "MicroRNA-17-3p Is a Prostate Tumor Suppressor in Vitro and in Vivo, and

Is Decreased in High Grade Prostate Tumors Analyzed by Laser Capture Microdissection." *Clinical & Experimental Metastasis* 26.8 (2009): 965-79. Web.

33) Huggett, J., K. Dheda, S. Bustin, and A. Zumla. "Real-time RT-PCR Normalisation; Strategies and Considerations." *Genes and Immunity*6.4 (2005): 279-84. Web.

34) Melo, Sonia A., Hikaru Sugimoto, Joyce T. O'Connell, Noritoshi Kato, Alberto Villanueva, August Vidal, Le Qiu, Edward Vitkin, Lev T. Perelman, Carlos A. Melo, Anthony Lucci, Christina Ivan, and George A. Calin. "Cancer Exosomes Perform Cell-Independent MicroRNA Biogenesis and Promote Tumorigenesis." *Cancer Cell* 26 (2014): 707-21. Web.

35) Song, Chunjiao, Huan Chen, Tingzhang Wang, Weiguang Zhang, Guomei Ru, and Juan Lang. "Expression Profile Analysis of MicrRNAs in Prostate Cancer by Next-Generation Sequencing." *The Prostate* 75 (2015): 500-16. Print.

36) Cheng, Lesley, Robyn A. Sharples, Benjamin J. Scicluna, and Andrew F. Hill. "Exosomes Provide a Protective and Enriched Source of MiRNA for Biomarker Profiling Compared to Intracellular and Cell-free Blood."*Journal of Extracellular Vesicles* 3.0 (2014): n. pag. Web.

37) Truong, Matthew, Bing Yang, and David F. Jarrard. "Toward the Detection of Prostate Cancer in Urine: A Critical Analysis." *The Journal of Urology*189.2 (2013): 422-29. Web.

38) Mogilyansky, E., and I. Rigoutsos. "The MiR-17/92 Cluster: A Comprehensive Update on Its Genomics, Genetics, Functions and Increasingly Important and Numerous Roles in Health and Disease." *Cell Death and Differentiation*20.12 (2013): 1603-614. Web.

39) Bae, Victoria L., Colleen K. Jackson-Cook, Arthur R. Brothman, Susan J. Maygardens, and Joy L. Ware. "Tumorigenicity of SV40 T Antigen Immortalized Human Prostate Epithelial Cells: Association with Decreased Epidermal Growth Factor Receptor (EGFR) Expression." *International Journal of Cancer* 58.5 (1994): 721-29. Web.

40) Astbury, Caroline, Colleen K. Jackson-Cook, Stephen H. Culp, Thomas E. Paisley, and Joy L. Ware. "Suppression of Tumorigenicity in the Human Prostate Cancer Cell Line M12 via Microcell-mediated Restoration of Chromosome 19." *Genes, Chromosomes and Cancer* 31.2 (2001): 143-55. Web.

41) Vandesompele, Jo, Mikeal Kubista, and Micheal W. Pfaffl. "Reference Gene Validation Software for Improved Normalization." *Real-time PCR: Current Technology and Applications*. By Julie Logan, Kirstin Edwards, and Nick Saunders. Norfolk, UK: Caister Academic, 2009. 47-63. Print.

42) Redshaw, Nicholas, Timothy Wilkes, Alexandra Whale, Simon Cowen, Jim Huggett, and Carole Foy. "A Comparison of MiRNA Isolation and RT-qPCR Technologies and

Their Effects on Quantification Accuracy and Repeatability." *BioTechniques* 54.3 (2013): 155-63. Web.

43) Pfaffl, Michael W., Ales Tichopad, Christian Prgomet, and Tanja P. Neuvians. "Determination of Stable Housekeeping Genes, Differentially Regulated Target Genes and Sample Integrity: BestKeeper – Excel-based Tool Using Pair-wise Correlations." *Biotechnology Letters* 26.6 (2004): 509-15. Web.

44) Andersen, C. L. "Normalization of Real-Time Quantitative Reverse Transcription-PCR Data: A Model-Based Variance Estimation Approach to Identify Genes Suited for Normalization, Applied to Bladder and Colon Cancer Data Sets." *Cancer Research* 64.15 (2004): 5245-250. Web.

45) Mestdagh, Pieter, and Jo Vandesompele. "Evaluation of Quantitative MiRNA Expression Platforms in the MicroRNA Quality Control (miRQC) Study."*Nature Methods* 8.11 (2014): 809-15. Web.

46) Pabinger, Stephan, Stefan Rodiger, Albert Kriegner, Klemens Vierlinger, and Andreas Weinhausen. "A Survey of Tools for the Analysis of Quantitative PCR (qPCR) Data." *Biomolecular Detection and Quantification* 1 (2014): 23-33. Web.

47) Baker, Monya. "MicroRNA Profiling: Separating Signal from Noise." *Nat Meth Nature Methods* 7.9 (2010): 687-92. Web.

48) Leucci, Eleonora, Anna Onnis, Mario Cocco, Giulia De Falco, Francesco Imperatore, Antonicelli Giuseppina, Valentina Costanzo, Giovanna Cerino, Susanna Mannucci, Rocco Cantisani, Joshua Nyagol, Walter Mwanda, Robert Iriso, Martin Owang, Karin Schurfeld, Cristiana Bellan, Stefano Lazzi, and Lorenzo Leoncini. "B-cell Differentiation in EBV-positive Burkitt Lymphoma Is Impaired at Posttranscriptional Level by MiRNA-altered Expression."*International Journal of Cancer* (2010): NA. Web.

49) Zhang, X., M. V. Fournier, J. L. Ware, M. J. Bissell, A. Yacoub, and Z. E. Zehner. "Inhibition of Vimentin or 1 Integrin Reverts Morphology of Prostate Tumor Cells Grown in Laminin-rich Extracellular Matrix Gels and Reduces Tumor Growth in Vivo." *Molecular Cancer Therapeutics* 8.3 (2009): 499-508. Web.

50) Saito, Yoshimasa, Gangning Liang, Gerda Egger, Jeffrey M. Friedman, Jody C. Chuang, Gerhard A. Coetzee, and Peter A. Jones. "Specific Activation of MicroRNA-127 with Downregulation of the Proto-oncogene BCL6 by Chromatin-modifying Drugs in Human Cancer Cells." *Cancer Cell*9.6 (2006): 435-43. Web.

51) Wu, S., S. Huang, J. Ding, Y. Zhao, L. Liang, T. Liu, R. Zhan, and X. He. "Multiple MicroRNAs Modulate P21Cip1/Waf1 Expression by Directly Targeting Its 3′ Untranslated Region." *Oncogene* 29.15 (2010): 2302-308. Web.

52) Ostling, P., S.-K. Leivonen, A. Aakula, P. Kohonen, R. Makela, Z. Hagman, A. Edsjo, S. Kangaspeska, H. Edgren, D. Nicorici, A. Bjartell, Y. Ceder, M. Perala, and O. Kallioniemi. "Systematic Analysis of MicroRNAs Targeting the Androgen Receptor in Prostate Cancer Cells." *Cancer Research* 71.5 (2011): 1956-967. Web.

53) Dolgin, Elie. "Phylogeny: Rewriting Evolution." *Nature* 486.7404 (2012): 460-62. Web.

54) Meyer, S. N., M. Amoyel, C. Bergantinos, C. De La Cova, C. Schertel, K. Basler, and L. A. Johnston. "An Ancient Defense System Eliminates Unfit Cells from Developing Tissues during Cell Competition." *Science*346.6214 (2014): 1258236. Web.

55) Mazzali, M., V. Ophascharoensuk, T. Kipari, J. A. Wesson, R. Johnson, and J. Hughes. "Osteopontin--a Molecule for All Seasons." *Q J Med* 95.1 (2002): 3-13. Web.

56) Meyer, Swanhild U., Micheal W. Pfaffl, and Susanne E. Ulbrich. "Normalization Strategies for MicroRNA Profiling Experiments: A 'normal' Way to a Hidden Layer of Complexity?" *Biotechnology Letters* (2010): n. pag. Web.

57) Chugh, Pauline, and Dirk P. Dittmer. "Potential Pitfalls in MicroRNA Profiling." *Wiley Interdisciplinary Reviews: RNA* 3.5 (2012): 601-16. Web.

58) Ling, Hui, Muller Fabbri, and George A. Calin. "MicroRNAs and Other Non-coding RNAs as Targets for Anticancer Drug Development." *Nat Rev Drug Discov Nature Reviews Drug Discovery* 12.11 (2013): 847-65. Web.

59) Koshiol, J., E. Wang, Y. Zhao, F. Marincola, and M. T. Landi. "Strengths and Limitations of Laboratory Procedures for MicroRNA Detection."*Cancer Epidemiology Biomarkers & Prevention* 19.4 (2010): 907-11. Web.

60) Hébert, Sébastien S., and Peter T. Nelson. "Studying MicroRNAs in the Brain: Technical Lessons Learned from the First Ten Years." *Experimental Neurology* 235.2 (2012): 397-401. Web.

61) Ha, Minju, and V. Narry Kim. "Regulation of MicroRNA Biogenesis." *Nature Reviews Molecular Cell Biology Nat Rev Mol Cell Biol* 15.8 (2014): 509-24. Web.

62) Eng J. ROC analysis: web-based calculator for ROC curves. Baltimore: Johns Hopkins University [updated 2014 March 19; cited <*date*>]. Available from: http://www.jrocfit.org.

63) Brosnahan, Amanda J., Lucy Vulchanova, Samantha R. Witta, Yuying Dai, Bryan J. Jones, and David R. Brown. "Norepinephrine Potentiates Proinflammatory Responses of Human Vaginal Epithelial Cells."*Journal of Neuroimmunology* 259.1-2 (2013): 8-16. Web.

64) Wang, W. C. H., A. H. Juan, A. Panebra, and S. B. Liggett. "MicroRNA Let-7 Establishes Expression of 2-adrenergic Receptors and Dynamically Down-regulates Agonist-promoted Down-regulation." *Proceedings of the National Academy of Sciences* 108.15 (2011): 6246-251. Web.

65) Seashols, Sarah Joy. "VCU Scholars Compass." *Site*. N.p., Dec. 2013. Web. 17 June 2015.

66) Shen, J., and M.-C. Hung. "Signaling-Mediated Regulation of MicroRNA Processing." *Cancer Research* 75.5 (2015): 783-91. Web.

67) Carter, H. Ballentine. "American Urological Association (AUA) Guideline on Prostate Cancer Detection: Process and Rationale." *BJU International BJU Int* 112.5 (2013): 543-47. Web.

68) Unternaehrer, Juli J., Rui Zhao, Kitai Kim, Marcella Cesana, John T. Powers, Sutheera Ratanasirintrawoot, Tamer Onder, Tsukasa Shibue, Robert A. Weinberg, and George Q. Daley. "The Epithelial-Mesenchymal Transition Factor SNAIL Paradoxically Enhances Reprogramming." *Stem Cell Reports* 3.5 (2014): 691-98. Web.

69) Robinson, MD, and Oshlack, A. A scaling normalization method for differential expression analysis of RNA-seq data. Genome Biology . 2012:11; R25.

70) Mortazavi A, Williams BA, McCue K, Schaeffer L, Wold B: Mapping and quantifying mammalian transcriptomes by RNA-Seq. Nat Methods. 2008, 5:621-628.

71) Gene Specfic Analysis White Paper. Partek.com. Date of access: May 3, 2015.

72) Chen, Y. McCarthy, D. Robinson, M. Smyth G. edgeR: differential expression analysis of digital gene expression User's Guide. 2014.

73) Dillies et al. A comprehensive evaluation of normalization methods for Illumina high-throughput RNA sequencing data analysis. Brief Bioinform. 2012. DOI: 10.1093/bib/bbs046.

74) McCarthy, DJ, Chen, Y, Smyth, GK. Differential expression analysis of multifactor RNA-Seq experiments with respect to biological variation. Nucleic Acids Research. 2012: 40, 4288- 4297.

75) Fagerland, M. W., L. Sandvik, and P. Mowinckel. Parametric methods outperformed non-parametric methods in comparisons of discrete numerical variables. 2011. BMC Medical Research Methodology 11-44.

76) Benjamini, Y., and Y. Hochberg. Controlling the false discovery rate: a practical and powerful approach to multiple testing. Journal of the Royal Statistical Society. 1995: 57, 289-300.

77) Wu, Qianni. N.d. MS. Virginia Commonwealth University Richmond, Virginia, n.p.

78) Pritchard, Colin C., Heather H. Cheng, and Muneesh Tewari. "MicroRNA Profiling: Approaches and Considerations." *Nat Rev Genet Nature Reviews Genetics* 13.5 (2012): 358-69. Web.

79) Jalava, S. E., A. Urbanucci, L. Latonen, K. K. Waltering, B. Sahu, O. A. Jänne, J. Seppälä, H. Lähdesmäki, T. L J Tammela, and T. Visakorpi. "Androgen-regulated MiR-32 Targets BTG2 and Is Overexpressed in Castration-resistant Prostate Cancer." *Oncogene* 31.41 (2012): 4460-471. Web.

80) Pang, Y., C. Y. F. Young, and H. Yuan. "MicroRNAs and Prostate Cancer."*Acta Biochimica Et Biophysica Sinica* 42.6 (2010): 363-69. Web.

81) Dai, Y., D. Ngo, J. Jacob, L. W. Forman, and D. V. Faller. "Prohibitin and the SWI/SNF ATPase Subunit BRG1 Are Required for Effective Androgen Antagonist-mediated Transcriptional Repression of Androgen Receptor-regulated Genes." *Carcinogenesis* 29.9 (2008): 1725-733. Web.

82) Rodriguez-Nieto, S., and M. Sanchez-Cespedes. "BRG1 and LKB1: Tales of Two Tumor Suppressor Genes on Chromosome 19p and Lung Cancer." *Carcinogenesis* 30.4 (2009): 547-54. Web.

83) "ETV4 Gene(Protein Coding)." *ETV4 Gene*. N.p., n.d. Web. 13 July 2015.

84) Castilla, María Ángeles, Juan Díaz-Martín, David Sarrió, Laura Romero-Pérez, María Ángeles López-García, Begoña Vieites, Michele Biscuola, Susana Ramiro-Fuentes, Clare M. Isacke, and José Palacios. "MicroRNA-200 Family Modulation in Distinct Breast Cancer Phenotypes." *PLoS ONE* 7.10 (2012): n. pag. Web.

85) Vrba, Lukas, Taylor J. Jensen, James C. Garbe, Ronald L. Heimark, Anne E. Cress, Sally Dickinson, Martha R. Stampfer, and Bernard W. Futscher. "Role for DNA Methylation in the Regulation of MiR-200c and MiR-141 Expression in Normal and Cancer Cells." *PLoS ONE* 5.1 (2010): n. pag. Web.

86) Katz, Betina, Sabrina T. Reis, Nayara I. Viana, Denis R. Morais, Caio M. Moura, Nelson Dip, Iran A. Silva, Alexandre Iscaife, Miguel Srougi, and Katia R. M. Leite. "Comprehensive Study of Gene and MicroRNA Expression Related to Epithelial-Mesenchymal Transition in Prostate Cancer." *PLoS ONE* 9.11 (2014): n. pag. Web.

87) Hyun, Seogang, Jung Hyun Lee, Hua Jin, Jinwu Nam, Bumjin Namkoong, Gina Lee, Jongkyeong Chung, and V. Narry Kim. "Conserved MicroRNA MiR-8/miR-200 and Its Target USH/FOG2 Control Growth by Regulating PI3K." *Cell* 139.6 (2009): 1096-108. Web.

88) Vallejo, Diana M., Esther Caparros, and Maria Dominguez. "Targeting Notch Signalling by the Conserved MiR-8/200 MicroRNA Family in Development and Cancer Cells." *The EMBO Journal* 30.4 (2011): 756-69. Web.

89) Mcglinn, E., S. Yekta, J. H. Mansfield, J. Soutschek, D. P. Bartel, and C. J. Tabin. "In Ovo Application of AntagomiRs Indicates a Role for MiR-196 in Patterning the Chick Axial Skeleton through Hox Gene Regulation."*Proceedings of the National Academy of Sciences* 106.44 (2009): 18610-8615. Web.

90) Bulun, S.e. "MicroRNAs Exhibit High Frequency Genomic Alterations in Human Cancer." *Yearbook of Obstetrics, Gynecology and Women's Health* 2007 (2007): 21-22. Web.

91) Srikantan, Subramanya, Kumiko Tominaga, and Myriam Gorospe. "Functional Interplay between RNA-Binding Protein HuR and MicroRNAs." *CPPS Current Protein & Peptide Science* 13.4 (2012): 372-79. Web.

92) Fatima, Roshan, Vijay Suresh Akhade, Debosree Pal, and Satyanarayana Mr Rao. "Long Noncoding RNAs in Development and Cancer: Potential Biomarkers and Therapeutic Targets." *Mol and Cell Ther Molecular and Cellular Therapies* 3.1 (2015): n. pag. Web.

93) Zehavi, Liron, Roi Avraham, Aviv Barzilai, Dalia Bar-Ilan, Roy Navon, Yechezkel Sidi, Dror Avni, and Raya Leibowitz-Amit. "Silencing of a Large MicroRNA Cluster on Human Chromosome 14q32 in Melanoma: Biological Effects of Mir-376a and Mir-376c on Insulin Growth Factor 1 Receptor." *Molecular Cancer Mol Cancer* 11.1 (2012): 44. Web.

94) Keniry, Andrew, David Oxley, Paul Monnier, Michael Kyba, Luisa Dandolo, Guillaume Smits, and Wolf Reik. "The H19 LincRNA Is a Developmental Reservoir of MiR-675 That Suppresses Growth and Igf1r." *Nat Cell Biol Nature Cell Biology* 14.7 (2012): 659-65. Web.

95) Zhu, Miaojun, Qin Chen, Xin Liu, Qian Sun, Xian Zhao, Rong Deng, Yanli Wang, Jian Huang, Ming Xu, Jianshe Yan, and Jianxiu Yu. "LncRNA H19/miR-675 Axis Represses Prostate Cancer Metastasis by Targeting TGFBI." *FEBS Journal FEBS J* 281.16 (2014): 3766-775. Web.

96) Zhou, Y., Y. Zhong, Y. Wang, X. Zhang, D. L. Batista, R. Gejman, P. J. Ansell, J. Zhao, C. Weng, and A. Klibanski. "Activation of P53 by MEG3 Non-coding RNA." *Journal of Biological Chemistry* 282.34 (2007): 24731-4742. Web.

97) Wu, Hailong, Shoumin Zhu, and Yin-Yuan Mo. "Suppression of Cell Growth and Invasion by MiR-205 in Breast Cancer." *Cell Res Cell Research* 19.4 (2009): 439-48. Web.

98) Fazi, Francesco, Alessandro Rosa, Alessandro Fatica, Vania Gelmetti, Maria Laura De Marchis, Clara Nervi, and Irene Bozzoni. "A Minicircuitry Comprised of MicroRNA-223 and Transcription Factors NFI-A and C/EBPα Regulates Human Granulopoiesis." *Cell* 123.5 (2005): 819-31. Web.

99) Lin, E. A., L. Kong, X.-H. Bai, Y. Luan, and C.-J. Liu. "MiR-199a*, a Bone Morphogenic Protein 2-responsive MicroRNA, Regulates Chondrogenesis via Direct Targeting to Smad1." *Journal of Biological Chemistry* 284.17 (2009): 11326-1335. Web.

100) Watahiki, Akira, Yuwei Wang, James Morris, Kristopher Dennis, Helena M. O'dwyer, Martin Gleave, Peter W. Gout, and Yuzhuo Wang. "MicroRNAs Associated with Metastatic Prostate Cancer." *PLoS ONE*6.9 (2011): n. pag. Web.

101) Kitade, Yukio, and Yukihiro Akao. "MicroRNAs and Their Therapeutic Potential for Human Diseases: MicroRNAs, MiR-143 and -145, Function as Anti-oncomirs and the Application of Chemically Modified MiR-143 as an Anti-cancer Drug." *J Pharmacol Sci Journal of Pharmacological Sciences* 114.3 (2010): 276-80. Web.

102) Foley, Niamh H., Isabella M. Bray, Amanda Tivnan, Kenneth Bryan, Derek M. Murphy, Patrick G. Buckley, Jacqueline Ryan, Anne O'meara, Maureen O'sullivan, and Raymond L. Stallings. "MicroRNA-184 Inhibits Neuroblastoma Cell Survival through Targeting the Serine/threonine Kinase AKT2." *Molecular Cancer Mol Cancer* 9.1 (2010): 83. Web.

103) Thompson, Ian M. "Operating Characteristics of Prostate-Specific Antigen in Men With an Initial PSA Level of 3.0 Ng/mL or Lower." *Jama* 294.1 (2005): 66. Web.

104) Wei, Yongbao, Jinrui Yang, Lu Yi, Yinhuai Wang, Zhitao Dong, Ziting Liu, Shifeng Ou-Yang, Hongtao Wu, Zhaohui Zhong, Zhuo Yin, Keqin Zhou, Yunliang Gao, Bin Yan, and Zhao Wang. "MiR-223-3p Targeting SEPT6 Promotes the Biological Behavior of Prostate Cancer." *Scientific Reports Sci. Rep.* 4 (2014): 7546. Web.

105) Todorova, Krassimira, Metodi V. Metodiev, Gergana Metodieva, Diana Zasheva, Milcho Mincheff, and Soren Hayrabedyan. "MiR-204 Is Dysregulated in Metastatic Prostate Cancer In Vitro." *Mol. Carcinog. Molecular Carcinogenesis* (2015): n. pag. Web.

106) Todorova, Krassimira, Metodi V. Metodiev, Gergana Metodieva, Diana Zasheva, Milcho Mincheff, and Soren Hayrabedyan. "MiR-204 Is Dysregulated in Metastatic Prostate Cancer In Vitro." *Mol. Carcinog. Molecular Carcinogenesis* (2015): n. pag. Web.

Appendix

Table 21: Extended NGS Analysis for Urine

Gene Name	logFC	locCPM	LR	PValue	PAdjusted
hsa-miR-223-3p	5.940734	10.614319	16.24019	5.58E-05	0.013335658
hsa-miR-223-5p	5.95683	7.6441786	13.45336	0.000245	0.029225904
hsa-miR-142-3p	6.801603	9.4414229	12.68913	0.000368	0.029300375
hsa-miR-199a-3p	4.884872	8.3158747	11.69224	0.000628	0.037499873
hsa-miR-363-3p	-2.4222	11.602927	11.15461	0.000838	0.040067362
hsa-miR-199b-5p	4.974522	7.5241254	10.1309	0.001458	0.058078823
hsa-miR-199b-3p	4.59329	7.3669649	9.558437	0.00199	0.067955399
hsa-miR-143-3p	3.957342	10.998673	8.453135	0.003644	0.108868889
hsa-miR-184	5.863426	12.214555	7.873185	0.005017	0.133237726
hsa-miR-629-5p	2.227044	9.2003383	7.185232	0.007351	0.175679457
hsa-miR-941	2.812312	10.376636	6.913948	0.008553	0.185824598
hsa-miR-205-5p	2.799235	11.093862	6.44201	0.011145	0.221976188
hsa-miR-146a-5p	2.617289	11.905298	6.268341	0.012291	0.224995801
hsa-miR-185-5p	1.792165	10.981644	6.009805	0.014227	0.224995801
hsa-miR-204-5p	-2.28501	11.863405	5.651272	0.017443	0.224995801
hsa-miR-221-3p	2.323762	11.741003	5.607212	0.017887	0.224995801
hsa-miR-34c-5p	4.915895	9.5787856	5.939451	0.014806	0.224995801
hsa-miR-375	-2.25697	15.598242	5.837234	0.01569	0.224995801
hsa-miR-618	4.634886	8.8283879	5.737391	0.016607	0.224995801
hsa-miR-145-5p	4.683413	7.6031015	5.48455	0.019185	0.229263865
hsa-miR-135a-5p	-2.25086	9.7143463	5.31853	0.0211	0.240001966
hsa-miR-3613-5p	2.656422	8.6492001	5.238507	0.022092	0.240001966
hsa-miR-224-5p	4.2514	7.5193947	4.93534	0.026313	0.24582941
hsa-miR-30b-5p	-1.86501	9.0509587	5.032267	0.024879	0.24582941
hsa-miR-338-5p	2.660272	8.1421914	4.90733	0.026743	0.24582941
hsa-miR-378a-3p	2.340643	14.428333	5.045535	0.024689	0.24582941
hsa-miR-106b-3p	1.754481	9.994472	4.798615	0.028483	0.252123979
hsa-miR-142-5p	2.641637	7.5290462	4.502165	0.033852	0.259292108
hsa-miR-194-5p	-2.04975	10.826673	4.524387	0.033415	0.259292108
hsa-miR-335-3p	-2.42317	7.0238824	4.677256	0.030565	0.259292108

hsa-miR-378c	2.163248	11.654233	4.459043	0.034717	0.259292108
hsa-miR-7706	2.934246	7.0007226	4.460831	0.034681	0.259292108
hsa-miR-20b-5p	-2.88384	7.4043395	4.21983	0.039954	0.289364984
hsa-miR-18a-3p	2.27682	7.2060772	3.981565	0.046001	0.323358661
hsa-miR-181a-5p	1.588965	12.463507	3.798065	0.051312	0.349502663
hsa-miR-210-3p	2.308042	8.6079003	3.709392	0.054107	0.349502663
hsa-miR-382-5p	3.957323	7.591024	3.751917	0.052747	0.349502663
hsa-miR-203a-3p	1.8338	14.43704	3.347386	0.067312	0.407257978
hsa-miR-3529-3p	1.612157	11.583631	3.326777	0.06816	0.407257978
hsa-miR-500a-3p	2.410842	7.3620295	3.384309	0.06582	0.407257978
hsa-miR-22-3p	1.662862	15.848046	3.218368	0.072816	0.422801075
hsa-miR-29a-3p	-1.31887	10.858349	3.159242	0.075498	0.422801075
hsa-miR-99a-5p	-1.28535	14.669096	3.146955	0.076069	0.422801075
hsa-miR-135b-5p	2.544828	7.711581	3.03227	0.081624	0.42408849
hsa-miR-23a-3p	1.845069	11.166412	3.05629	0.080425	0.42408849
hsa-miR-361-3p	1.325939	10.239265	3.0998	0.078302	0.42408849
hsa-miR-15b-5p	1.779465	7.9188845	2.900423	0.088556	0.450318343
hsa-miR-574-3p	-1.7858	8.9486664	2.812291	0.093545	0.465774519
hsa-miR-10b-5p	-1.57388	15.415848	2.724711	0.098806	0.475890367
hsa-miR-185-3p	2.117409	7.4792644	2.681074	0.101547	0.475890367
hsa-miR-34a-5p	2.174507	7.8564769	2.636348	0.104443	0.475890367
hsa-miR-3615	1.935132	8.2198082	2.59025	0.107523	0.475890367
hsa-miR-452-5p	2.417074	8.5605751	2.633221	0.104649	0.475890367
hsa-miR-576-3p	1.97834	6.8467383	2.618304	0.105637	0.475890367
hsa-miR-615-3p	-1.8157	8.4008804	2.420809	0.119733	0.520294811
hsa-miR-508-3p	2.40192	6.988689	2.365041	0.124081	0.529558413
hsa-let-7i-5p	1.174783	13.456275	2.214528	0.136717	0.545840497
hsa-miR-1301-3p	1.533529	7.5259215	2.194434	0.13851	0.545840497
hsa-miR-150-5p	1.391047	8.4929822	2.268832	0.131999	0.545840497
hsa-miR-17-5p	-1.45356	8.3589481	2.225052	0.135788	0.545840497
hsa-miR-934	2.007721	8.8790982	2.18551	0.139315	0.545840497
hsa-miR-10a-5p	-1.40733	15.075426	1.937447	0.163946	0.55187454
hsa-miR-16-5p	1.028633	9.5983274	2.064657	0.150749	0.55187454
hsa-miR-222-3p	1.260597	9.1522395	2.08909	0.148354	0.55187454
hsa-miR-30a-5p	-1.09524	14.020108	2.025666	0.154661	0.55187454
hsa-miR-30c-5p	-1.08	11.508867	2.047487	0.152458	0.55187454
hsa-miR-31-5p	2.059023	7.4618987	1.966738	0.160795	0.55187454
hsa-miR-339-5p	-1.63516	7.646961	2.123894	0.145017	0.55187454
hsa-miR-425-5p	1.165469	9.7911464	1.948502	0.162748	0.55187454
hsa-miR-769-5p	1.445804	9.3599063	1.947235	0.162885	0.55187454
hsa-miR-93-5p	1.158637	10.704653	2.007314	0.156542	0.55187454

hsa-let-7f-2-3p	-1.83447	6.9021967	1.884003	0.16988	0.556182113
hsa-miR-4516	2.535969	7.0990241	1.889215	0.169291	0.556182113
hsa-miR-192-5p	-1.13134	12.636514	1.82492	0.176729	0.556388654
hsa-miR-24-3p	1.228274	12.316643	1.860406	0.172578	0.556388654
hsa-miR-509-3p	2.234188	7.6173777	1.82325	0.176927	0.556388654
hsa-miR-10a-3p	-1.52778	8.2616514	1.787996	0.181171	0.558102418
hsa-miR-125b-5p	-0.99019	12.159405	1.691233	0.193439	0.558102418
hsa-miR-1287-5p	1.831372	7.4062168	1.745971	0.186384	0.558102418
hsa-miR-181b-5p	1.179	10.596126	1.685387	0.19421	0.558102418
hsa-miR-197-3p	1.519523	9.8423829	1.736972	0.187523	0.558102418
hsa-miR-224-3p	2.018405	6.7094447	1.716731	0.190114	0.558102418
hsa-miR-29c-3p	-1.55311	9.5344584	1.695269	0.192908	0.558102418
hsa-miR-582-3p	1.295381	7.2272314	1.670787	0.196153	0.558102418
hsa-miR-127-3p	2.104886	7.0465542	1.55704	0.212099	0.589438236
hsa-miR-25-3p	0.876096	12.732683	1.562199	0.211343	0.589438236
hsa-miR-125a-3p	1.094682	7.2026524	1.509864	0.21916	0.602059593
hsa-miR-141-3p	-1.29889	10.741446	1.405796	0.235755	0.604689108
hsa-miR-181a-3p	1.433398	6.9958551	1.363756	0.242888	0.604689108
hsa-miR-374b-5p	-1.05493	7.6279577	1.37916	0.240244	0.604689108
hsa-miR-374c-3p	-1.05514	7.6279577	1.374266	0.24108	0.604689108
hsa-miR-425-3p	1.481974	7.512011	1.372764	0.241338	0.604689108
hsa-miR-484	1.051318	10.572526	1.431092	0.231586	0.604689108
hsa-miR-542-3p	1.075885	7.6999108	1.38348	0.239509	0.604689108
hsa-miR-660-5p	-1.43373	7.5509697	1.442304	0.229767	0.604689108
hsa-miR-99b-5p	-0.9183	12.268869	1.421832	0.233102	0.604689108
hsa-miR-128-3p	-0.79693	10.230627	1.332768	0.248313	0.611823645
hsa-let-7c-5p	-1.12959	12.216749	1.317865	0.250976	0.612073166
hsa-miR-155-5p	-1.13839	8.6408106	1.284241	0.257112	0.618381929
hsa-miR-196a-5p	-1.17834	9.5608818	1.273414	0.259127	0.618381929
hsa-miR-584-5p	1.185308	9.4131734	1.261726	0.261325	0.618381929
hsa-miR-221-5p	1.439904	7.0291555	1.220318	0.269298	0.624876689
hsa-miR-499a-5p	-1.31607	7.3947201	1.22459	0.268462	0.624876689
hsa-miR-129-5p	1.244769	7.1954452	1.176863	0.277996	0.638855328
hsa-let-7g-5p	0.946926	14.97011	1.145196	0.284557	0.647706186
hsa-miR-30d-3p	-1.31195	7.1178337	1.131943	0.287361	0.647918217
hsa-miR-149-5p	-1.14834	9.8564527	1.102254	0.293772	0.656182052
hsa-miR-103a-3p	0.76367	10.992585	1.031106	0.309899	0.666971637
hsa-miR-103b	0.763898	10.992585	1.036608	0.308612	0.666971637
hsa-miR-140-3p	0.753401	9.4584128	1.019845	0.312556	0.666971637
hsa-miR-23b-3p	-1.2533	8.4086539	1.020777	0.312335	0.666971637
hsa-miR-30a-3p	-0.88467	12.506809	1.023248	0.31175	0.666971637

hsa-miR-450a-5p	1.071002	8.3415863	0.995493	0.318404	0.673437632
hsa-miR-514a-3p	1.12481	8.6371099	0.926653	0.335734	0.703863979
hsa-let-7b-3p	-0.91672	7.5056897	0.886563	0.346411	0.719931446
hsa-let-7e-5p	-0.87016	9.363299	0.859982	0.353744	0.7213812
hsa-miR-151a-3p	0.739576	11.726425	0.851377	0.356163	0.7213812
hsa-miR-181a-2-3p	-0.87729	7.5396238	0.856033	0.354851	0.7213812
hsa-miR-125a-5p	-0.66648	12.794758	0.812233	0.367461	0.738009517
hsa-miR-26a-5p	-0.75643	14.605994	0.80039	0.370977	0.738862208
hsa-miR-486-5p	0.730327	16.244364	0.784264	0.37584	0.742362281
hsa-miR-200b-3p	0.932365	13.749107	0.77115	0.379861	0.744154701
hsa-miR-1180-3p	0.864256	10.187516	0.748352	0.386998	0.74583312
hsa-miR-378a-5p	1.018679	7.2739192	0.755861	0.384627	0.74583312
hsa-miR-421	-0.82075	7.4961372	0.738692	0.39008	0.74583312
hsa-miR-1307-3p	0.736694	9.8132621	0.726515	0.394015	0.747378241
hsa-miR-140-5p	0.801628	8.0546998	0.679131	0.409886	0.752859232
hsa-miR-28-5p	-0.83576	8.5648107	0.671138	0.412655	0.752859232
hsa-miR-30d-5p	-0.59802	12.318839	0.678252	0.410189	0.752859232
hsa-miR-449c-5p	1.216989	6.7866859	0.683502	0.408384	0.752859232
hsa-miR-6087	-1.26265	6.9454955	0.69931	0.403016	0.752859232
hsa-miR-10b-3p	-0.7495	8.417257	0.644384	0.422128	0.758560528
hsa-miR-30e-3p	0.65092	10.213295	0.64554	0.421712	0.758560528
hsa-miR-146b-5p	0.772095	8.9693704	0.581008	0.445917	0.786460081
hsa-miR-152-3p	0.757186	9.464975	0.557559	0.455246	0.786460081
hsa-miR-28-3p	0.580208	10.408234	0.587205	0.443502	0.786460081
hsa-miR-30c-2-3p	0.651444	9.4977678	0.552256	0.457397	0.786460081
hsa-miR-374a-5p	-0.84624	7.765129	0.573262	0.448965	0.786460081
hsa-miR-582-5p	1.014564	6.7948591	0.555297	0.456161	0.786460081
hsa-miR-126-3p	-0.54452	8.4566623	0.517901	0.471738	0.788429661
hsa-miR-181d-5p	1.218029	7.5618856	0.518671	0.471409	0.788429661
hsa-miR-203b-5p	0.881604	9.8042724	0.535991	0.464099	0.788429661
hsa-miR-96-5p	-0.74472	7.8129823	0.522664	0.469707	0.788429661
hsa-miR-32-5p	-0.76836	7.8389839	0.493167	0.482518	0.799299487
hsa-miR-708-5p	0.912175	7.3963661	0.487755	0.484931	0.799299487
hsa-miR-132-3p	0.866036	7.130833	0.464477	0.495539	0.803367374
hsa-miR-23c	-0.7005	8.3158521	0.446074	0.504205	0.803367374
hsa-miR-3184-3p	0.448782	11.459004	0.454393	0.500256	0.803367374
hsa-miR-423-5p	0.448814	11.459004	0.452919	0.500952	0.803367374
hsa-miR-652-3p	0.628272	8.6999016	0.46131	0.497012	0.803367374
hsa-miR-148a-3p	-0.56148	15.457351	0.423959	0.514968	0.80534939
hsa-miR-27b-3p	-0.68293	12.96632	0.420665	0.516605	0.80534939
hsa-miR-423-3p	0.450973	14.069983	0.420907	0.516485	0.80534939

hsa-miR-92a-3p	0.464458	14.618178	0.416023	0.518928	0.80534939
hsa-let-7b-5p	-0.41652	12.815815	0.28883	0.590971	0.815541785
hsa-miR-106a-5p	0.667345	9.5701581	0.334483	0.563031	0.815541785
hsa-miR-106b-5p	0.619592	7.2591352	0.376208	0.53964	0.815541785
hsa-miR-1290	0.827504	7.0878356	0.314267	0.575074	0.815541785
hsa-miR-148a-5p	-0.43351	8.7009787	0.272519	0.601647	0.815541785
hsa-miR-151a-5p	0.578661	6.9543925	0.267522	0.604999	0.815541785
hsa-miR-15a-5p	0.567429	6.8846508	0.387827	0.533444	0.815541785
hsa-miR-186-5p	0.418498	10.862124	0.377459	0.538966	0.815541785
hsa-miR-23b-5p	0.811317	6.8660568	0.338481	0.560707	0.815541785
hsa-miR-26b-5p	-0.55522	11.507932	0.318765	0.572351	0.815541785
hsa-miR-27b-5p	0.597064	7.4734448	0.321358	0.570793	0.815541785
hsa-miR-29b-3p	-0.63324	7.7126068	0.266382	0.605769	0.815541785
hsa-miR-320b	-0.63986	11.309314	0.259007	0.610803	0.815541785
hsa-miR-339-3p	0.436579	7.580464	0.263409	0.607788	0.815541785
hsa-miR-362-5p	-0.68801	6.8831844	0.290659	0.589799	0.815541785
hsa-miR-374a-3p	-0.70429	6.903374	0.277316	0.598466	0.815541785
hsa-miR-449a	0.707319	7.1738906	0.26791	0.604737	0.815541785
hsa-miR-450b-5p	0.597008	6.9648557	0.274462	0.600354	0.815541785
hsa-miR-532-5p	-0.42383	11.679605	0.327338	0.567231	0.815541785
hsa-miR-598-3p	0.620447	7.1412008	0.308179	0.5788	0.815541785
hsa-miR-664a-5p	0.583614	8.3986854	0.349184	0.554575	0.815541785
hsa-miR-744-5p	-0.43236	10.564927	0.324956	0.568645	0.815541785
hsa-miR-92b-3p	0.459972	8.0969897	0.302407	0.582377	0.815541785
hsa-miR-98-5p	0.656272	11.543766	0.313011	0.575838	0.815541785
hsa-miR-99b-3p	0.617464	7.7242429	0.354147	0.551775	0.815541785
hsa-miR-148b-3p	0.411804	11.6944	0.24427	0.621139	0.820976005
hsa-miR-20a-5p	-0.46117	9.7100253	0.238656	0.625178	0.820976005
hsa-miR-429	-0.49702	12.148174	0.241064	0.623438	0.820976005
hsa-miR-200b-5p	-0.5376	9.8354871	0.229757	0.631704	0.823063935
hsa-miR-30e-5p	-0.41913	9.8912822	0.227136	0.633656	0.823063935
hsa-miR-193a-5p	0.412648	11.408706	0.219856	0.639149	0.825711901
hsa-miR-107	0.399244	8.6348749	0.186616	0.665748	0.846349796
hsa-miR-21-5p	0.424921	15.605387	0.192542	0.660809	0.846349796
hsa-miR-29c-5p	-0.43363	7.9730302	0.189158	0.663618	0.846349796
hsa-miR-3184-5p	-0.35109	9.5390259	0.182246	0.66945	0.846553651
hsa-miR-22-5p	0.371383	9.1984617	0.175799	0.675009	0.8490897
hsa-miR-451a	0.324515	16.397745	0.157973	0.69103	0.86469193
hsa-miR-191-5p	0.260682	13.440101	0.147479	0.700956	0.872544106
hsa-let-7a-5p	-0.32923	16.345996	0.115813	0.73362	0.872846438
hsa-miR-1-3p	-0.48282	7.6747278	0.132573	0.715779	0.872846438

hsa-miR-100-5p	0.323166	14.368302	0.127479	0.72106	0.872846438
hsa-miR-200a-5p	-0.40083	8.8829552	0.130879	0.717523	0.872846438
hsa-miR-2110	0.409964	8.1529223	0.139777	0.708503	0.872846438
hsa-miR-424-3p	0.323625	7.9585278	0.123483	0.725287	0.872846438
hsa-miR-4488	-0.44849	7.782507	0.128613	0.719874	0.872846438
hsa-miR-504-5p	-0.44546	7.2183624	0.11541	0.734068	0.872846438
hsa-miR-874-3p	0.391261	6.7963615	0.120287	0.728723	0.872846438
hsa-miR-196b-5p	-0.40703	9.5067384	0.107008	0.743577	0.879776542
hsa-miR-19a-3p	0.398072	6.9502228	0.084633	0.771114	0.907862993
hsa-let-7d-3p	-0.27558	10.195543	0.079932	0.777389	0.909917347
hsa-miR-200a-3p	0.291708	13.614122	0.077675	0.780473	0.909917347
hsa-miR-101-3p	-0.19888	10.967683	0.058803	0.808398	0.922240334
hsa-miR-200c-3p	-0.25903	15.331867	0.061801	0.803672	0.922240334
hsa-miR-204-3p	0.388138	8.7170939	0.062346	0.802826	0.922240334
hsa-miR-320a	-0.28819	15.036824	0.066632	0.796305	0.922240334
hsa-miR-424-5p	0.329176	7.6192269	0.057596	0.810337	0.922240334
hsa-miR-182-5p	0.161408	10.623732	0.050619	0.821989	0.931068234
hsa-miR-324-5p	0.242013	6.9771132	0.04712	0.828152	0.932447136
hsa-miR-335-5p	-0.18641	7.3765432	0.039372	0.842714	0.932447136
hsa-miR-502-3p	-0.1876	8.3272378	0.039712	0.842045	0.932447136
hsa-miR-532-3p	0.182299	7.8862883	0.04048	0.840545	0.932447136
hsa-miR-7704	-0.2011	9.1348154	0.04143	0.83871	0.932447136
hsa-let-7d-5p	-0.1593	10.553354	0.026416	0.870888	0.954781328
hsa-miR-218-5p	-0.17003	7.1465665	0.026974	0.869543	0.954781328
hsa-miR-9-5p	0.143642	8.8394647	0.021938	0.882253	0.962824372
hsa-miR-144-3p	-0.13792	7.278947	0.013572	0.907258	0.96801203
hsa-miR-183-5p	-0.09587	9.9540567	0.013607	0.907137	0.96801203
hsa-miR-345-5p	-0.10947	7.291081	0.015997	0.899351	0.96801203
hsa-miR-455-5p	-0.18113	7.2724557	0.018401	0.892099	0.96801203
hsa-miR-501-3p	0.092629	8.202342	0.014765	0.903285	0.96801203
hsa-miR-27a-3p	-0.08653	11.99531	0.008104	0.928271	0.976368263
hsa-miR-328-3p	0.087142	9.3043696	0.009527	0.922245	0.976368263
hsa-miR-342-3p	-0.06731	7.3940077	0.00765	0.930304	0.976368263
hsa-miR-361-5p	-0.07828	8.5256917	0.007404	0.931431	0.976368263
hsa-miR-21-3p	0.08556	6.8639263	0.005286	0.942042	0.983178981
hsa-miR-193b-3p	0.084254	8.3841002	0.004494	0.946553	0.983591596
hsa-miR-19b-3p	-0.03645	8.5633183	0.002498	0.960142	0.989111909
hsa-miR-4497	0.063175	7.4202507	0.002777	0.957976	0.989111909
hsa-let-7f-5p	0.013499	13.614829	0.000133	0.990814	0.995958467
hsa-miR-125b-2-3p	0.01143	6.7902867	0.000962	0.975259	0.995958467
hsa-miR-1307-5p	0.015023	8.1094631	0.000159	0.989929	0.995958467

hsa-miR-193b-5p	0.014656	7.5314755	0.000195	0.988848	0.995958467
hsa-miR-320c	0.01255	8.7207467	9.49E-05	0.992229	0.995958467
hsa-miR-340-5p	0.004386	10.301802	2.57E-05	0.995958	0.995958467
hsa-miR-95-3p	-0.03531	9.1361922	0.001293	0.971311	0.995958467

Table 22: NGS Results Reanalyzed without the Outlier 10242013 G6 (significant values only)

Gene Name	logFC	logCPM	LR	PValue	FDR
hsa-miR-223-3p	**6.058034**	**10.920572**	**18.6917**	**1.54E-05**	**0.003672**
hsa-miR-135a-5p	**-3.74411**	**9.7413361**	**16.13384**	**5.90E-05**	**0.007053**
hsa-miR-142-3p	**6.838292**	**9.8458739**	**14.13144**	**0.00017**	**0.011801**
hsa-miR-223-5p	**5.654684**	**8.0163204**	**13.85467**	**0.000198**	**0.011801**
hsa-miR-363-3p	**-2.50551**	**11.791686**	**11.73019**	**0.000615**	**0.029394**
hsa-miR-199b-3p	4.541513	7.8019737	10.65301	0.001099	0.039301
hsa-miR-199a-3p	**4.606071**	**8.1449676**	**10.46955**	**0.001214**	**0.039301**
hsa-miR-20b-5p	-5.2	7.6765883	10.27568	0.001348	0.039301
hsa-miR-199b-5p	4.873913	7.8268478	10.10341	0.00148	0.039301
hsa-miR-335-3p	-4.20383	7.4143649	9.32286	0.002263	0.053027
hsa-miR-148a-3p	-1.96908	15.022611	8.767695	0.003066	0.053027
hsa-miR-141-3p	-2.93239	10.480757	8.766494	0.003068	0.053027
hsa-miR-18a-3p	2.63595	7.72636	8.657284	0.003258	0.053027
hsa-miR-143-3p	**4.044592**	**11.182106**	**8.64716**	**0.003276**	**0.053027**
hsa-miR-26b-5p	-2.25021	11.007079	8.567721	0.003422	0.053027
hsa-miR-200c-3p	-2.28666	14.64529	8.420047	0.003711	0.053027
hsa-miR-184	**6.013703**	**12.486412**	**8.390545**	**0.003772**	**0.053027**
hsa-miR-941	2.960932	10.667177	8.191066	0.00421	0.055896
hsa-miR-30d-3p	-3.8984	7.3098222	7.785788	0.005266	0.066239
hsa-miR-429	-2.2439	11.655725	7.65768	0.005653	0.066846
hsa-miR-618	4.717046	9.2540133	7.588716	0.005873	0.066846
hsa-miR-145-5p	4.678684	8.1148049	7.452943	0.006333	0.068802
hsa-miR-629-5p	2.18884	9.0952823	6.969643	0.00829	0.086148
hsa-miR-28-5p	-2.44446	8.2959277	6.719835	0.009535	0.094949
hsa-miR-29c-3p	-3.00686	9.4359788	6.599694	0.0102	0.097508
hsa-miR-375	**-2.39585**	**15.732764**	**6.25059**	**0.012415**	**0.114124**
hsa-miR-185-5p	1.766215	10.97283	5.932252	0.014866	0.131594
hsa-miR-338-5p	2.789545	8.5425559	5.815708	0.015884	0.135578
hsa-miR-205-5p	**2.621553**	**10.832302**	**5.696611**	**0.016998**	**0.140085**
hsa-miR-3613-5p	2.736128	8.9034732	5.53656	0.018623	0.142586
hsa-miR-362-5p	-3.20117	7.0637951	5.501983	0.018995	0.142586
hsa-miR-7706	3.062136	7.440193	5.493157	0.019091	0.142586
hsa-miR-106b-3p	1.855044	10.197222	5.426127	0.019838	0.143673

hsa-let-7c-5p	-2.10493	12.03373	5.342758	0.020809	0.146272
hsa-miR-374a-3p	-3.20561	7.0625966	5.230147	0.022199	0.151585
hsa-miR-142-5p	2.750075	7.958257	5.098495	0.023947	0.156714
hsa-miR-378a-3p	2.34489	14.462887	5.075865	0.024261	0.156714
hsa-miR-499a-5p	-2.90046	7.5751569	4.968956	0.025806	0.157202
hsa-miR-200a-3p	-1.7102	12.746068	4.943868	0.026183	0.157202
hsa-miR-204-5p	**-2.13617**	**12.09691**	**4.922713**	**0.026506**	**0.157202**
hsa-miR-374a-5p	-2.48276	7.731995	4.892872	0.026968	0.157202
hsa-miR-196b-5p	-2.50038	8.8013411	4.662995	0.030819	0.175314
hsa-miR-3615	2.145313	8.6951132	4.594493	0.032075	0.175314
hsa-miR-221-3p	1.99	11.403436	4.583806	0.032275	0.175314
hsa-miR-29a-3p	-1.56991	10.950711	4.538318	0.033144	0.176032
hsa-miR-194-5p	-2.08035	11.035454	4.338388	0.037262	0.193601
hsa-miR-26a-5p	-1.56089	14.407557	4.299118	0.038132	0.193906
hsa-miR-378c	2.117121	11.50856	4.262065	0.038973	0.194051
hsa-miR-382-5p	4.079753	8.1052867	4.178959	0.040929	0.194612
hsa-miR-30b-5p	-1.78232	9.361434	4.169492	0.041158	0.194612
hsa-miR-200a-5p	-2.0379	8.4756649	4.131579	0.04209	0.194612
hsa-miR-146a-5p	**1.879016**	**11.066714**	**4.121463**	**0.042342**	**0.194612**
hsa-miR-210-3p	2.441074	8.8114332	4.0693	0.043669	0.196839
hsa-miR-27b-3p	-1.91852	12.638123	4.038468	0.044474	0.196839

Table 23: The Cancer Genome Atlas NGS Analysis

Gene Name	logFC	logCPM	LR	PValue	FDR
hsa-mir-153-2	2.375872	4.2179218	134.3074	4.68E-31	4.90E-28
hsa-mir-93	1.189148	10.550639	119.7268	7.26E-28	3.80E-25
hsa-mir-3074	1.814727	1.568247	108.3875	2.21E-25	7.71E-23
hsa-mir-92a-1	1.564023	8.3213546	107.1198	4.19E-25	1.10E-22
hsa-mir-20a	1.132973	6.8277576	90.2482	2.10E-21	4.39E-19
hsa-mir-891a	-4.69622	5.7882076	82.21717	1.22E-19	2.13E-17
hsa-mir-148a	1.108021	14.993064	68.8513	1.06E-16	1.39E-14
hsa-mir-221	-1.2587	8.3836717	68.56983	1.22E-16	1.39E-14
hsa-mir-19b-2	1.065629	6.4343874	68.52597	1.25E-16	1.39E-14
hsa-mir-27b	-0.80095	11.045283	68.40606	1.33E-16	1.39E-14
hsa-mir-200c	1.159767	12.559697	67.30591	2.32E-16	2.21E-14
hsa-mir-3648	2.114903	1.752852	66.47013	3.55E-16	3.10E-14
hsa-mir-92a-2	0.880161	12.000063	64.57169	9.31E-16	7.49E-14
hsa-mir-204	-1.92817	5.272123	63.19781	1.87E-15	1.40E-13
hsa-mir-96	1.521856	3.6452804	61.95647	3.51E-15	2.45E-13
hsa-mir-17	0.852782	8.3718011	61.82654	3.75E-15	2.45E-13
hsa-mir-3653	1.376266	2.1313151	60.26718	8.28E-15	5.10E-13
hsa-mir-153-1	1.911868	1.04943	59.08511	1.51E-14	8.77E-13
hsa-mir-3651	2.366102	-0.051638	58.82416	1.72E-14	9.49E-13
hsa-mir-708	1.081198	3.9738929	58.62231	1.91E-14	9.99E-13
hsa-mir-143	-0.95183	19.164957	57.06874	4.21E-14	2.10E-12
hsa-mir-130b	1.021477	3.1036429	55.8414	7.86E-14	3.74E-12
hsa-mir-187	-2.39347	4.4546513	55.31364	1.03E-13	4.67E-12
hsa-mir-222	-0.93211	6.1568708	51.57749	6.88E-13	3.00E-11
hsa-mir-133b	-1.31753	5.379416	51.33117	7.80E-13	3.26E-11
hsa-mir-19b-1	0.949312	1.8721361	50.60346	1.13E-12	4.55E-11
hsa-mir-141	1.022551	9.7097178	50.44562	1.23E-12	4.75E-11
hsa-mir-23c	-1.83966	2.5130641	50.11969	1.45E-12	5.40E-11
hsa-mir-629	0.704272	5.7138313	49.96907	1.56E-12	5.63E-11
hsa-mir-19a	1.161695	3.7454592	49.89754	1.62E-12	5.65E-11
hsa-mir-1224	-4.30229	1.2200315	49.05925	2.48E-12	8.38E-11
hsa-mir-133a-2	-1.35028	3.4053011	48.93359	2.65E-12	8.65E-11
hsa-mir-10a	-1.81014	12.372823	48.84375	2.77E-12	8.79E-11
hsa-mir-126	0.734171	9.9003198	48.05625	4.14E-12	1.24E-10
hsa-mir-889	-1.04511	4.1637969	48.04553	4.16E-12	1.24E-10
hsa-mir-375	1.60362	15.632796	46.46021	9.35E-12	2.72E-10

hsa-mir-378c	-1.02956	3.3046928	44.90335	2.07E-11	5.70E-10
hsa-mir-7-1	0.896851	3.6806218	44.90242	2.07E-11	5.70E-10
hsa-mir-381	-0.82828	5.6754016	44.56851	2.46E-11	6.59E-10
hsa-mir-196b	0.792775	9.0507603	44.21714	2.94E-11	7.69E-10
hsa-mir-20b	1.143666	6.8579937	42.27071	7.95E-11	2.03E-09
hsa-mir-1275	2.361612	-0.028257	41.71947	1.05E-10	2.62E-09
hsa-mir-184	-2.50435	2.5996989	41.10668	1.44E-10	3.51E-09
hsa-mir-873	-2.2561	-0.088651	40.82375	1.67E-10	3.96E-09
hsa-mir-892a	-4.87136	0.9964634	40.47178	1.99E-10	4.64E-09
hsa-mir-452	-0.758	5.5046358	39.81024	2.80E-10	6.36E-09
hsa-mir-25	0.800304	11.867799	39.03831	4.16E-10	9.25E-09
hsa-mir-615	2.180022	-0.057721	35.88002	2.10E-09	4.57E-08
hsa-mir-182	1.245345	12.93727	34.69345	3.86E-09	8.24E-08
hsa-mir-888	-5.66614	0.3677875	33.31146	7.85E-09	1.64E-07
hsa-mir-3189	2.62196	-0.982561	32.66443	1.10E-08	2.23E-07
hsa-mir-379	-0.7396	9.1201181	32.63807	1.11E-08	2.23E-07
hsa-mir-3687	1.707156	0.4725616	32.59746	1.13E-08	2.24E-07
hsa-mir-3170	1.591742	-0.616192	32.44443	1.23E-08	2.38E-07
hsa-mir-425	0.76313	5.7920194	32.30154	1.32E-08	2.51E-07
hsa-mir-1-2	-0.87472	7.9576222	31.13993	2.40E-08	4.47E-07
hsa-mir-3607	1.184976	4.5866887	31.11324	2.43E-08	4.47E-07
hsa-mir-542	-0.96701	6.8026582	30.8819	2.74E-08	4.95E-07
hsa-mir-106a	0.919663	5.5517447	30.81021	2.85E-08	5.04E-07
hsa-mir-1258	-1.34897	1.1020469	30.15134	4.00E-08	6.97E-07
hsa-mir-1251	-2.29768	2.8075032	29.50735	5.57E-08	9.55E-07
hsa-mir-135b	-1.52791	0.8813382	29.47205	5.67E-08	9.57E-07
hsa-mir-561	1.133266	0.2380957	29.02588	7.14E-08	1.19E-06
hsa-mir-490	-2.74685	2.1406113	28.72398	8.35E-08	1.36E-06
hsa-mir-106b	0.526667	7.8125021	28.46152	9.56E-08	1.54E-06
hsa-mir-32	0.773088	4.8223119	27.83285	1.32E-07	2.10E-06
hsa-mir-218-2	-0.46608	5.7003667	27.66883	1.44E-07	2.25E-06
hsa-mir-23b	-0.55774	10.960628	27.41853	1.64E-07	2.52E-06
hsa-mir-323b	-1.82248	1.326315	27.38474	1.67E-07	2.53E-06
hsa-mir-654	-0.60883	4.3471905	26.81406	2.24E-07	3.35E-06
hsa-mir-24-2	-0.52602	10.48834	26.46609	2.68E-07	3.95E-06
hsa-mir-191	0.631971	7.8381464	26.06139	3.31E-07	4.80E-06
hsa-mir-423	0.493807	5.7133823	25.73824	3.91E-07	5.60E-06
hsa-mir-299	-0.69771	1.5389282	25.64819	4.10E-07	5.79E-06
hsa-mir-934	-1.2634	0.6017654	25.09668	5.45E-07	7.60E-06
hsa-mir-616	0.998361	0.1730767	24.92321	5.97E-07	8.21E-06
hsa-mir-30d	0.403105	12.398191	24.43917	7.67E-07	1.04E-05

hsa-mir-487b	-0.73082	2.2862904	24.35392	8.02E-07	1.07E-05
hsa-mir-342	0.482584	5.5961014	24.34723	8.04E-07	1.07E-05
hsa-mir-27a	-0.47366	9.3506832	24.27636	8.35E-07	1.09E-05
hsa-mir-133a-1	-0.8883	7.1426282	24.2585	8.42E-07	1.09E-05
hsa-mir-1269	3.5489	4.4194509	24.14436	8.94E-07	1.14E-05
hsa-mir-18a	0.70535	1.7441356	23.90582	1.01E-06	1.26E-05
hsa-mir-576	0.597962	2.2538887	23.90079	1.01E-06	1.26E-05
hsa-mir-449a	2.819635	-0.159285	23.69269	1.13E-06	1.39E-05
hsa-mir-99b	-0.35597	13.823526	23.62524	1.17E-06	1.42E-05
hsa-mir-378	-0.6635	8.9037056	23.35121	1.35E-06	1.62E-05
hsa-mir-363	0.699295	6.4066321	23.3231	1.37E-06	1.63E-05
hsa-mir-891b	-5.14585	-0.130729	23.2777	1.40E-06	1.65E-05
hsa-mir-183	1.103625	11.367074	23.25485	1.42E-06	1.65E-05
hsa-mir-500a	0.523525	6.2745502	23.13477	1.51E-06	1.74E-05
hsa-mir-330	-0.57455	3.5008487	22.70964	1.88E-06	2.14E-05
hsa-mir-134	-0.52931	7.0027908	22.57249	2.02E-06	2.28E-05
hsa-mir-152	-0.60935	8.3401442	22.49824	2.10E-06	2.34E-05
hsa-mir-21	0.471152	16.196297	21.92	2.84E-06	3.13E-05
hsa-mir-652	-0.96209	3.8734763	21.75394	3.10E-06	3.38E-05
hsa-mir-3664	1.680061	-0.776448	21.6186	3.33E-06	3.59E-05
hsa-mir-196a-1	-0.87573	2.1546557	21.15967	4.23E-06	4.51E-05
hsa-mir-541	-1.51921	-0.580814	21.14076	4.27E-06	4.51E-05
hsa-mir-24-1	-0.44331	4.439857	21.07526	4.42E-06	4.62E-05
hsa-mir-618	1.694674	-0.772066	20.94669	4.72E-06	4.89E-05
hsa-mir-496	-0.69917	1.1432969	20.75066	5.23E-06	5.36E-05
hsa-mir-411	-0.6642	2.8882369	20.44708	6.13E-06	6.23E-05
hsa-mir-1291	1.237728	-0.494637	20.42559	6.20E-06	6.24E-05
hsa-mir-127	-0.51892	9.0653456	20.24933	6.80E-06	6.77E-05
hsa-mir-142	0.798764	8.9525854	19.92059	8.07E-06	7.97E-05
hsa-mir-210	1.111234	5.8703593	19.81764	8.52E-06	8.33E-05
hsa-mir-491	0.627844	1.3230771	19.75425	8.81E-06	8.53E-05
hsa-mir-1304	1.606437	-0.445973	19.15283	1.21E-05	0.000116
hsa-mir-769	0.391005	4.0479618	19.10706	1.24E-05	0.000118
hsa-mir-22	-0.31887	15.574185	19.08515	1.25E-05	0.000118
hsa-mir-3614	1.144672	-0.428612	18.82959	1.43E-05	0.000133
hsa-mir-760	-1.00978	0.023289	18.72802	1.51E-05	0.00014
hsa-mir-451	-1.02134	7.0260939	18.61829	1.60E-05	0.000147
hsa-mir-744	0.527733	4.487698	18.52389	1.68E-05	0.000153
hsa-mir-410	-0.55338	3.5086681	18.49244	1.71E-05	0.000154
hsa-mir-892b	-4.02234	-0.677826	18.3868	1.80E-05	0.000161
hsa-mir-146b	0.757807	7.2233514	18.36164	1.83E-05	0.000162

hsa-mir-944	-1.04098	1.3734933	18.15102	2.04E-05	0.000179
hsa-mir-100	-0.46524	13.170244	18.02096	2.18E-05	0.00019
hsa-mir-514-3	-1.45621	0.1594851	17.59132	2.74E-05	0.000237
hsa-mir-3612	-1.62059	-1.267406	17.51498	2.85E-05	0.000244
hsa-mir-450b	-0.87174	3.0927677	17.30202	3.19E-05	0.000271
hsa-mir-758	-0.49704	3.4817026	17.2797	3.23E-05	0.000272
hsa-mir-26a-2	-0.45882	11.094345	17.09713	3.55E-05	0.000297
hsa-mir-1248	0.846675	0.9442437	17.05347	3.63E-05	0.000302
hsa-mir-1976	0.533807	1.8627077	17.00728	3.72E-05	0.000307
hsa-mir-514-2	-1.50625	0.1951512	16.66533	4.46E-05	0.000364
hsa-mir-190b	1.259403	-0.35248	16.25653	5.53E-05	0.000447
hsa-mir-432	-0.62185	2.325647	16.24684	5.56E-05	0.000447
hsa-mir-651	0.612704	0.7319562	16.22105	5.64E-05	0.00045
hsa-mir-224	-0.54797	3.1618562	16.09485	6.02E-05	0.000477
hsa-mir-370	-0.57781	2.4921079	15.97631	6.41E-05	0.000504
hsa-mir-876	-1.54566	-1.034093	15.80843	7.01E-05	0.000547
hsa-mir-514-1	-1.42358	0.1829902	15.51246	8.20E-05	0.000635
hsa-mir-590	0.420038	3.1638283	14.76732	0.000122	0.000935
hsa-mir-424	-0.64829	4.7932847	14.75247	0.000123	0.000936
hsa-mir-219-2	-1.59514	-0.297982	14.53728	0.000137	0.001042
hsa-mir-493	-0.5778	2.7048661	14.45822	0.000143	0.001078
hsa-mir-212	-0.50694	2.8662911	14.37463	0.00015	0.001119
hsa-mir-376c	-0.61721	2.200399	14.08588	0.000175	0.001296
hsa-mir-559	1.600928	-1.160333	14.01829	0.000181	0.001334
hsa-mir-671	0.446058	1.5714286	13.8932	0.000193	0.001415
hsa-mir-197	0.417267	6.6372194	13.87261	0.000196	0.001421
hsa-mir-501	0.440567	3.2742846	13.67462	0.000217	0.001568
hsa-mir-29a	-0.35551	12.707552	13.54894	0.000232	0.001665
hsa-mir-3676	1.017736	2.2830318	13.28862	0.000267	0.0019
hsa-mir-660	0.404794	5.012233	13.1476	0.000288	0.002035
hsa-mir-508	-1.2397	2.3448322	13.07565	0.000299	0.0021
hsa-mir-338	-0.61435	7.8877981	13.05297	0.000303	0.002112
hsa-mir-548t	1.280678	-0.799869	13.01175	0.00031	0.002144
hsa-mir-145	-0.45408	12.363643	12.74921	0.000356	0.002443
hsa-mir-675	-1.20006	2.5301579	12.74318	0.000357	0.002443
hsa-mir-107	-0.26893	5.1128204	12.43036	0.000422	0.002869
hsa-mir-592	1.112876	0.0786445	12.40798	0.000428	0.002885
hsa-mir-505	-0.48984	4.355685	12.29427	0.000454	0.003046
hsa-mir-144	-0.84323	5.0465558	12.21289	0.000475	0.003151
hsa-mir-890	-2.26721	-1.19492	12.20763	0.000476	0.003151
hsa-mir-431	-0.6881	2.2115542	11.98578	0.000536	0.003527

hsa-mir-154	-0.42403	2.2543405	11.9715	0.00054	0.003532
hsa-mir-3152	1.547579	-0.676012	11.93548	0.000551	0.003578
hsa-mir-382	-0.44196	3.1450414	11.75463	0.000607	0.003915
hsa-mir-98	-0.32418	4.7639758	11.74473	0.00061	0.003915
hsa-mir-663	1.363497	-0.765854	11.7246	0.000617	0.003934
hsa-mir-488	-1.27539	-0.10305	11.32988	0.000763	0.004833
hsa-mir-377	-0.47003	1.4469292	11.31949	0.000767	0.004833
hsa-mir-129-1	-0.88255	1.202866	11.02947	0.000897	0.005617
hsa-mir-205	-0.81572	10.109087	10.95431	0.000934	0.005814
hsa-mir-2114	-1.13975	-0.0336	10.77982	0.001026	0.006341
hsa-mir-383	-0.90911	1.6392219	10.77182	0.001031	0.006341
hsa-mir-627	0.625524	0.2908571	10.67323	0.001087	0.006649
hsa-mir-676	-0.68021	0.3620714	10.59113	0.001136	0.00691
hsa-mir-188	0.477346	1.2396901	10.56898	0.00115	0.006943
hsa-mir-376a-1	-0.66012	0.1372532	10.56094	0.001155	0.006943
hsa-mir-509-3	-1.54933	-0.272854	10.43443	0.001237	0.007393
hsa-mir-552	-1.15865	-0.980088	10.34536	0.001298	0.007714
hsa-mir-486	-0.77592	5.3991957	10.19518	0.001408	0.008321
hsa-mir-450a-2	-0.61022	0.9699993	10.10317	0.00148	0.008698
hsa-mir-412	-1.00977	1.5010153	9.905115	0.001648	0.009631
hsa-mir-543	-0.55986	0.4045636	9.750433	0.001793	0.010418
hsa-mir-3658	1.085486	-1.307106	9.629619	0.001915	0.011065
hsa-mir-376a-2	-0.7518	-0.5099	9.54603	0.002004	0.011516
hsa-mir-129-2	-0.8246	1.2402839	9.437361	0.002126	0.012152
hsa-mir-1296	0.46015	2.391548	9.250943	0.002354	0.013381
hsa-mir-3923	-1.12384	-1.307406	8.928845	0.002807	0.015871
hsa-mir-1-1	-0.67784	-0.080493	8.900593	0.002851	0.016032
hsa-mir-484	0.421845	4.4109294	8.867331	0.002903	0.016239
hsa-mir-532	0.349094	9.2625446	8.829194	0.002964	0.016494
hsa-mir-323	-0.77066	0.8079309	8.803072	0.003007	0.016643
hsa-mir-485	-0.49873	0.7664848	8.732438	0.003126	0.017209
hsa-mir-454	0.33438	2.0117732	8.523015	0.003507	0.019205
hsa-mir-15a	0.270969	6.1167716	8.418911	0.003713	0.02023
hsa-mir-147b	1.213297	-0.653303	8.332971	0.003893	0.021039
hsa-mir-181d	-0.34867	3.7627408	8.328802	0.003902	0.021039
hsa-mir-3622b	-1.37434	-1.293387	8.282237	0.004003	0.021475
hsa-mir-200b	0.512001	9.1454824	8.216699	0.004151	0.022151
hsa-mir-369	-0.43261	3.0787675	8.119267	0.00438	0.023255
hsa-mir-449b	1.970322	-1.08281	7.964609	0.00477	0.0252
hsa-let-7c	-0.30802	12.656205	7.902721	0.004936	0.025945
hsa-mir-3193	-0.9805	-0.78771	7.829555	0.00514	0.026882

hsa-mir-3195	-1.26913	-1.124426	7.775057	0.005297	0.027567
hsa-mir-214	-0.28483	3.8830032	7.716223	0.005473	0.02828
hsa-mir-628	-0.34764	2.988739	7.711054	0.005488	0.02828
hsa-mir-103-2	0.343933	1.71964	7.687482	0.005561	0.028511
hsa-mir-494	-0.62473	0.2759539	7.639594	0.00571	0.029135
hsa-mir-513c	-1.20781	-1.255094	7.57005	0.005935	0.030134
hsa-mir-589	0.233194	4.8469167	7.450223	0.006343	0.031996
hsa-mir-3154	-1.19174	-1.06453	7.444645	0.006363	0.031996
hsa-mir-653	0.459498	0.87323	7.419811	0.006451	0.032286
hsa-mir-376b	-0.55901	0.1533243	7.20836	0.007256	0.036144
hsa-mir-539	-0.54821	1.7863857	7.150319	0.007495	0.037156
hsa-mir-23a	-0.28687	10.739657	7.093859	0.007735	0.038163
hsa-mir-1255a	0.610042	-0.35008	7.022879	0.008047	0.03952
hsa-mir-30b	0.402195	8.5344667	6.958267	0.008343	0.040781
hsa-mir-219-1	0.399761	0.8042959	6.814108	0.009044	0.043945
hsa-mir-509-1	-1.00122	-0.45673	6.799211	0.00912	0.043945
hsa-mir-2278	1.070325	-1.286556	6.793383	0.00915	0.043945
hsa-mir-136	-0.46398	5.5384516	6.786174	0.009187	0.043945
hsa-mir-450a-1	-0.55158	0.9146509	6.783435	0.009201	0.043945
hsa-mir-181a-2	-0.33465	7.713994	6.744644	0.009403	0.044707
hsa-mir-3613	0.423838	2.8163195	6.728623	0.009488	0.044906
hsa-mir-632	0.993626	-0.9512	6.703287	0.009624	0.045343
hsa-mir-3622a	-0.61936	-0.45416	6.609157	0.010146	0.047589
hsa-mir-139	-0.36296	6.2422859	6.524153	0.010642	0.04969
hsa-mir-495	-0.34241	2.2711025	6.516373	0.010689	0.04969
hsa-mir-150	0.466193	7.9079427	6.506354	0.010749	0.04975
hsa-mir-497	0.280251	4.9098755	6.369655	0.011609	0.053493
hsa-mir-329-2	-0.60551	-0.410151	6.291365	0.012133	0.055662
hsa-mir-3662	1.135779	-1.266248	6.168184	0.013007	0.059117
hsa-mir-3943	-0.78855	-0.534875	6.163351	0.013042	0.059117
hsa-mir-1225	-0.91101	-1.113035	6.161568	0.013056	0.059117
hsa-mir-585	-0.88169	-0.49172	6.122093	0.01335	0.060191
hsa-mir-550a-1	0.459876	0.2001389	6.068211	0.013764	0.061789
hsa-mir-181b-1	-0.2924	6.1014706	6.029579	0.014068	0.062886
hsa-mir-95	0.448455	0.6233907	5.96929	0.014557	0.064795
hsa-mir-125a	-0.25369	9.1056048	5.880956	0.015306	0.067837
hsa-mir-4284	-0.96183	-1.294707	5.819267	0.015852	0.069961
hsa-mir-206	-1.83627	6.7549515	5.693307	0.01703	0.074845
hsa-mir-1274b	0.571288	2.2075754	5.685597	0.017105	0.07486
hsa-mir-15b	0.313265	6.2310564	5.66825	0.017275	0.075289
hsa-mir-31	-0.54201	2.0714663	5.63074	0.017648	0.076597

hsa-mir-103-1	0.246508	13.002564	5.464777	0.019404	0.083868
hsa-mir-670	-0.78546	-1.32823	5.39122	0.020238	0.087116
hsa-mir-935	0.695878	-0.388736	5.381551	0.020351	0.087241
hsa-mir-668	-1.08927	-1.164109	5.37052	0.02048	0.087437
hsa-mir-1237	-0.77066	-1.3284	5.34717	0.020756	0.088255
hsa-mir-581	0.64162	-0.768555	5.329895	0.020963	0.088773
hsa-mir-1179	-0.78141	-0.947104	5.304739	0.021267	0.089701
hsa-mir-3180-4	-0.72341	-1.32902	5.195204	0.022649	0.095145
hsa-mir-26a-1	0.416579	0.3972515	5.187801	0.022746	0.095169
hsa-mir-105-1	1.207705	-0.331231	5.167196	0.023017	0.095921
hsa-mir-655	-0.36388	0.6473016	5.13758	0.023413	0.097184
hsa-mir-1539	0.714487	-1.329103	5.12272	0.023615	0.097632
hsa-let-7a-2	0.22847	13.407557	5.096461	0.023975	0.09873
hsa-mir-326	-0.30874	2.1257736	5.047497	0.024662	0.101161
hsa-mir-498	0.685741	-1.329539	5.024415	0.024992	0.102117
hsa-mir-3146	0.681822	-1.329602	5.010132	0.025199	0.102562
hsa-mir-3647	0.486405	1.9821505	4.995338	0.025416	0.103042
hsa-mir-555	0.672077	-1.329734	4.980918	0.025628	0.103503
hsa-mir-612	1.369552	-1.110237	4.963316	0.025891	0.10416
hsa-mir-345	0.266392	2.473808	4.913869	0.026642	0.10639
hsa-mir-130a	-0.27107	6.0258603	4.913443	0.026648	0.10639
hsa-mir-3065	0.39577	4.9858477	4.895791	0.026922	0.107075
hsa-mir-548e	0.702434	-0.861516	4.851402	0.027624	0.109448
hsa-mir-362	0.301661	2.625225	4.792975	0.028576	0.112794
hsa-let-7a-1	0.227778	12.407351	4.741326	0.029446	0.115793
hsa-mir-105-2	1.248527	-0.21597	4.727204	0.029689	0.11631
hsa-let-7a-3	0.225029	12.414	4.671376	0.030669	0.119702
hsa-mir-3650	0.898982	-1.259267	4.604422	0.03189	0.124002
hsa-mir-339	0.230297	3.8974532	4.594222	0.03208	0.12428
hsa-mir-4286	0.803333	-1.032317	4.560788	0.032712	0.126261
hsa-mir-599	-0.89787	-1.197875	4.525217	0.033399	0.128438
hsa-mir-378b	-0.83605	-1.174776	4.490212	0.034089	0.130614
hsa-mir-556	0.710719	-0.62805	4.474166	0.034411	0.131365
hsa-mir-2115	0.865139	-0.902961	4.448892	0.034924	0.132838
hsa-mir-198	0.843868	-1.300827	4.365231	0.03668	0.13901
hsa-mir-125b-2	-0.20212	5.9984506	4.299676	0.03812	0.143946
hsa-mir-30e	-0.1728	13.216998	4.263042	0.03895	0.146553
hsa-mir-937	0.543025	-0.368983	4.243216	0.039407	0.147743
hsa-mir-4326	0.487951	0.4040128	4.206982	0.040258	0.150392
hsa-mir-574	0.237821	5.7688801	4.191981	0.040616	0.151188
hsa-mir-3909	-0.55831	-0.789732	4.116423	0.042469	0.157526

hsa-mir-372	0.895694	-0.893316	4.097254	0.042953	0.158616
hsa-mir-181c	-0.21991	6.5870333	4.088872	0.043166	0.158616
hsa-mir-3611	0.851846	-1.245825	4.086868	0.043218	0.158616
hsa-mir-2110	0.393347	0.5408299	4.079816	0.043398	0.158723
hsa-mir-335	0.274122	5.0125101	4.069488	0.043665	0.15914
hsa-mir-3161	1.172215	-1.248226	4.050552	0.044157	0.160375
hsa-mir-215	-0.37529	0.6691823	4.037941	0.044488	0.161019
hsa-mir-1231	-0.5923	-1.335904	4.009117	0.045255	0.162738
hsa-mir-3937	0.605495	-1.335697	4.0084	0.045274	0.162738
hsa-mir-155	0.294701	6.2326402	3.997428	0.04557	0.16324
hsa-mir-570	0.655976	-0.776421	3.978735	0.046078	0.164497
hsa-mir-1285-1	0.582635	-1.335965	3.955972	0.046705	0.166169
hsa-mir-622	0.571268	-1.336162	3.918812	0.047749	0.169305
hsa-mir-3907	-0.55352	-1.336432	3.907852	0.048061	0.169837
hsa-mir-3121	-0.55213	-1.33652	3.892043	0.048515	0.170713
hsa-mir-3918	-0.79349	-1.287335	3.882747	0.048785	0.170713
hsa-mir-200a	0.382774	8.57815	3.880845	0.04884	0.170713
hsa-mir-943	-0.79195	-1.288203	3.876283	0.048973	0.170713
hsa-let-7e	-0.25991	9.3482691	3.871083	0.049125	0.170713
hsa-mir-3927	-0.53496	-1.336734	3.85234	0.049677	0.171815
hsa-mir-1277	0.556949	-0.301321	3.849172	0.049771	0.171815

Table 24: P69 vs M12 Microarray Analysis

Gene Name	Fold change	Gene Name	Fold change	Gene Name	Fold change
hsa-miR-548m-5p	-500	hsa-miR-135b-3p	-6.84932	hsa-miR-500-5p	-3.1348
hsa-miR-127-3p	-500	hsa-miR-132-3p	-6.45161	hsa-miR-2113-5p	-3.125
hsa-miR-411-5p	-200	hsa-miR-520a-5p	-6.41026	hsa-miR-1227-5p	-3.03951
hsa-miR-138-1-3p	-200	hsa-miR-29c-3p	-6.32911	hsa-miR-425-3p	-3.003
hsa-miR-891b-5p	-142.857	hsa-miR-514-5p	-6.25	hsa-miR-146b-5p	-2.99401
hsa-miRPlus-C1089	-111.111	hsa-miR-489-5p	-6.21118	hsa-miR-140-3p	-2.95858
hsa-miR-1248-5p	-58.8235	hsa-miR-145-3p	-6.17284	hsa-miR-127-5p	-2.90698
hsa-miR-299-5p	-50	hsa-miR-342-5p	-6.06061	hsa-miR-1181-5p	-2.86533
hsa-miR-379-5p	-50	hsa-miR-23b-3p	-5.91716	hsa-miR-587-5p	-2.83286
hsa-miR-889-5p	-40	hsa-miR-556-3p	-5.78035	hsa-miR-379-3p	-2.7933
hsa-miR-548a-5p	-35.7143	hsa-miR-23a-3p	-5.61798	hsa-miR-1182-5p	-2.78552
hsa-miR-323a-3p	-32.2581	hsa-miR-1265-5p	-5.34759	hsa-miR-876-3p	-2.73973
hsa-miRPlus-D1061	-27.7778	hsa-miR-148a-3p	-5.29101	hsa-miR-296-3p	-2.7027
hsa-miR-34b-3p	-27.027	hsa-miR-143-3p	-5.2356	hsa-let-7a-2-3p	-2.69542
hsa-miR-487b-5p	-25.641	hsa-miR-1267-5p	-5.18135	hsa-miR-603-5p	-2.68817
hsa-miR-1238-5p	-25.641	hsa-miR-376a-3p	-5.05051	hsa-miR-411-3p	-2.6738
hsa-miR-409-3p	-23.8095	hsa-miR-105-3p	-5.02513	hsa-miR-144-5p	-2.6738
hsa-miR-135b-5p	-23.2558	hsa-miR-1260a-5p	-4.7619	hsa-miR-1538-5p	-2.6455
hsa-miR-614-5p	-23.2558	hsa-miR-27a-5p	-4.7619	hsa-miR-323-5p	-2.6178
hsa-miR-504-5p	-22.7273	hsa-miR-125b-1-3p	-4.71698	hsa-miR-758-5p	-2.59067
hsa-miR-1914-3p	-22.2222	hsa-miR-380-5p	-4.71698	hsa-miR-770-5p	-2.55102
hsa-miR-520d-3p	-21.2766	hsa-miR-369-5p	-4.6729	hsa-miR-15b-5p	-2.55102
hsa-miR-382-5p	-20.8333	hsa-miR-572-5p	-4.65116	hsa-miR-27b-5p	-2.53165
hsa-miR-1185-5p	-20	hsa-miR-100-5p	-4.5045	SNORD38B	-2.51256
hsa-miR-579-5p	-19.6078	hsa-miR-1206-5p	-4.44444	hsa-miR-1270-5p	-2.5
hsa-miR-659-5p	-19.6078	hsa-miR-19b-2-3p	-4.34783	hsa-miR-339-5p	-2.48139
hsa-miR-136-5p	-18.1818	hsa-miR-138-2-3p	-4.31034	hsa-miR-654-5p	-2.47525
hsa-miR-452-3p	-17.5439	hsa-miR-598-5p	-4.2735	hsa-miR-19b-5p	-2.46914
hsa-miR-377-5p	-17.2414	hsa-miR-376c-5p	-4.25532	hsa-miR-630-5p	-2.45098
hsa-miR-490-5p	-16.9492	hsa-miR-31-5p	-4.21941	hsa-miR-449b-3p	-2.42131
hsa-miR-936-5p	-15.625	hsa-miR-376b-5p	-4.14938	hsa-miR-1256-5p	-2.40964
hsa-miR-362-3p	-13.8889	hsa-miR-1258-5p	-4.13223	hsa-miR-378a-3p	-2.40385
hsa-miR-616-5p	-12.5	hsa-miR-543-5p	-3.90625	hsa-miR-212-5p	-2.33645
hsa-miR-432-5p	-11.7647	hsa-miR-191-5p	-3.87597	hsa-miR-142-5p	-2.32019
hsa-miR-619-5p	-11.6279	hsa-miR-432-3p	-3.74532	hsa-miR-302d-3p	-2.24215

hsa-miR-509-3p	-10.989	hsa-miR-181a-2-3p	-3.74532	hsa-miR-100-3p	-2.23214
hsa-miR-1237-5p	-10.5263	hsa-miR-302e-5p	-3.74532	hsa-miR-555-5p	-2.20264
hsa-miR-541-3p	-10.4167	hsa-miR-448-5p	-3.67647	hsa-miR-23b-5p	-2.1978
hsa-miR-1179-5p	-10.2041	hsa-miR-376a-5p	-3.663	hsa-miR-146a-5p	-2.17865
hsa-miR-1236-5p	-10	hsa-miR-1245a-5p	-3.63636	hsa-miR-769-3p	-2.17391
hsa-miR-640-5p	-9.52381	hsa-miR-493-3p	-3.63636	hsa-miR-125a-3p	-2.1322
hsa-miR-135a-5p	-8.19672	hsa-miR-649-5p	-3.62319	hsa-miR-1253-5p	-2.12314
hsa-miR-888-3p	-8.06452	hsa-miR-924-5p	-3.59712	hsa-miR-34c-5p	-2.11864
hsa-miR-342-3p	-7.87402	hsa-miR-191-3p	-3.43643	hsa-miR-224-3p	-2.10526
hsa-miR-588-5p	-7.69231	hsa-miR-875-3p	-3.27869	hsa-miR-591-5p	-2.08768
hsa-miR-527-5p	-7.57576	hsa-miR-218-1-3p	-3.26797	hsa-miR-450b-5p	-2.05339
hsa-miR-141-3p	-7.40741	hsa-miR-526b-3p	-3.26797	hsa-miR-636-5p	-2.04499
hsa-miR-196b-3p	-7.29927	hsa-miR-138-5p	-3.22581	hsa-miR-720-5p	-2.04082
hsa-miR-125b-5p	-6.89655	hsa-miR-21-5p	-3.20513	hsa-miR-1914-5p	-2.03252
hsa-miR-516b-3p	-6.84932	hsa-miR-1913-5p	-3.16456	hsa-miR-203-5p	-2.0284

Gene Name	Fold change	Gene Name	Fold change	Gene Name	Fold change
hsa-miRPlusA1027	2.003	hsa-miR-200c-3p	3.487	hsa-miR-486-5p	9.078
hsa-miR-126-5p	2.004	hsa-miR-188-5p	3.557	hsa-miR-570-5p	9.152
hsa-miR-34c-3p	2.006	hsa-miR-642-5p	3.597	hsa-miR-195-3p	9.307
hsa-miR-515-3p	2.007	hsa-miR-326-5p	3.606	hsa-miR-933-5p	9.341
hsa-miR-621-5p	2.012	hsa-miR-490-3p	3.612	hsa-miR-663b-5p	9.506
hsa-miR-34a-3p	2.015	hsa-miR-193b-3p	3.617	hsa-miR-337-5p	9.977
hsa-miR-22-5p	2.026	hsa-miR-450a-5p	3.62	hsa-miR-551a-5p	10.377
hsa-miR-365-5p	2.042	hsa-miR-181c-5p	3.65	hsa-miR-592-5p	10.486
hsa-miR-491-5p	2.071	hsa-miR-208b-5p	3.741	hsa-miR-513c-5p	10.656
hsa-miR-96-3p	2.084	hsa-miR-628-5p	3.746	hsa-miR-211-5p	10.954
hsa-miR-1264-5p	2.092	hsa-miR-154-3p	3.751	hsa-miR-299-3p	11.371
hsa-miR-141-5p	2.093	hsa-miR-7-1-3p	3.787	hsa-miR-623-5p	11.895
hsa-miR-589-5p	2.094	hsa-miR-942-5p	3.83	hsa-miR-508-3p	12.437
hsa-miR-26b-5p	2.105	hsa-miR-187-5p	3.83	hsa-miR-19b-1-3p	12.583
hsa-miR-187-3p	2.157	hsa-miR-135a-3p	3.855	hsa-miR-517-3p	12.739
hsa-miR-330-3p	2.168	hsa-miR-595-5p	3.858	hsa-miR-767-3p	12.925
hsa-miR-32-5p	2.175	hsa-miR-1244-5p	3.885	hsa-miR-363-3p	13.28
hsa-miR-885-3p	2.211	hsa-miR-558-5p	3.986	hsa-miR-662-5p	13.298
hsa-miR-346-5p	2.219	hsa-miR-647-5p	4.044	hsa-miR-520b-5p	13.474
hsa-miR-28-3p	2.227	hsa-miR-943-5p	4.137	hsa-miR-196a-5p	13.48
hsa-miR-30a-3p	2.277	hsa-miR-34a-5p	4.183	hsa-miR-620-5p	13.515
hsa-miR-668-5p	2.285	hsa-let-7d-5p	4.191	hsa-miR-518c-3p	13.62
hsa-miR-628-3p	2.295	hsa-miR-429-5p	4.224	hsa-miR-3180-3p	13.753

hsa-miR-1205-5p	2.307	hsa-miR-675-3p	4.326	hsa-miR-562-5p	15.051
hsa-miR-1296-5p	2.322	hsa-miR-548k-5p	4.433	hsa-miR-767-5p	15.266
hsa-miR-30e-5p	2.327	hsa-miR-370-5p	4.444	hsa-miR-501-3p	15.48
hsa-miR-200b-3p	2.34	hsa-miR-519e-5p	4.471	hsa-miR-486-3p	16.75
hsa-miR-125b-2-3p	2.352	hsa-miR-520f-5p	4.509	hsa-miR-371-5p	16.886
hsa-miR-526b-5p	2.391	hsa-miR-130a-5p	4.531	hsa-miR-106a-3p	17.1
hsa-miR-502-5p	2.396	hsa-miR-580-5p	4.63	hsa-miR-338-5p	17.177
hsa-miR-137-5p	2.417	hsa-miR-548i-5p	4.639	hsa-miR-33b-5p	17.468
hsa-miR-214-5p	2.435	hsa-miR-890-5p	4.692	hsa-miR-616-3p	17.628
hsa-miR-223-5p	2.437	hsa-miR-146a-3p	4.81	hsa-miR-374b-3p	17.749
hsa-miR-744-5p	2.443	hsa-miR-583-5p	5.012	**hsa-miRPlusA1031**	17.818
hsa-miR-325-5p	2.483	hsa-miR-188-3p	5.021	hsa-miR-1269-5p	17.957
hsa-miR-7-5p	2.49	hsa-miR-222-3p	5.023	hsa-miR-372-5p	18.745
hsa-miR-210-5p	2.497	hsa-miR-518b-5p	5.143	hsa-miR-557-5p	18.817
hsa-miR-33b-3p	2.499	hsa-miR-548o-5p	5.164	hsa-miR-512-5p	19.327
hsa-miR-518e-5p	2.514	hsa-miR-124-5p	5.174	hsa-miR-202-5p	19.695
hsa-miR-1249-5p	2.515	hsa-miR-885-5p	5.175	hsa-miR-18b-3p	20
hsa-miR-339-3p	2.528	hsa-miR-146b-3p	5.355	**hsa-miRPlusD1033**	20.163
hsa-miR-760-5p	2.529	hsa-miR-600-5p	5.403	hsa-miR-675b-5p	21.361
hsa-miR-30d-5p	2.555	hsa-miR-597-5p	5.554	hsa-miR-873-5p	21.467
hsa-miR-1911-3p	2.561	hsa-miR-15b-3p	5.574	hsa-miR-1-5p	23.538
hsa-miR-605-5p	2.583	hsa-miR-381-5p	5.729	hsa-miR-412-5p	23.833
hsa-miR-148b-5p	2.601	hsa-miR-99a-5p	5.742	hsa-miR-491-3p	24.61
hsa-miR-877-3p	2.603	hsa-miR-223-3p	5.753	hsa-miR-498-5p	25.427
hsa-miR-200a-5p	2.655	hsa-miR-634-5p	5.801	hsa-miR-937-5p	26.513
hsa-miR-421-5p	2.664	hsa-miR-518a-3p	5.86	hsa-miR-451-5p	27.084
hsa-miR-499-5p	2.731	hsa-miR-596-5p	5.881	hsa-miR-520d-5p	27.591
hsa-miR-1263-5p	2.741	hsa-miR-30c-1-3p	5.921	hsa-miR-556-5p	27.696
hsa-miR-26a-1-3p	2.751	hsa-miR-516a-5p	6.019	hsa-miR-147-5p	27.998
hsa-miR-25-3p	2.777	hsa-miR-335-3p	6.032	hsa-miR-92b-3p	28.949
hsa-miR-564-5p	2.805	hsa-miR-554-5p	6.091	hsa-miR-515-5p	30.258
hsa-miR-545-5p	2.807	hsa-miR-150-5p	6.103	hsa-miR-517c-5p	31.942
hsa-miR-22-3p	2.811	hsa-miR-521-5p	6.14	hsa-miR-373-3p	34.484
hsa-miR-548d-5p	2.836	hsa-miR-615-3p	6.17	hsa-miR-524-3p	34.725
hsa-miR-891a	2.84	hsa-miR-551b-3p	6.242	hsa-miR-454-3p	35.91
hsa-miR-26a-2-3p	2.88	hsa-miR-199a-3p	6.426	hsa-miR-133a-5p	37.907
hsa-let-7c-5p	2.932	hsa-miR-10a-3p	6.566	hsa-miR-133b-5p	38.93
hsa-miR-200a-3p	2.943	hsa-miR-497-5p	6.572	hsa-miR-181c-3p	42.935
hsa-miR-30c-2-3p	3.05	hsa-miR-9-5p	6.676	hsa-miR-373-5p	45.111
hsa-miR-184-5p	3.077	hsa-miR-516b-5p	6.816	hsa-miR-518f-5p	47.556
hsa-miR-1271-5p	3.082	hsa-miR-525-3p	6.817	hsa-miR-921-5p	69.187

hsa-miR-302a-5p	3.167	hsa-miR-541-5p	7.187	hsa-miR-548l-5p	76.18
hsa-miR-149-3p	3.175	hsa-miR-139-5p	7.456	hsa-miR-375-5p	81.495
hsa-miR-552-5p	3.302	hsa-miR-129-3p	7.465	hsa-miR-143-5p	83.063
hsa-miR-510-5p	3.344	hsa-miR-362-5p	7.488	hsa-miR-631-5p	85.097
hsa-miR-10a-5p	3.349	hsa-miR-217-5p	7.616	hsa-miR-153-5p	100.736
hsa-miR-130b-5p	3.361	hsa-miR-888-5p	7.62	hsa-miR-105-5p	131.645
hsa-miR-96-5p	3.388	hsa-miR-301b-5p	7.815	hsa-miR-622-5p	147.739
hsa-miR-608-5p	3.404	hsa-miR-1224-3p	7.95	hsa-miR-122-5p	198.567
hsa-miR-485-3p	3.414	hsa-miR-519a-5p	8.064	hsa-miR-147b-5p	201.357
hsa-miR-615-5p	3.421	hsa-miR-338-3p	8.159	hsa-miR-551b-5p	264.961
hsa-miR-149-5p	3.432	hsa-miR-198-5p	8.234	hsa-miRPlusC1076	1046.216
hsa-miR-302c-5p	3.435	hsa-miR-610-5p	8.235		
hsa-miR-130b-3p	3.448	hsa-miR-517a-5p	8.245		
hsa-miR-1255b-5p	3.461	hsa-miR-10b-5p	8.885		

The low inter- and intra-platform consistency of different miRNA profiling technologies is troubling. Because of this, it is considered good practice to validate one's profiling results with another platform. In Chapter 1, we validated our urinary sequencing results with qRT-PCR but we did not have the time to validate each one of the large number of miRNAs profiled in Chapter 2. So in the place of validation by qRT-PCR, a miRNA microarray representing the work of a previous graduate student in our laboratory is reproduced here. It duplicates the comparison between the P69 and M12 cell lines only.

Table 25: Detailed Legend for Figure 14 A)

Gene	Fold Change	logCPM	LR	PValue
hsa-mir-770	-0.57267	-1.19553	1.920108	0.165845
hsa-mir-370	-0.57781	2.492108	15.97631	6.41E-05
hsa-mir-493	-0.5778	2.704866	14.45822	0.000143
hsa-mir-337	-0.09373	3.893152	0.623334	0.429811
hsa-mir-665	-0.18132	-0.76107	0.376376	0.539549
hsa-mir-431	-0.6881	2.211554	11.98578	0.000536
hsa-mir-433	-0.15849	0.00032	0.458814	0.498179
hsa-mir-127	-0.51892	9.065346	20.24933	6.80E-06
hsa-mir-432	-0.62185	2.325647	16.24684	5.56E-05
hsa-mir-136	-0.46398	5.538452	6.786174	0.009187
hsa-mir-379	-0.7396	9.120118	32.63807	1.11E-08
hsa-mir-299	-0.69771	1.538928	25.64819	4.10E-07
hsa-mir-380	-0.36248	0.149918	3.385694	0.065764
hsa-mir-323	-0.77066	0.807931	8.803072	0.003007
hsa-mir-758	-0.49704	3.481703	17.2797	3.23E-05
hsa-mir-329	-0.60551	-0.41015	6.291365	0.012133
hsa-mir-494	-0.62473	0.275954	7.639594	0.00571
hsa-mir-543	-0.55986	0.404564	9.750433	0.001793
hsa-mir-495	-0.34241	2.271103	6.516373	0.010689
hsa-mir-376c	-0.61721	2.200399	14.08588	0.000175
hsa-mir-376a	-0.7518	-0.5099	9.54603	0.002004
hsa-mir-654	-0.60883	4.34719	26.81406	2.24E-07
hsa-mir-376b	-0.55901	0.153324	7.20836	0.007256
hsa-mir-300	0	-1.35774	0	1
hsa-mir-381	-0.82828	5.675402	44.56851	2.46E-11
hsa-mir-487b	-0.73082	2.28629	24.35392	8.02E-07
hsa-mir-539	-0.54821	1.786386	7.150319	0.007495
hsa-mir-889	-1.04511	4.163797	48.04553	4.16E-12
hsa-mir-544b	0.562399	-1.32198	1.530385	0.216055
hsa-mir-655	-0.36388	0.647302	5.13758	0.023413
hsa-mir-487a	-0.07083	0.116702	0.133341	
hsa-mir-382	-0.44196	3.145041	11.75463	0.000607
hsa-mir-134	-0.52931	7.002791	22.57249	2.02E-06
hsa-mir-668	-1.08927	-1.16411	5.37052	0.02048
hsa-mir-485	-0.49873	0.766485	8.732438	0.003126
has-mir-453	NA	NA	NA	NA

hsa-mir-154	-0.42403	2.25434	11.9715	0.00054
hsa-mir-496	-0.69917	1.143297	20.75066	5.23E-06
hsa-mir-377	-0.47003	1.446929	11.31949	0.000767
hsa-mir-541	-1.51921	-0.58081	21.14076	4.27E-06
hsa-mir-409	-0.09061	3.994212	0.545747	0.460061
hsa-mir-412	-1.00977	1.501015	9.905115	0.001648
hsa-mir-410	-0.55338	3.508668	18.49244	1.71E-05
hsa-mir-656	-0.29756	-0.02532	1.917731	0.166107

Table 26: Detailed Legend for Figure 14 B)

Gene	logFC	logCPM	LR	P-value
hsa-miR-127-3p	-7.8541	8.32929	26.14608	3.17E-07
hsa-miR-127-5p	-4.60846	2.749087	3.722337	0.053689
hsa-miR-134-5p	-5.29173	5.857574	16.06363	6.12E-05
hsa-miR-136-3p	-7.86219	5.174953	15.66054	7.58E-05
hsa-miR-136-5p	-5.97326	3.613491	7.000483	0.008149
hsa-miR-154-3p	-4.34619	2.621537	3.187705	0.074194
hsa-miR-299-3p	-6.79296	4.220381	8.727155	0.003135
hsa-miR-323a-3p	-7.70687	5.011052	12.82824	0.000341
hsa-miR-323b-3p	-6.99059	4.390966	9.755046	0.001788
hsa-miR-329-3p	-5.52909	3.316172	5.974179	0.014517
hsa-miR-337-3p	-5.00872	2.970253	4.698453	0.03019
hsa-miR-370-3p	-11.4301	8.603022456	31.87442999	1.64E-08
hsa-miR-376a-3p	-5.06654	2.980456303	4.289050984	0.038358571
hsa-miR-376c-3p	-5.58019	3.330567	6.153677	0.013114
hsa-miR-377-3p	-6.02292	3.627183	6.614553	0.010115
hsa-miR-379-3p	-4.37378	2.626862	3.123234	0.077183
hsa-miR-379-5p	-10.5752	7.760063	27.68123	1.43E-07
hsa-miR-382-3p	-5.18441	3.071711	5.080347	0.024199

hsa-miR-382-5p	-8.0011	5.28569	15.5985	7.83E-05
hsa-miR-409-3p	-10.0685	7.261611	26.51293	2.62E-07
hsa-miR-409-5p	-5.59927	3.335382	6.021738	0.014131
hsa-miR-410-3p	-5.90353	3.505032	5.272944	0.021659
hsa-miR-431-3p	-4.37504	2.626862	3.105295	0.078038
hsa-miR-433-3p	-6.37965	3.878968	6.847639	0.008876
hsa-miR-485-3p	-5.9428	3.562994	6.262382	0.012333
hsa-miR-485-5p	-4.83709	2.866527	4.101107	0.042855
hsa-miR-487b-3p	-5.39577	3.231627	5.629107	0.017665
hsa-miR-493-3p	-8.74440	5.989907002	22.46513627	2.14E-06
hsa-miR-493-5p	-9.76754	6.963052438	22.87421627	1.73E-06
hsa-miR-494-3p	-4.04009	2.487355	2.753955	0.097014
hsa-miR-495-3p	-6.93181	4.342174	9.656266	0.001887
hsa-miR-539-3p	-6.45383	3.967528	8.123694	0.004369
hsa-miR-543	-9.50421	6.707409	23.09731	1.54E-06
hsa-miR-654-3p	-10.1712	7.363168	27.41589	1.64E-07
hsa-miR-654-5p	-7.0784	4.480912	10.64118	0.001106
hsa-miR-656-3p	-5.81706	3.486217	6.44361	0.011135
hsa-miR-758-3p	-7.72285	5.032793	13.41604	0.000249
hsa-miR-889-3p	-7.65758	4.965643	12.29348	0.000455

Vita

Gene Chatman Clark was born on July 29, 1990 in Richmond, Virginia. Starting in 2008, he attended Virginia Polytechnic Institute where he earned a Bachelor of Science degree in Biochemistry while studying Lipid A biosynthesis in mycobacterium tuberculosis with Dr. Marcy Hernick. Upon graduating in 2012, he became a non-degree seeking student at Virginia Commonwealth University School of Medicine while studying bacterial vaginosis with Dr. Kimberly Jefferson and working full time as a project manager at Movement Mortgage. In 2014, he completed the Graduate Health Sciences Certificate Program at Virginia Commonwealth University and has recently matriculated to the Doctor of Medicine program at Virginia Commonwealth University School of Medicine where was awarded the Dean's Merit Scholarship. His dream is to one day go into academic medicine.